DEVELOPMENT AND REACTIVITY OF NOVEL HETEROGENEOUS CATALYSTS FOR HYDROCARBON CONVERSIONS

By

STEVEN C. PETROSIUS

A DISSERTATION PRESENTED TO THE GRADUATE SCHOOL
OF THE UNIVERSITY OF FLORIDA IN PARTIAL FULFILLMENT
OF THE REQUIREMENTS FOR THE DEGREE OF
DOCTOR OF PHILOSOPHY

UNIVERSITY OF FLORIDA

1992

This work is dedicated to my wife, Sandra, and my son, Nicholas. It has truly been their dedication which has made it possible.

"The known is finite, the unknown infinite; intellectually we stand on an islet in the midst of an illimitable ocean of inexplicability. Our business in every generation is to reclaim a little more land."

- T. X. Huxley, 1887

ACKNOWLEDGEMENTS

The content of this thesis and the years of study it represents have in no small way been inspired by a multitude of friends, family and co-workers. Initially, I would like to express my gratitude to Dr. Russell Drago, my research advisor, for his helpful criticisms and for sharing his enthusiasm of chemistry. Doc's ideas about dedication and fairness will stay with me for many years. Appreciation goes to Ruth Drago for her always generous hospitality and for making UF a "home away from home" for myself and my family. Maribel Lisk and April Kirch deserve special thanks for their assistance in cutting through the seemingly endless amounts of red tape one encounters at UF.

Present Drago group members Mike Naughton, Don Ferris, Steve Showalter, Doug Patton, John Hage, Chris Chronister, Todd Lafrenz, Mike Robbins, Robert Beer, Krzysztof Jurczyk, Phil Kaufman and Karen Frank have all been invaluable sources of ideas as well as good friends. Former group members Al Goldstein, Tom Cundari, Jerry Grunewald and Bob Taylor deserve recognition for showing me the ropes and tolerating sometimes stupid questions. The UF glass shop and machine shop are acknowledged for their technical contributions.

Finally, I would like to thank my family. Mom and Dad P. as well as Mom and Dad H. have shown exceptional moral support in this endeavor despite the

fact that I cannot always abbreviate the chemical jargon adequately to explain my work. The two people who deserve my deepest gratitude are my wife, Sandra, and my son, Nicholas. They have never faltered in their love or support. That they have endured being 1500 miles from home and living the modest lifestyle of graduate school is a testament to their dedication which I will cherish always.

TABLE OF CONTENTS

ACKNOWLEDGEMENTS iv

LIST OF TABLES viii

LIST OF FIGURES x

ABSTRACT xii

CHAPTERS

1 GENERAL INTRODUCTION 1

2 REACTIVITY AND STRUCTURAL CHARACTERISTICS OF A NOVEL SUPPORTED ALUMINUM CHLORIDE CATALYST 6

Background 6
Reactivity Studies 6
Synthetic Studies 12
Experimental 17
Results and Discussion 24
Reactivity of $AlCl_2(SG)_n$ in Hydrocarbon Conversions .. 24
Dehydrohalogenation and hydrodehalogenation .. 25
Friedel-Crafts alkylation 30
Low-temperature isomerization of butane 34
Reactions of n-hexane with $AlCl_2(SG)_n$ 42
Cracking of hydrocarbon polymers 46
Synthesis Variations 54
Silica hydration studies 54
Sealed-system catalyst preparation 67
Conclusions 74
Reactivity Studies 74
Synthetic Studies 77

3 POROUS, CARBONACEOUS ADSORBENTS AS CATALYSTS AND CATALYST SUPPORTS FOR ACIDIC METAL OXIDES 79

Background 79
Experimental 93
Results and Discussion 98
Catalytic Combustion Reactivity Studies 98
Kinetic Experiments 106
Oxidative Dehydrogenation of 1-Butene 120
Catalyst Characterization 123
X-ray photoelectron spectroscopy 123
Magnetic susceptibility 129
Scanning electron microscopy 133
Porosimetry 136
Conclusions 142

4 SUMMARY 148

Supported Aluminum Chloride 148
Porous Carbon Adsorbents 149

REFERENCE LIST 151

BIOGRAPHICAL SKETCH 161

LIST OF TABLES

Table		Page
2-1.	Product Distributions for the Reaction of 1,2-Dichloroethane Over Various Metal-Doped Catalysts.	26
2-2.	Friedel-Crafts Alkylation with $AlCl_2(SG)_n$.	32
2-3.	Products from the Reaction of N-Hexane over $AlCl_2(SG)_n$.	44
2-4.	Product Distribution from the Reaction of N-Hexane Over $AlCl_2(SG)_n$. 1-Hexene Promoter Present.	45
2-5.	Cracking of Polymers Over $AlCl_2(SG)_n$.	48
2-6.	Reactivity of $AlCl_2(SG)_n$ Catalyst Samples Prepared with Silica in Varying Degrees of Hydration.	59
3-1.	Structural Parameters of Carbonaceous Adsorbents.	94
3-2.	Activity of Various Metal Oxide/Porous Carbon Catalysts in the Catalytic Combustion of Methylene Chloride.	100
3-3.	Activity of Base-Treated Carbon Adsorbents for the Catalytic Combustion of Methylene Chloride.	102
3-4.	Values of the Rate Constant for the Catalytic Combustion of Methylene Chloride at Various Flow Rates.	107
3-5.	Reactivity of CrO_3/563 in the Catalytic Combustion of Halogenated Organics.	111
3-6.	Influence of Water on 1,2-Dichloroethane Reactivity Over Carbon and Zeolite Catalysts.	113
3-7.	Bond Energies for Chlorinated Methane Compounds.	115

Table | Page

3-8. Deep Oxidation of CCl_4 Over Ambersorb® 563. 116

3-9. Elemental Analysis of Ambersorb® 563 Before and After CCl_4 Deep Oxidation. 118

3-10. Summary of XPS Data for Chromium Catalysts. 128

3-11. Porosimetry of Ambersorb® 563 and CrO_3/563. 141

LIST OF FIGURES

Figure		Page
1-1.	Proposed Structure of $AlCl_2(SG)_n$.	2
2-1.	Reaction of Al_2Cl_6 with Sulfonated Resins.	7
2-2.	Structures of Various Hydrocarbon Polymers.	11
2-3.	^{27}Al SS MAS NMR Spectrum of $AlCl_2(SG)_n$.	15
2-4.	Equilibrium of Silanol Groups with Siloxane Groups on Silica.	16
2-5.	Schematic of Batch Reactor.	20
2-6.	Schematic of Flow System.	21
2-7.	Dehydrohalogenation of 1,1,1-Trichloroethane Over $RuCl_3{\cdot}ZnCl_2{\cdot}AlCl_2(SG)_n$.	29
2-8.	Cumene Dealkylation.	35
2-9.	Mechanism for the Promotion of Butane Isomerization by 1-Butene.	38
2-10.	Isomerization of N-Butane over $AlCl_2(SG)_n$.	39
2-11.	Sequential Batch Cracking of Poly(ethylene) with $AlCl_2(SG)_n$.	53
2-12.	Model of Silica Gel Surface Illustrating the Dehydration/Rehydration Equilibrium.	57
2-13.	Infrared Spectra of Pyridine Adsorbed on $AlCl_2(SG)_n$ Prepared with Conditioned Silica and Dry Silica.	63

Figure Page

2-14. SS NMR of $AlCl_2(SG)_n$ Catalysts.
a) Prepared with Dry Silica.
b) Prepared with Conditioned Silica. 65

2-15. Infrared Spectra of Pyridine Adsorbed on $AlCl_2(SG)_n$ Samples Prepared in CCl_4 and in a Sealed System, 72 Hour Reaction. 68

2-16. Infrared Spectrum of Pyridine Adsorbed on $AlCl_2(SG)_n$ Prepared in Sealed System, 18 Hour Reaction. 69

2-17. Infrared Spectrum of Pyridine Adsorbed on $AlCl_2(SG)_n$ Prepared in a Sealed System, Desorbed at 300 °C. 71

2-18. SS MAS NMR of $AlCl_2(SG)_n$ Prepared in a Sealed System. 73

3-1. Structure of Pyrolyzed Poly(styrene/divinylbenzene) at Various Temperatures. 81

3-2. Proposed Surface Structure of Silica-supported Chromium(VI) Oxide. 91

3-3. Influence of Air on the Catalytic Activity of CrO_3/563 in CH_2Cl_2 Deep Oxidation. 104

3-4. Arrhenius Plot for CH_2Cl_2 Deep Oxidation with Ambersorb® 563. . . 109

3-5. Low-Temperature Catalytic Combustion Using a Water Co-Feed. . . . 121

3-6. Oxydehydrogenation of 1-Butene with Various Catalysts. 124

3-7. XPS Spectrum of CrO_3/563 Before Reaction, θ = 0 °. 125

3-8. XPS Spectrum of CrO_3/563 Before Reaction, θ = 90 °. 127

3-9. SEM of Ambersorb® 563, 6000 Magnification. 134

3-10. SEM of Ambersorb® 563, 30,000 Magnification. 135

3-11. SEM of 563/CrO_3, 6000 Magnification. 137

3-12. SEM of 563/CrO_3, 30,000 Magnification. 138

Abstract of Dissertation Presented to the Graduate School
of the University of Florida in Partial Fulfillment of the
Requirements for the Degree of Doctor of Philosophy

DEVELOPMENT AND REACTIVITY OF NOVEL HETEROGENEOUS CATALYSTS FOR HYDROCARBON CONVERSIONS

By

Steven C. Petrosius

August, 1992

Chairperson: Dr. Russell S. Drago
Major Department: Chemistry

Preparation of the novel solid acid catalyst $AlCl_2(SG)_n$ has been accomplished in a sealed tube vapor deposition process using an extended time period comparable to that for a previously reported CCl_4 synthesis. Reactivity studies and spectroscopic investigations indicate a similar structure for surface acid sites in the catalysts prepared via the two different methods. It has also been determined that excessively dry silica is deficient in surface silanol (Si-OH) moieties such that effective reaction of Al_2Cl_6 is not achieved. Exposure to humid air is sufficient to hydrate the silica to a level where the active catalyst can be prepared.

The activity of $AlCl_2(SG)_n$ in a number of acid-catalyzed reactions has been studied. In the alkylation of benzene and toluene, the catalyst was found to

be active in batch reactions but gives poor selectivity at elevated temperature in a flow reactor. The isomerization of butane and hexane have been examined with especially successful results obtained for the butane reactant. Cracking of hydrocarbon polymers as a possible recycling procedure is promising with $AlCl_2(SG)_n$. At 100 °C in a batch reactor the activity of the catalyst for cracking polymers is comparable to that observed with n-hexadecane.

Catalysts comprised of metal oxides dispersed on porous carbons are very effective in the oxidative decomposition of halogenated hydrocarbons at 250 °C in air. Methylene chloride, 1,2-dichloroethane, 1,2,4-trichlorobenzene, tetrachloroethylene, tetrachloroethane and carbon tetrachloride are decomposed to CO_2, CO and HCl over the carbon catalysts with high selectivity to HCl for the chlorinated products. Trends in reactivity with support variation indicate that a determining factor in the activity of the catalysts appears to be the micropore volume of the carbon support. The presence of water in the reaction mixture has no effect on the activity of the carbon catalysts. Reactions comparing CH_2Cl_2 with CD_2Cl_2 indicate a rate dependence on cleavage of a carbon-hydrogen bond. Kinetic studies in the methylene chloride experiment show a first order dependence on CH_2Cl_2 concentration and an activation energy of 11.0 kcal/mol.

CHAPTER 1
GENERAL INTRODUCTION

Solid acid catalysis is an indispensable tool for modern industrial chemistry. The ability of heterogeneous acids to activate carbon-hydrogen bonds is a key aspect to their versatility. In fact, the conversion of crude oil to hydrocarbon fuels is the biggest use of heterogeneous acid catalysis today; at 1 x 10^{12} kg/year, crude oil refining even outpaces sulfuric acid production in volume.[1] Solid acids typically exist in one of three forms: inorganic oxides (SiO_2, TiO_2, ZrO_2, etc.), organic polymers with acidic functional groups (ion-exchange resins) or acidic metal compounds deposited on supports, which may be either inert or active themselves.

A novel solid acid has been developed which consists of chemisorbed aluminum chloride on silica gel, denoted $AlCl_2(SG)_n$.[2-4] Characterization by IR and NMR spectroscopy[3] indicates the presence of surface tetrahedral aluminum sites; an example is illustrated in Figure 1-1. This representation is a simplified model of one possible surface site. It is well established that the catalyst possesses both Lewis acid sites (Al centers) as well as Brönsted sites (adjacent -OH groups). The unique stability observed for the catalyst arises from the condensation of Al_2Cl_6 with the surface hydroxyl groups on the silica support. There is a 72 hour reflux period for the catalyst preparation which allows full reaction of the metal species, in contrast to typical vapor deposition methods[5-11] which use shorter

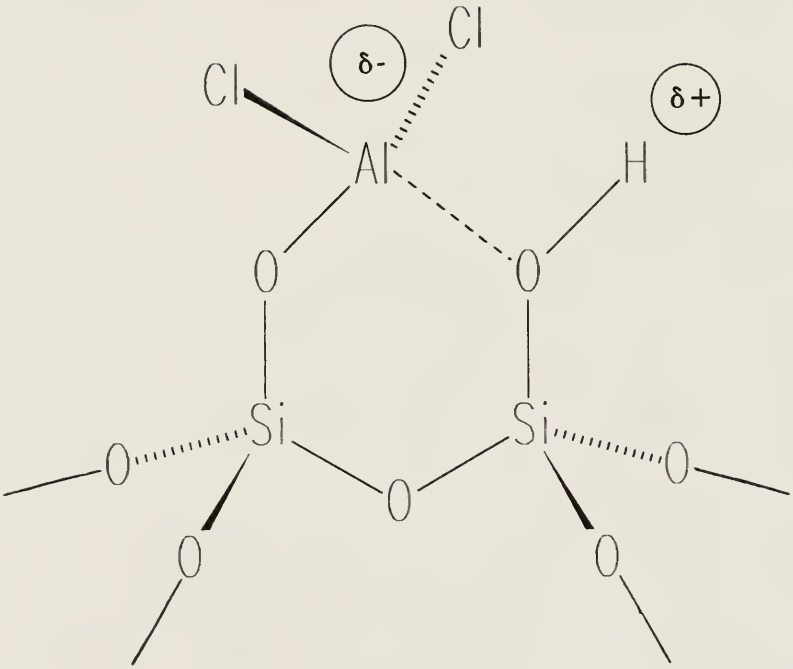

Figure 1-1. Proposed Structure of $AlCl_2(SG)_n$.

contact times and produce catalysts with very short lifetimes due to desorption of Al_2Cl_6 from the support. $AlCl_2(SG)_n$ has been shown to be active in cracking[3,4] and dehydrohalogenation/hydrodehalogenation reactions[12] under conditions where typical zeolite or silica/alumina catalysts are inactive.

The application of $AlCl_2(SG)_n$ to a number of other acid-catalyzed reactions is presented in Chapter 2. The catalyst has demonstrated activity in dehydrohalogenation of 1,1,1-trichloroethane, alkylation of benzene and toluene with a wide range of alkylating agents, room temperature isomerization of n-butane, cracking and isomerization of n-hexane and finally cracking of hydrocarbon-based polymer materials. The reactivity profile generated by these studies is valuable for understanding catalyst structure, such as the existence of Brönsted acid sites and the relative acidity of $AlCl_2(SG)_n$ as compared to other strong acids.

Structural examinations of $AlCl_2(SG)_n$ are also presented in Chapter 2. A sealed-system catalyst preparation method was devised to avoid the use of potentially hazardous chlorinated solvents. Spectroscopic investigations and reactivity comparisons indicate a virtually identical structure for the sealed-system and CCl_4-prepared catalysts. An important aspect of this synthesis procedure is the extended time period, greater than 24 hours, that the components are allowed to react. The hydroxyl content of the silica support is a parameter which was found to notably influence catalyst structure and reactivity. Examination of catalysts prepared with silica at varying degrees of hydration has illustrated that

the active catalyst can only be prepared with "conditioned" silica; that is, silica with sufficient quantity of geminal hydroxyl groups ($>Si(OH)_2$). The facile condensation of these groups under relatively mild conditions has been investigated in terms of catalyst structure and reactivity.

The $AlCl_2(SG)_n$ catalyst is an example of a conventional acidic metal species supported on an inorganic oxide; the preparation itself imparts unique features on the catalyst structure. Chapter 3 presents the investigations of catalysts where the supports themselves are novel materials: highly porous carbonaceous adsorbents prepared by a patented pyrolysis of macroreticular polymers. These materials are essentially hydrophobic in nature, consisting of an extended aromatic framework[13] which can be modified by various activation methods to contain a selected level of surface hydrophilic character. The carbons are studied as both catalysts and catalyst supports. Low-temperature oxidative decomposition of chlorinated hydrocarbons has been very successful using metal oxides supported on carbon adsorbents. Complete oxidation of methylene chloride to carbon monoxide, carbon dioxide and hydrogen chloride is accomplished at 250 °C under an air atmosphere. Other halogenated hydrocarbons show comparable reactivity in this reaction. One other successful reaction using the carbon catalysts is the oxidative dehydrogenation of 1-butene. Carbonaceous materials are known to catalyze oxidative dehydrogenation reactions, predominantly with ethylbenzene, and in this study the activity of metal doped carbons surpasses conversions and selectivities of conventional metal oxide catalysts.

A number of experiments have been performed to reveal mechanistic information about the reactions performed with the carbon catalysts. Parameters such as catalyst acidity, pore structure, surface area, oxygen concentration and metal dopants are examined with respect to the reactivity of the catalysts in standard catalytic combustion reactions. Catalyst characterization also reveals information about how the carbons function as catalysts supports and as catalysts without metal dopants.

CHAPTER 2
REACTIVITY AND STRUCTURAL CHARACTERISTICS OF A NOVEL SUPPORTED ALUMINUM CHLORIDE CATALYST

Background

The idea of using a support to modify the reactivity of anhydrous aluminum chloride was attempted as early as the 1950s by combining Al_2Cl_6 with oxide supports.[14] This work continued sporadically throughout the 1960s and early 1970s[5,8,11,15] but it was not until the OPEC oil embargo of the late 1970's that vigorous efforts to improve upon existing technology resulted in many new catalysts and processes being developed based on Al_2Cl_6.[6,7,9,10,16-22]

Reactivity Studies

Fuentes and Gates[19] and Fuentes et al.[23] have investigated the vapor deposition of Al_2Cl_6 onto sulfonated silica and sulfonated poly(styrene-divinylbenzene) ion exchange resins. Elemental analyses and observation of HCl evolution indicated that aluminum chloride was chemically bound to the supports, as shown in Figure 2-1.[24] Isomerization of n-hexane and n-butane at temperatures less than 100 °C was accomplished using these "superacid" catalysts. The preparation of the Gates catalysts and their proposed structures are

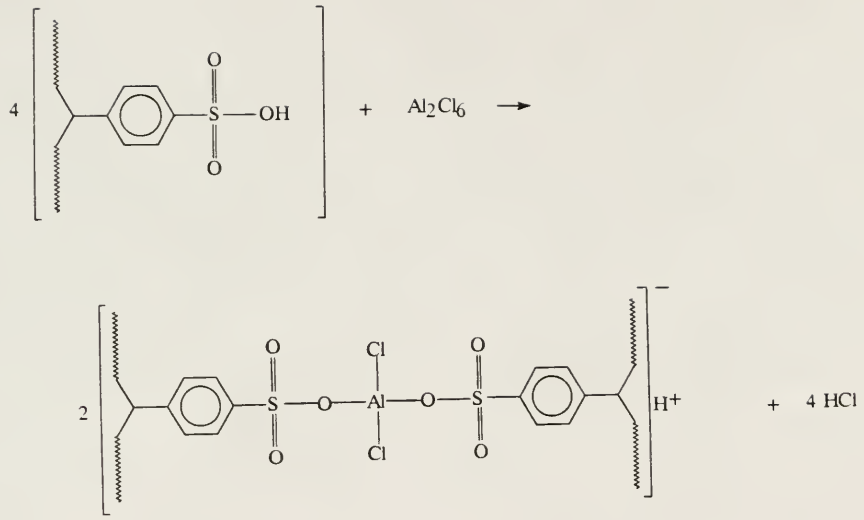

Figure 2-1. Reaction of Al_2Cl_6 with Sulfonated Resins.

remarkably similar to that for $AlCl_2(SG)_n$; it is expected, therefore, that similar reactivity in hydrocarbon conversion reactions can be demonstrated.

Aluminum chloride is probably best known as a catalyst for the alkylation of aromatic compounds, the so-called "Friedel-Crafts" reaction.[25-27] Most of the recent developments in this area involve using various metal salts as homogeneous catalysts. Olah and co-workers, for example, have recently developed boron, gallium and aluminum trifluoromethanesulfonate (triflate) catalysts for aromatic alkylation.[28] The reported advantages of these triflate catalysts over the chloride analogs are improved activity and, in particular, decreased volatility. Application of these materials as heterogeneous catalysts was mentioned as well. It is apparent that a need exists for more convenient Friedel-Crafts catalysts; solid acids are a natural choice in this application.

Studies have been done with transition metals supported on inorganic oxides[29] in the alkylation of benzene with aromatic halides, offering fairly successful results. No mention is made, however, of the use of less reactive aliphatic halides. The superacid polymer, Nafion-H®, has been utilized in these alkylation reactions[30] and offers impressive reactivity even with relatively unreactive alkenes, but the polymer is cost-prohibitive for use in any large-scale operations. These examples illustrate the need for more efficient heterogeneous catalysts in Friedel-Crafts systems. The $AlCl_2(SG)_n$ catalyst has been shown to have more moderate activity than pure, anhydrous Al_2Cl_6; therefore, application of supported aluminum chloride in aromatic alkylations may offer such advantages

as less polyalkylation products (improved selectivity) and the typical assets accorded to heterogeneous systems such as ease of separation from reaction mixtures and better stability.[24]

The initial step of the Friedel-Crafts reaction with alkyl halides generally entails coordination of the halide to the Lewis acid center to form an ion pair, as illustrated in equation 2-1:[25]

$$R\text{-}X + AlCl_3 \quad <======> \quad R^+AlCl_4^- \qquad (2\text{-}1)$$

Once this species is formed, the carbocation R^+ will normally undergo reaction with the aromatic reactant, generating a proton which can regenerate the Lewis acid by formation of $HCl_{(g)}$.

In the absence of other reactants, the carbonium ion R^+ can undergo deprotonation to produce an olefin.[31] Once again, the catalyst can be regenerated by HCl formation and this reactivity is the basis for acid-catalyzed dehydrochlorination chemistry, illustrated in equation 2-2:

$$R\text{-}CH_2\text{-}CH_2\text{-}X + AlCl_3 \text{ ----> } [R\text{-}CH^+\text{-}CH_3/AlCl_4^-]$$
$$\text{----> } R\text{-}CH{=}CH_2 + AlCl_3 + HCl \qquad (2\text{-}2)$$

The $AlCl_2(SG)_n$ catalyst has been used in the dehydrochlorination of 1,2-dichloroethane and 1,1,1-trichloroethane. The results will be discussed later in this chapter.

Cracking of aliphatic, long-chain hydrocarbons with $AlCl_2(SG)_n$ has been thoroughly explored by Drago and Getty.[2b,3,4] Exceptional activity and selectivity to C3 - C5 products was observed with n-hexadecane. An interesting similarity exists between hydrocarbon polymers and long-chain hydrocarbons; namely, the structures consist mainly of repeating $-CH_2-$ units along with $-CH_3$ end groups. Because the important step in catalytic cracking of paraffins involves hydride abstraction from a $-CH_2-$ unit to produce a carbonium ion, cracking of polymers should be feasible over acid catalysts much in the same way hydrocarbons are cracked. Figure 2-2 presents the structures for a selected group of polymers utilized in cracking experiments with $AlCl_2(SG)_n$.

There has been a limited amount of work done in catalytic polymer degradation using silica/alumina[32-34] and activated carbon catalysts.[34,35] These systems, however, have a number of disadvantages for practical applications. The temperatures reported in these studies are at minimum 280 °C, with temperatures of 500 - 600 °C generally needed to effect reasonable conversions. One apparatus used[34] consists of a pressurized liquid flow system which is elaborate and can present difficulties in separating reactants, products and catalyst. These studies indicate that $AlCl_2(SG)_n$ should be useful in polymer cracking because the reported conditions with silica/alumina are the same as for cracking of monomeric

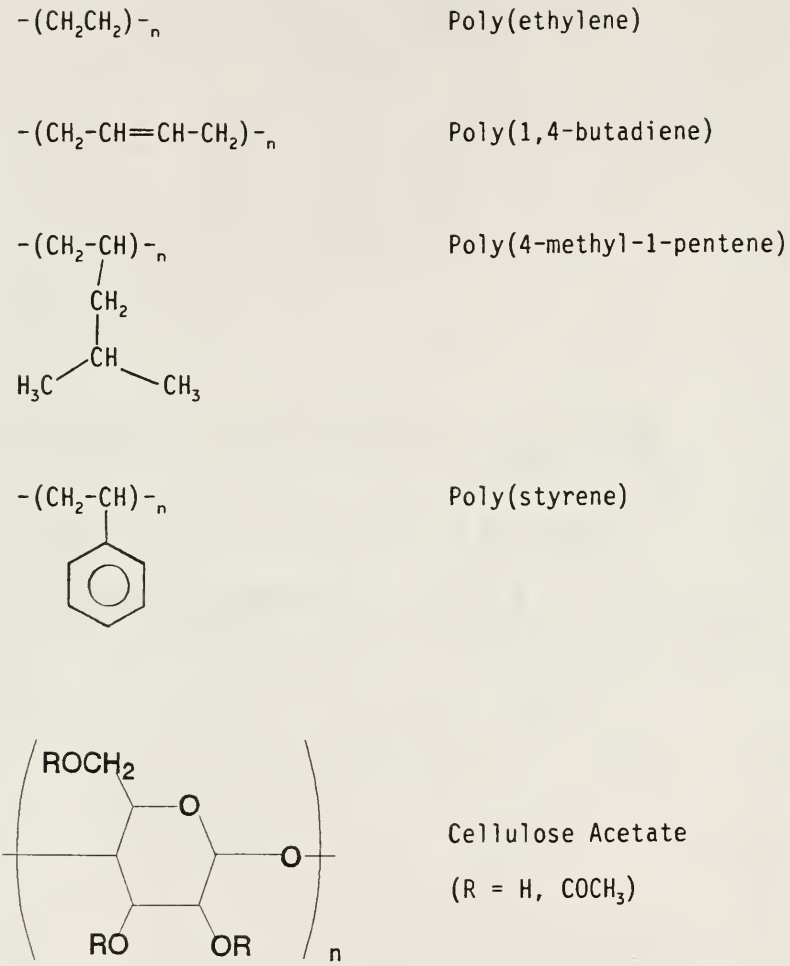

Figure 2-2. Structures of Various Hydrocarbon Polymers.

hydrocarbons. Furthermore, $AlCl_2(SG)_n$ is known to be active at lower temperatures and pressures where aluminosilicates are inactive.

Synthetic Studies

Schmidt and co-workers have outlined a process for synthesizing and utilizing an aluminum chloride (on alumina) catalyst for the isomerization and decyclization of hydrocarbon feeds comprised of C4 to C6 aliphatic hydrocarbons[36] and in some cases solely C6 hydrocarbons.[37] Certain aspects of their catalyst which make it noteworthy to the research presented in this thesis include the use of an inorganic oxide support (alumina), use of Al_2Cl_6 as the acidic component in the level of 2 - 10 % by weight, need for a chloride source in the reaction feeds to maintain catalyst activity, deactivation by contact with water or organic oxygenates and finally deactivation by aromatics. These characteristics are virtually identical to those observed with $AlCl_2(SG)_n$.[2-4] The patents which delineate the Schmidt procedure offer no physical characterization of the catalyst with which to compare to $AlCl_2(SG)_n$, so the solid acids cannot be compared spectroscopically.

Preparation of the Schmidt catalyst entails contacting alumina with sublimed Al_2Cl_6 at high temperature for an extended period of time, reported to be a minimum of 45 minutes at 550 °C. This is considerably longer than the contact times utilized in typical vapor deposition techniques and, as suggested by the CCl_4 studies, may therefore be the distinguishing feature which allows the

catalyst to possess its unique reactivity. Carbon tetrachloride itself is a solvent with poor solvating ability and has been used extensively in studies of donor-acceptor interactions to produce results consistent with the gas phase studies. Therefore, its only function in the synthesis of $AlCl_2(SG)_n$ could be to provide an inert medium for the reaction of Al_2Cl_6 with the support. By this reasoning, it should be possible to prepare $AlCl_2(SG)_n$ in the absence of CCl_4 if a suitable method is devised which affords long contact time and uniform contact of Al_2Cl_6 and silica. A sealed tube reactor containing silica gel and Al_2Cl_6 heated to just above the sublimation temperature of Al_2Cl_6 and kept at that temperature for a sufficient time period provides such conditions.

Spectroscopic investigations of surface acidity are useful methods for obtaining reasonable comparisons between various acid catalysts. One of the most straightforward methods of examining the types of acid sites and, in some cases, acid strengths is the infrared spectrum of adsorbed pyridine. Literature reports of this technique are abundant.[38-48] The physical basis for this method arises from the observation that pyridine bound in a coordinate fashion to Lewis acid sites exhibits different frequencies than that for pyridinium ion arising from protonation by Brönsted sites.[38] In addition, the shift of the predominant pyridine frequency bound to Lewis sites relative to free pyridine can give a qualitative empirical assessment of acid site strengths. This process has been used to evaluate $AlCl_2(SG)_n$ prepared in carbon tetrachloride.[3,49] Aluminum chloride-based

catalysts arising from alternate preparations can be contrasted to the literature results to assess differences in structure and acidity.

Nuclear magnetic resonance (NMR) has been used for many years as a successful technique in the examination of solution chemistry and since the advent of the magic angle spinning method, NMR has been applied to the solid state as well. Of particular interest to examination of $AlCl_2(SG)_n$, ^{27}Al solid state magic angle spinning NMR (SS MAS NMR) has been used with zeolites and amorphous aluminosilicates to elucidate the structures of these solids.[50-53] It has been determined that tetrahedral Al moieties show shifts of between 50 ppm, as observed for tetrahedral Al centers in zeolite ZSM-5,[51] and 105 ppm, as observed for pure Al_2Cl_6.[52] Figure 2-3 shows the ^{27}Al spectrum for $AlCl_2(SG)_n$ prepared in CCl_4 and will serve as the basis for evaluation of catalysts prepared via other routes.

Methods for pre-treating the silica gel support before catalyst preparation have the potential to significantly influence the structure and activity of the final catalyst. The surface structure of silica consists of hydroxyl (silanol, Si-OH) groups as well as siloxane (Si-O-Si) species. Dehydration of vicinal hydroxyl groups can result in the formation of siloxane bridges as pictured in Figure 2-4. This figure is a simplified representation of a three-dimensional silica surface which contains many different types of silanol environments. Because the process is reversible, the content of water in the atmosphere directly contacting the silica determines the relative amounts of both types of surface species. In addition, the

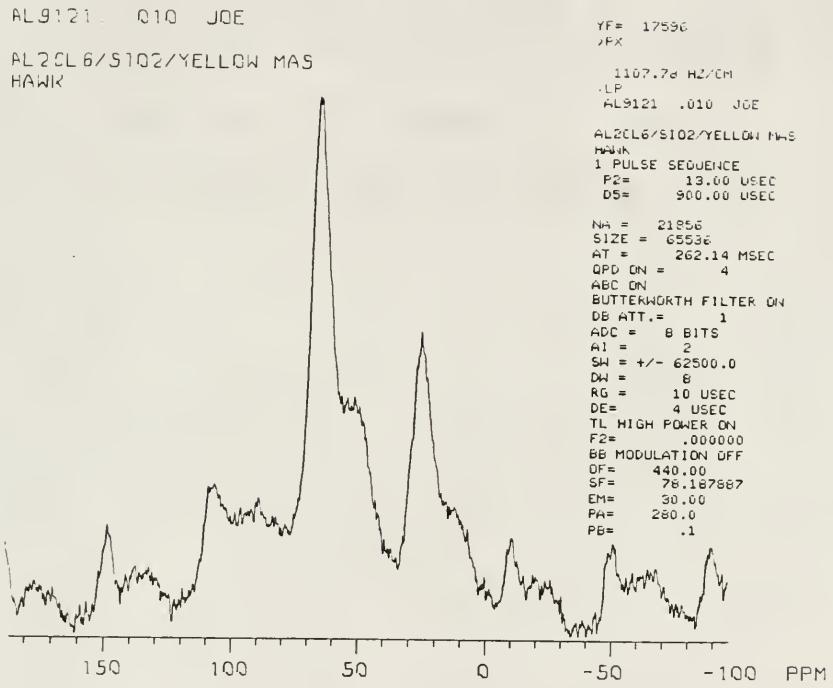

Figure 2-3. ^{27}Al SS MAS NMR Spectrum of $AlCl_2(SG)_n$.

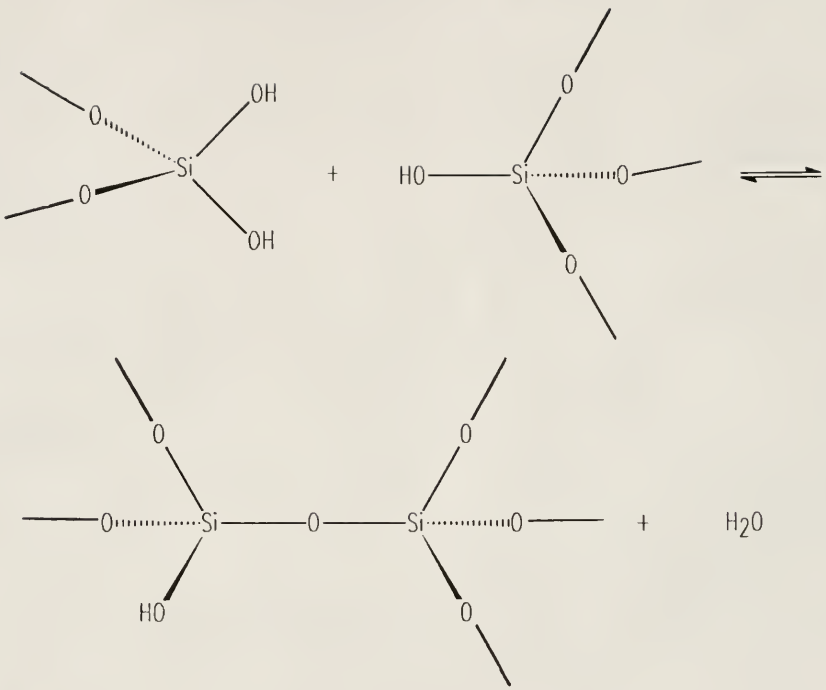

Figure 2-4. Equilibrium of Silanol Groups with Siloxane Groups on Silica.

temperature at which a sample of silica gel is dried is a factor in determining the concentration of surface hydroxyl groups obtained.[54] In addition to silanol groups, SiOH · n H_2O species exist in uncalcined silica which involves water hydrogen bonding to surface hydroxyl groups. In the synthesis of $AlCl_2(SG)_n$, the anhydrous Al_2Cl_6 can react with isolated SiOH species, geminal silanols ($>Si(OH)_2$ groups) and water producing a variety of mixed hydroxo, oxo and chloro species. Understanding these variables is vital for optimizing solid acid acidity and obtaining reproducibility in catalyst preparation.

Experimental

Reagents. The aluminum chloride used to prepare all catalysts was purchased from Alfa Chemicals with a purity of 99.997 % (anhydrous), lot number K17CG. The silica gel support was donated by W. R. Grace Company as Davison Grade #62. The silica gel has a mesh size of 60-200, surface area of 340 m^2/g and pore volume 1.1 cm^3/g. Preparation of the silica support prior to catalyst preparation consists of activation with 1 M HCl, water washing and drying at 80 °C for 72 hours under 1 mm Hg vacuum. It has been determined (vide supra) that following the drying period, adsorption of water at a level of 0.02 g H_2O per gram of dry silica hydrates the support sufficiently for complete reaction of 5.0 g of Al_2Cl_6 with 10.0 g of silica. This composition produces the most active catalyst that does not possess unreacted Al_2Cl_6. The hydration process will be referred to as conditioning of the silica and is accomplished by exposure of the dry silica to air (approx. 75 % humidity) for 24 hours. Hydrated silica will refer to silica with

excessive water content. Carbon tetrachloride, purchased from Aldrich Chemicals, was distilled over phosphorus (V) oxide under N_2 prior to use. All liquid hydrocarbon reactants (benzene, n-hexane, n-hexadecane, cumene, 1-hexene) were purified according to literature methods. Chlorinated organic reactants (1,2-dichloroethane, 1,1,1-trichloroethane, 2-chloropropane, 2-chloro-2-methylpropane) were purchased from Aldrich and used as received. Gaseous materials (ethylene, propylene, 1-butene, n-butane, isobutane, HCl) were purchased from Matheson as C. P. purity, with the exception of HCl which is technical grade. Poly(1,4-butadiene) was donated by Dr. Kenneth Wagener. The rubber tire used in the polymer cracking experiments was supplied by Mr. Todd Lafrenz. All other reagents and solvents were obtained from Aldrich Chemicals and were used as purchased unless stated otherwise.

Instrumentation. Gas chromatography analysis for hydrocarbon products was conducted on a Varian model 940 gas chromatograph equipped with a flame ionization detector and either a 1/8" x 8' stainless steel Hayesep Q (80-100 mesh) column or a 1/8" x 6' stainless steel VZ-10 (60-80 mesh) column. Chlorinated products were analyzed on a Varian 3700 GC with a thermal conductivity detector and a 1/8" x 9' s.s. Porapak Q (100-120 mesh) column. Aromatic hydrocarbons were analyzed on a Hewlett Packard model 5890A GC fitted with a Superox II column (15 m x 0.53 mm I.D. Non-Pakd). Gas chromatography/mass spectroscopy was performed on a Varian 3400 GC equipped with an 30 m x 0.32 mm RSL-160 column (5 μ capillary) interfaced to a Finnegan MAT ITDS 700 mass

spectrometer. A Nicolet 5DXB FTIR spectrometer was used for FTIR analysis. Magic angle spinning solid-state NMR was performed either by Dr. Gordon Kennedy at Mobil Research and Development Company on a Bruker AM-500 NMR spectrometer or by Mr. John West on a GE NT-300 superconducting, wide-bore 300 MHz FTNMR spectrometer operating at 7.02 Tesla. $Al(NO_3)_{3\ (aq)}$ was the reference for all ^{27}Al NMR studies.

Reactors. Reactions utilizing $AlCl_2(SG)_n$ are typically carried out in either a batch reactor as depicted in Figure 2-5 or a fixed bed flow system depicted in Figure 2-6, depending on the particular reaction requirements. The batch reactor consists of a 250 ml Parr pressure bottle with a stainless steel pressure head (comprised of fill/purge valves, pressure gauge and sample port) and a neoprene stopper gasket.[55]

The fixed bed flow system is designed such that gases can be passed over a catalyst powder at ambient or elevated temperatures. This is accomplished by using a 10 mm i.d. pyrex tube fitted with a fritted glass disk to support the solid catalyst while allowing reactant gases to flow through. The reaction tube is heated by either a commercially available Thermolyne Briskheat flexible electric heat tape or a resistance oven consisting of nichrome wire wrapped around a 4" pyrex tube with quartz wool packing material for even heating. The heating element is controlled by a digital temperature controller model CN-2041 (Omega Engineering) equipped with a J-type thermocouple. In all cases temperature varied only ± 2 °C once equilibrated. A 5-inch length of glass beads is placed

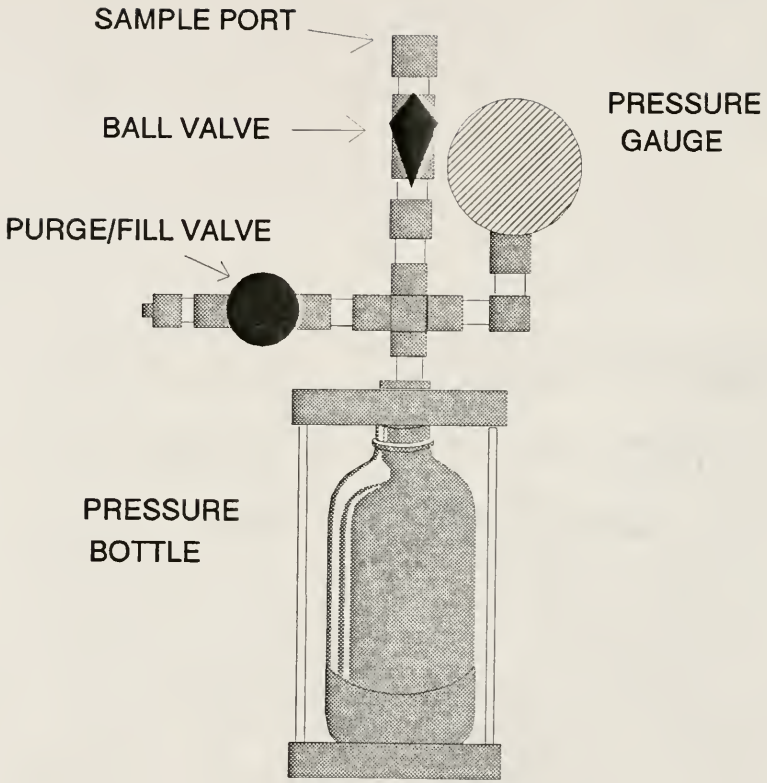

Figure 2-5. Schematic of Batch Reactor.

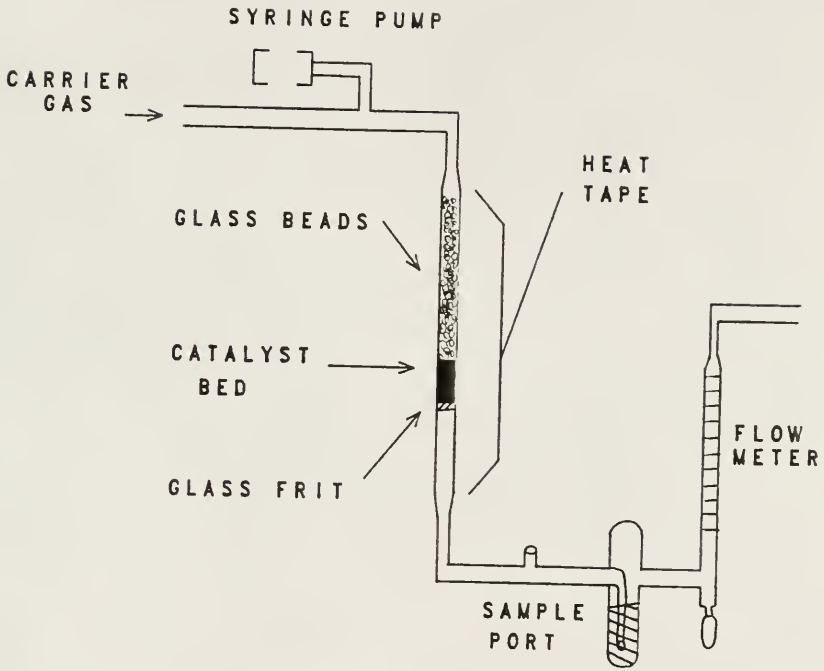

Figure 2-6. Schematic of Flow System.

over the catalyst in the reaction tube to ensure proper mixing and heating of the reactants. Rubber septa attached to the flow line at pre-catalyst and post-catalyst positions allow for gas sampling for GC analysis. A model FL-320 rotameter (Omega Engineering) is used to obtain flow control of gas feeds from 0.2 ml/min up to 50 ml/min. A soap bubble meter in the post-catalyst zone is used to determine overall flow rates of the gases. Liquid reactants are delivered to the catalyst zone via a syringe pump which provides a constant feed rate of reactant. The liquid reactant is vaporized once it contacts the heated catalyst zone. Volatile liquid reactants are delivered by bubbling the carrier gases through a saturation bubbler and over the catalyst bed.

Catalyst preparation. The supported aluminum chloride catalyst was prepared as follows. A 200 ml or 250 ml 3-neck round-bottom flask is thoroughly dried to remove residual water and equipped with a reflux condenser and a teflon-coated magnetic stir bar. An anhydrous N_2 purge is used to ensure a dry environment. To the flask is added 100 to 150 ml of CCl_4 along with 10.0 g of silica gel (activated according to previous specifications). To this slurry is added 5.0 g anhydrous Al_2Cl_6 and the mixture is heated to reflux. After a short time (30 minutes to 2 hours) the slurry changes from colorless to a dark brown color. This color remains for the entire catalyst preparation period. A minimum of 72 hours is generally required for full adsorption of Al_2Cl_6 to occur, as indicated by a gradual disappearance of Al_2Cl_6 crystals in the slurry.

At the end of the 72 hour period, the solid is filtered from the reflux solution and dried at room temperature under vacuum to obtain a tan solid. No further treatment of the catalyst is necessary for use in catalytic experiments. Catalysts which have additional metal promoters are prepared in the same way as mentioned above, with the exception of refluxing the silica in CCl_4 with 0.2 g of the metal chloride promoter for 24 hours prior to Al_2Cl_6 addition. In the catalysts where $ZnCl_2$ was used as an additional promoter, an amount equivalent to 3 times the molar amount of the first promoter is used. The $ZnCl_2$ is added to the slurry after the first promoter but before the Al_2Cl_6.

Sealed-system catalyst preparation. A sealed-system catalyst preparation method was devised to provide a vapor phase method for preparing the catalyst. A 250 ml Parr pressure bottle is dried to remove traces of water and 2.0 g silica gel (prepared as described previously) along with 1.0 g anhydrous Al_2Cl_6 is sealed in the bottle with a neoprene stopper. The pressure bottle is clamped into the same holder as used for the batch catalytic reactions. No pressure head is used for this process because $HCl_{(g)}$ is generated in the adsorption reaction and would corrode the stainless steel. Care was taken to determine appropriate amounts of reagents so that the pressure generated in the bottle from HCl formation would not exceed 60 psi, the maximum pressure rating for the bottle. The sealed system is placed in an oil bath in the temperature range 175 - 190 °C to volatilize the Al_2Cl_6. This reaction is allowed to proceed for a minimum of 72 hours after which time the bottle is cooled and the clamps are slowly loosened to carefully

break the seal and release the pressure arising from the HCl formed in the reaction. Once the pressure is relieved, the rubber stopper is replaced to inhibit water contacting the catalyst. A homogeneous-looking gray solid is obtained and is used in catalytic experiments without further treatment.

Procedure for pyridine adsorption for infrared analysis. A vacuum desiccator is used for all pyridine adsorption experiments. A sample of $AlCl_2(SG)_n$ is placed in the desiccator with a pyridine reservoir and the desiccator is evacuated to generate a pyridine atmosphere inside. The catalyst is kept in the pyridine environment at room temperature for 2 to 3 hours, during which time the catalyst changes from tan to off-white in color. The catalyst is then placed under vacuum for at least 2 hours to remove excess pyridine. This evacuation step is conducted at room temperature as well as elevated temperatures (150 and 300 °C) as a way of gauging the strength of pyridine adsorption. Infrared spectra are taken as a fluorolube mull of the catalyst on KBr plates. No attempt is made to keep the catalyst dry after pyridine adsorption. The region of 1700 to 1400 cm^{-1} is used as the fingerprint region for acid site adsorption of pyridine.

Results and Discussion

Reactivity of $AlCl_2(SG)_n$ in Hydrocarbon Conversions

A vital step in the development of novel heterogeneous acid catalysts is to determine their applicability in selected test reactions. This process is useful in assessing the overall strength and types of acid sites in addition to demonstrating

the potential utility of the catalyst in commercial processes. Isomerization of paraffins, cracking of hydrocarbons and alkylation reactions are among the most important acid-catalyzed reactions utilized industrially and will be the focus for reactivity studies with $AlCl_2(SG)_n$.

Dehydrohalogenation and hydrodehalogenation

One of the reported requirements for cracking with $AlCl_2(SG)_n$ is the presence of a chloride source, such as CCl_4, to maintain catalyst activity during the experiment. It has been noticed that chloroform and methylene chloride are side products when using carbon tetrachloride, indicating a hydrodechlorination (replacement of a chlorine atom with a hydrogen atom) pathway for catalyst regeneration.[2-4,49] Both hydrodechlorination and dehydrochlorination (removal of HCl from a chlorinated molecule) are known to be acid catalyzed;[56-61] therefore, the observation of products arising from hydrodechlorination of CCl_4 is not unexpected.

1,2-Dichloroethane is a simple molecule to study for dehydrochlorination:

$$Cl\text{-}CH_2CH_2\text{-}Cl \text{ -----> } CH_2{=}CH\text{-}Cl + HCl \qquad (2\text{-}4)$$

Conversion of dichloroethane to vinyl chloride is also the largest commercial dehydrochlorination reaction, although at present the reaction is performed thermally (450 - 500 °C) without the need for a catalyst.[62,63] The goal in studying this process is to find a catalytic route which can provide better conversion levels

Table 2-1. Product Distributions for the Reaction of 1,2-Dichloroethane Over Various Metal-Doped Catalysts.

CATALYST	T (°C)	PRODUCTS (MOL/MIN)		
		ETHANE	ETHYL CHLORIDE	VINYL CHLORIDE
$PdCl_2 \cdot (SG)_n AlCl_2$	150	1.7×10^{-5}	1.5×10^{-6}	5.0×10^{-7}
$RhCl_3 \cdot (SG)_n AlCl_2$	125	2.4×10^{-5}	5.0×10^{-7}	---
$RuCl_3 \cdot (SG)_n AlCl_2$	150	6.0×10^{-7}	5.0×10^{-7}	2.6×10^{-6}
$K_2PdCl_4 \cdot (SG)_n AlCl_2$	125	1.0×10^{-6}	---	---
$PdCl_2 \cdot RhCl_3 \cdot (SG)_n AlCl_2$	150	2.0×10^{-5}	3.5×10^{-6}	1.6×10^{-6}
$K_2PdCl_4 \cdot RhCl_3 \cdot (SG)_n AlCl_2$	150	2.5×10^{-6}	1.2×10^{-6}	---
$ZnCl_2 \cdot RhCl_3 \cdot (SG)_n AlCl_2$	150	8.8×10^{-6}	1.3×10^{-6}	2.1×10^{-6}
$ZnCl_2 \cdot RuCl_3 \cdot (SG)_n AlCl_2$	125	1.2×10^{-5}	5.9×10^{-6}	3.3×10^{-6}

with respect to the commercial process (50 - 60 %) while maintaining high selectivity (95 - 98 %) to vinyl chloride. It should be mentioned that hydrodechlorination of 1,2-dichloroethane to ethyl chloride is a side reaction that can occur when using acid catalysts.

Table 2-1 presents the product distributions for the reaction of 1,2-dichloroethane (abbreviated 1,2-dce) over a number of metal-promoted variations of $AlCl_2(SG)_n$.[12] The products obtained give some indication as to the function of the metal promoter(s) added. The feed rate of 1,2-dce is 1.26×10^{-4} moles/minute. The unpromoted $AlCl_2(SG)_n$ catalyst gives primarily 1,1-dichloroethane, most likely arising from acid-catalyzed Markownikov addition of HCl to vinyl chloride formed in a dehydrochlorination intermediate step. Metal promoters can function to modify the acidity of the tetrahedral Al sites on the catalyst and/or react with HCl to preclude addition of HCl to the olefin product; either possibility could account for the absence of 1,1-dichloroethane in the product stream when using metal-promoted catalysts. The extreme coking observed with unpromoted $AlCl_2(SG)_n$ is also inhibited by use of metal promoters.

The three products from the reaction over promoted $AlCl_2(SG)_n$ are ethane, ethyl chloride and vinyl chloride. Ethyl chloride is the hydrodehalogenation product and ethane can arise from hydrodehalogenation of the ethyl chloride product. As seen in Table 2-1, $PdCl_2$ and $RhCl_3$ are the most effective hydrodehalogenation promoters which indicates the need to activate H_2 in the hydrodechlorination process. $RuCl_3$, which is apparently less effective in

hydrogen activation, gives selectivity to vinyl chloride (70 %) but only <10 % conversion of 1,2-dichloroethane. A series of catalysts with two added promoters was investigated. The overall results show increased conversion of 1,2-dce but poor selectivity to vinyl chloride.

The persistence of 1,2-dichloroethane to undergo hydrodechlorination rather than dehydrochlorination led to the use of a different substrate with more potential for HCl removal. 1,1,1-trichloroethane (tce) was investigated with the most active catalyst from the dichloroethane studies, $ZnCl_2{\cdot}RuCl_3{\cdot}AlCl_2(SG)_n$. 1,1,1-trichloroethane is presently converted to 1,1-dichloroethylene stoichiometrically with a sacrificial base reagent.[63-67] A recent report details the use of CsCl on silica for the catalytic conversion of tce to 1,1-dichloroethylene at 150 - 300 °C in a flow system.[68] Conversion was typically ~100 % with selectivity of 80 % at 250 °C. Silica was reported to be a vital component in the activity of the catalyst, so $AlCl_2(SG)_n$ was used in hope of attaining a system which is active at lower temperature. Figure 2-7 shows the activity of $ZnCl_2{\cdot}RuCl_3{\cdot}AlCl_2(SG)_n$ at temperatures of 100 to 300 °C. A sample of the silica support was also used in the reaction as a comparison. The reaction was performed over a period of 12 hours (noncontinuous) which is not sufficient for assessment of catalyst longevity. In addition, because the temperature was changed during the run, the effect of time on catalyst activity is uncertain. It should be pointed out that dehydrochlorination was the major pathway here; less than 10 % of the products observed resulted from hydrodechlorination or any other side reactions. The

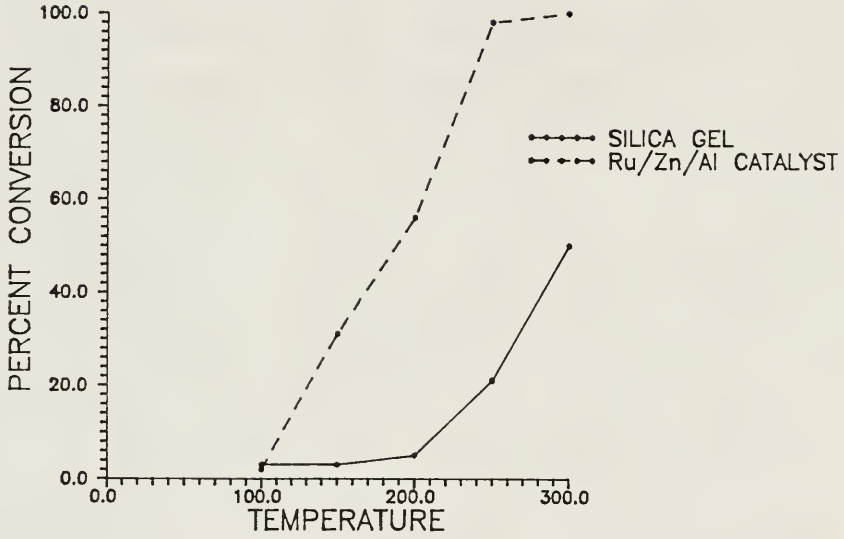

Figure 2-7. Dehydrohalogenation of 1,1,1-Trichloroethane Over $RuCl_3 \cdot ZnCl_2 \cdot AlCl_2(SG)_n$.

activity of the metal-promoted catalyst was considerable even at lower temperatures. Specifically, at 150 - 200 °C the silica showed < 20 % conversion whereas the promoted $AlCl_2(SG)_n$ catalyst approached 90 % conversion of the substrate. The selectivity seen in this reaction (90 + %) indicates that the substrate 1,1,1-trichloroethane is less prone to undergo hydrodechlorination with $AlCl_2(SG)_n$ to form dichloroethane than is dichloroethane susceptible to form ethyl chloride.

Friedel-Crafts alkylation

The alkylation of aromatic hydrocarbons with alkenes and alkyl halides is a classic acid-catalyzed reaction[25-27] and anhydrous aluminum chloride is one of the most effective catalysts known for this reaction. The search for a heterogeneous catalyst to perform Friedel-Crafts chemistry is an active area of research, with catalysts such as Nafion-H®,[69-72] clay-supported transition metals,[29,73,74] graphite-intercalated Al_2Cl_6[72,75] and modified alumina[76] reported within the past 15 years. In the specific case of graphite-intercalated Al_2Cl_6, the catalyst demonstrated very good activity initially but over a few hours the activity dropped to zero.[72] The two reasons given for this problem are hydrolysis of Al_2Cl_6 by water in the reaction feed and gradual desorption of Al_2Cl_6 from the graphite. Clearly, $AlCl_2(SG)_n$ offers significant improvement over graphite-intercalated aluminum chloride because Al_2Cl_6 is chemically bound to the silica and does not desorb even at 250 °C. Deactivation by water is an innate problem for catalysts possessing tetrahedral aluminum active sites and can be deterred by careful drying of the carrier gases.

Table 2-2 presents the results of using $AlCl_2(SG)_n$ in a series of aromatic alkylation reactions. The activity of the catalyst in both batch and flow systems has been investigated. In the batch reactions, it appears that the activity is directly influenced by the stability of the carbonium ion formed from the alkyl halide reactant. A reactant, denoted R_3C-Cl can react with a catalyst active site, depicted as S-O-$AlCl_2$ (S = support) to give an ion-pair: S-O-$AlCl_3^-$ R_3C^+. Alkyl chlorides in which the Cl atom is connected to a 3° carbon, such as t-butyl chloride (abbreviated t-BuCl), form very stable 3° carbonium ions upon abstraction of the chloride;[77] hence the relatively high activity of $AlCl_2(SG)_n$ for alkylation of benzene and toluene with t-BuCl. If an alkyl chloride is used which gives a 2° carbonium ion, i-propyl chloride (i-PrCl), the activity drops to 10 % conversion from 50 % with t-BuCl. In this instance, only the strongest acid sites are active for 2° carbonium ion generation. A number of species are formed in this system which can poison acid sites on $AlCl_2(SG)_n$, such as olefins, and the strongest acid sites will be poisoned first. The rate of this competing reaction may determine how far the reaction progresses toward the alkylaromatic; the faster a carbonium ion is generated, the better chance it has of reacting with the aromatic reactant to form the product before catalyst deactivation occurs. It can be speculated that the low activity of $AlCl_2(SG)_n$ with i-PrCl and benzene can be accounted for by complete poisoning of the active sites by benzene after only 10 % of the alkyl chloride has reacted.

Table 2-2. Friedel-Crafts Alkylation with $AlCl_2(SG)_n$.

Aromatic Reactant	Alkyl Reactant	Conditions	Conversion to Alkylaromatic Products
Toluene	t-Butyl Chloride	Batch	48 %
Benzene	t-Butyl Chloride	Batch	54 %
Benzene	i-Propyl Chloride	Batch	10 %
Benzene	1,2-Dichloroethane	Batch	0 %
Benzene	1-Hexene	Batch	0 %
Benzene	Acetyl Chloride	Batch	0 %
Benzene	t-Butyl Chloride	Flow	0 %
Benzene	Propylene	Flow	0 %
Benzene	i-Propyl Chloride	Flow	4 %

Conditions

Batch:
Reflux temperature, 50 ml CCl_4, 11 mmol reactants.

Flow:
100 - 175 °C, 5 - 30 ml/min N_2,
50/50 (mol/mol) reactant feed @ 0.6 ml/hr.

Protonation of an alkene will also provide carbonium ions in the Friedel-Crafts reaction. This process, however, appears to be less favorable than chloride abstraction over $AlCl_2(SG)_n$ given the lack of activity observed with 1-hexene as the reactant. Poisoning of the acid site by the olefin may also be involved with the lack of activity observed in this case. As expected, 1,2-dichloroethane, which would give a 1° carbonium ion, shows no activity as well. Finally, acetyl chloride was utilized in an acylation reaction (ArH + RCOCl ----> ArCOR + HCl) with no products observed. This is not an unexpected result because $AlCl_2(SG)_n$ loses activity in the presence of oxygen donor groups. Even pure Al_2Cl_6 is used in greater than stoichiometric quantity in acylation reactions due to total complexation of the acyl chloride, which necessitates hydrolysis of the complex to obtain the ketone product and thereby results in inefficient use of the aluminum chloride.

Different product selectivity is observed for the flow system as compared to the batch. Alkylaromatic products are not present in the flow system reaction with t-butyl chloride at 175 °C; propane, isobutane, isopentane and unreacted benzene are the only significant components of the post-catalyst stream. It can be proposed that formation of the expected t-butylbenzene product is unfavorable under the reaction conditions. Dealkylation of alkylaromatics is a known cracking pathway using acid catalysts; for example, t-butylbenzene is efficiently cracked to benzene and isobutylene at 280 °C over silica/alumina.[63] It has been previously established that $AlCl_2(SG)_n$ is significantly more acidic and more active in

cracking than silica/alumina. Therefore, it is reasonable to assume that at 175 °C the t-butyl chloride/benzene reaction equilibrium would lie in favor of the reactants in the presence of $AlCl_2(SG)_n$. The t-butyl cation generated by the acid is then free to undergo hydride transfer to give isobutane and disproportionate to give C3 and C5 products. The isopropyl chloride/benzene system also appears to show similar chemistry as minimal cumene is formed. In this instance, no C4 or C5 products are seen because of the inability of propyl carbonium ions to undergo disproportionation.

In order to substantiate the proposal that the alkylaromatic product can indeed dealkylate under the reaction conditions, the reaction of cumene over $AlCl_2(SG)_n$ was performed at the same temperature as the Friedel-Crafts reactions above and the results are presented in Figure 2-8. Initial conversion of cumene to benzene and C3 products at 160 °C is 100 % but drops rapidly due to coking or poisoning of the acid sites by coordination of the aromatic reactant. These results clearly demonstrate that $AlCl_2(SG)_n$ favors dealkylation over alkylation under the flow-system reaction conditions. As such, the catalyst offers no improvement over present alkylation processes.

Low-temperature isomerization of butane

The isomerization of n-butane to isobutane is a widely-used commercial reaction for obtaining the isobutane feedstock utilized in alkylation with 1-butene for the production of C8 hydrocarbons.[78] The highly-branched alkylates are used in gasoline in order to boost octane ratings. A number of commercial methods for

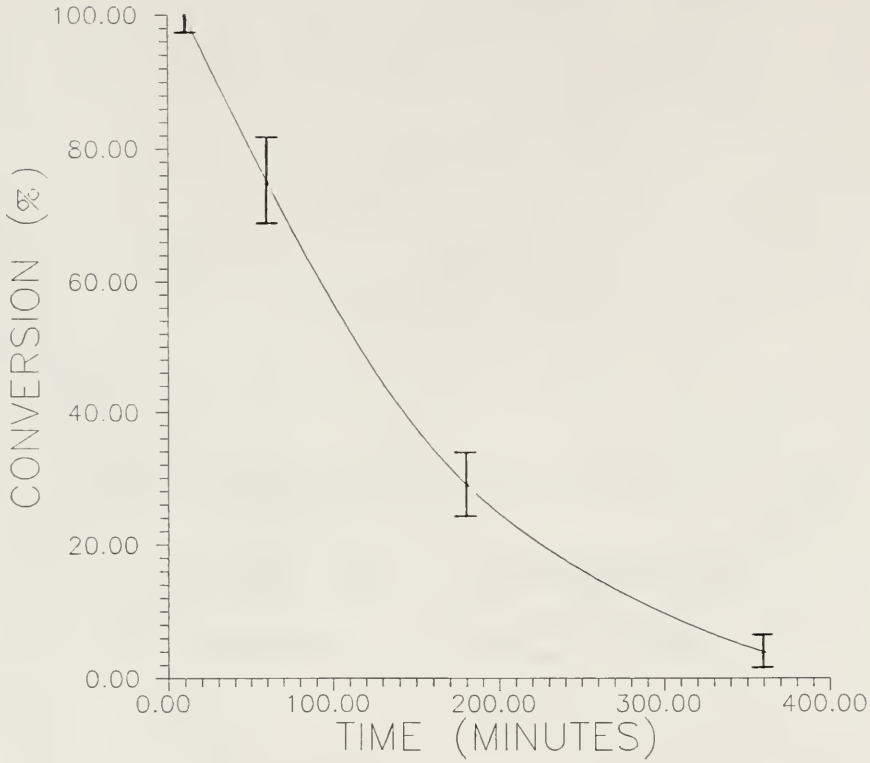

Conditions:

6 ml/min N_2, saturated with cumene vapors (from bubbler)

160 °C

1.0 g catalyst

Figure 2-8. Cumene Dealkylation.

this process are known, such as utilization of a platinum-on-alumina catalyst which is treated with polyhalides (CCl_4, e. g.)[79] and the Butamer process involving a proprietary Pt catalyst.[80] There has been a large amount of work done using Al_2Cl_6 for hydrocarbon isomerization. Ono and co-workers have delineated the use of Al_2Cl_6 in conjunction with metal salts for the isomerization of n-pentane at low temperature.[18,81-83] Of particular interest is a report by Fuentes et al. regarding the use of sulfonated silica-supported Al_2Cl_6 and polymer-supported Al_2Cl_6 in the isomerization of n-butane.[23] It was reported that addition of HCl to the reactant feed resulted in an increased rate of isomerization. This observation was attributed to the fact that isomerization requires both Brönsted and Lewis acid sites; protons serve to regenerate Brönsted sites lost during reaction and Cl^- acts to keep the Cl/Al ratio high, thereby maintaining stronger Lewis acid sites.

Isomerization of butane at low temperature (less than 100 °C) is important not only from the standpoint of using less energy to attain high temperatures but also for maximizing the potential yield of isobutane which is limited by the isomerization equilibrium. Equation 2-3 expresses the equilibrium temperature dependence:[31]

$$R(\ln K) = (2318/T) - 4.250 \qquad (2\text{-}3)$$

where R is the ideal gas constant in J/mol·K, T is the temperature in Kelvin and K is the ratio of isobutane to n-butane. The result is that as the temperature

increases, the isobutane to n-butane ratio decreases concurrently which lowers the maximum amount of isobutane which can be produced in an isomerization procedure.

The addition of small amounts of olefins to the saturated hydrocarbon feed has been found to have dramatic effects on the levels of isomerization observed. Early work done by Pines and Wackher[84] showed that the addition of even 0.01% butenes to an n-butane/HCl mixture in the presence of pure Al_2Cl_6 at 100 °C changed conversion from < 0.1 % to 11.8 %. As depicted in Figure 2-9, protonation of the butene results in a carbonium ion, $CH_3CH_2CH^+CH_3$, which can act as a catalytic agent in the reaction. After rearrangement of the straight-chain cation to the isobutyl cation, hydride abstraction from an n-butane molecule can occur to form the isobutane product and regenerate the straight-chain carbonium ion, thereby continuing the catalytic cycle.

The investigation of n-butane isomerization at various temperatures with $AlCl_2(SG)_n$ was done in order to determine effects of olefins and HCl on the activity. Figure 2-10 shows the results for n-butane isomerization over time in the presence of 4 % 1-butene. The goal was to obtain conditions whereby the conversion of n-butane is relatively high and stable over extended time periods. For the case where $AlCl_2(SG)_n$ is used with n-butane and 4 % 1-butene (no HCl), the conversion is initially very high (ca. 50 %) but drops rapidly to a level of 5 % after 25 hours. Two reasons for this decline in activity can be proposed. In cases where catalysts of high acidity are used for hydrocarbon conversions, coking of the

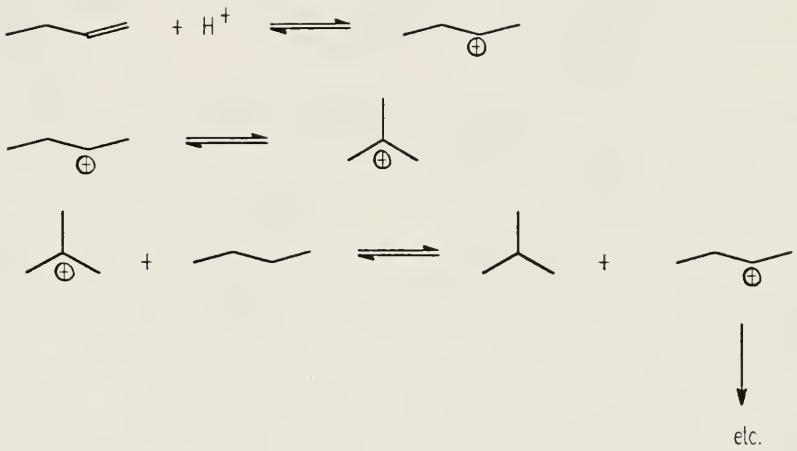

Figure 2-9. Mechanism for the Promotion of Butane Isomerization by 1-Butene.

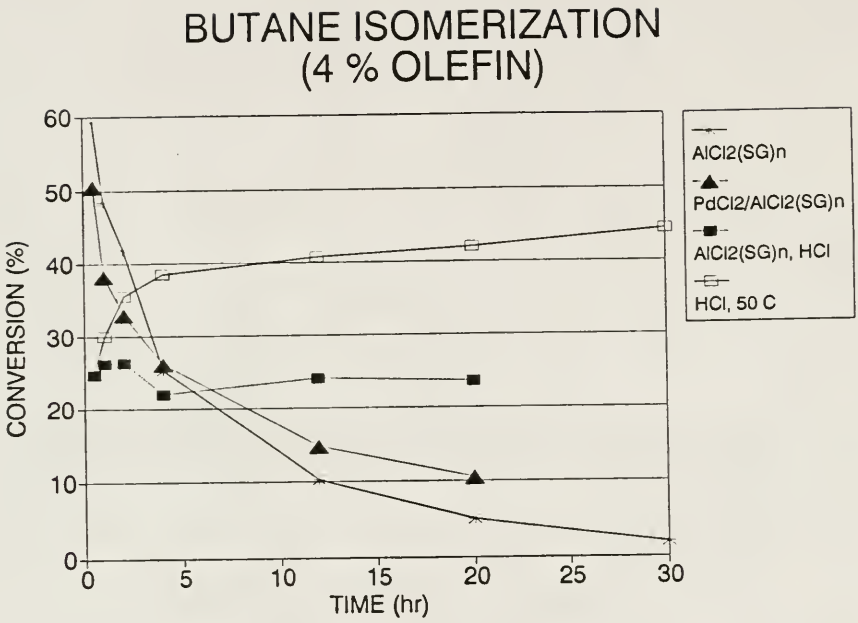

Conditions:

25 °C (Unless otherwise noted)

0.70 - 1.0 g catalyst

Hydrocarbon flow rate: 4 ml/min

HCl flow rate (when used): 0.01 - 0.05 ml/min

Figure 2-10. Isomerization of N-Butane over $AlCl_2(SG)_n$.

catalyst (specifically, irreversible adsorption of hydrocarbon fragments which become highly unsaturated and form a carbonaceous polymer on the catalyst surface) can result in deactivation of the acid sites. The other explanation is simple depletion of Brönsted acid sites during the reaction. Experiments can be performed to determine the deactivation pathway and thereby formulate a way to extend the catalyst lifetime.

It has been shown previously[49] that addition of 2 % of a noble metal promoter (Rh, Ru, Pd, Pt) will decrease the rate of coking and prolong catalyst activity by hydrogenating the carbonaceous deposits on the catalyst surface. In view of this, a catalyst was prepared by reacting $PdCl_2$ with silica in CCl_4 and then treating the $PdCl_2$/silica with Al_2Cl_6 to make a noble-metal promoted solid acid catalyst. As seen in Figure 2-10, no apparent advantage is observed in this experiment as the $PdCl_2$ promoted catalyst shows the same decline in activity over the same time period. This observation, along with the fact that the catalyst did not darken in color as is usual in cases where coking occurs, leads to the conclusion that coking is not involved in catalyst deactivation. It should be mentioned that the addition of an organic chloride, CCl_4, to the gas stream which is reportedly useful in maintaining activity in cracking reactions also does not change the rate of catalyst deactivation.

To test the proposed pathway of Brönsted site depletion, $HCl_{(g)}$ at 10 % by volume was added to the gas stream. The results in this case are notably different, with activity maintained at 25 to 30 % even after 20 hours with no

decline. Based on this data, it can be said that protonic acidity is crucial to maintaining catalytic activity in butane isomerization when olefins are present.

The selectivity to isobutane in all of the butane isomerization experiments mentioned thus far meets or exceeds 85 %. The other products obtained are propane and isopentane arising from a dimerization/cracking pathway. This cracking side-reaction is temperature dependent, with more cracking observed as the temperature is increased. The efficiency of butane isomerization at elevated temperature is therefore limited by the selectivity to the desired isobutane product. Our supported aluminum chloride catalyst has been used at elevated temperature, with the optimal temperature apparently being 50 °C. The data for this experiment is also presented in Figure 2-10. A conversion of 45 % can be maintained for a minimum of 30 hours with 85 % selectivity to isobutane. The theoretical limit according to equation 2-3 is 58 % conversion at 50 °C. Therefore, the activity of the catalyst is approaching the maximum that can be obtained with any system. If the reaction is performed at 100 °C, initial conversion of n-butane is approximately 100 % but selectivity to isobutane is only 65 %. After 20 hours of reaction at 100 °C the conversion drops to only 40 % and the catalyst is black, which is a sign that coking is deactivating the catalyst at 100 °C.

The blank reaction using HCl, 1-butene and n-butane (no solid catalyst) results in no observed production of isobutane which proves that $AlCl_2(SG)_n$ is required in this reaction. Another blank reaction where 1-butene is omitted from

the reaction feed results in only 3 % conversion to isobutane with a very rapid decline to 0 % after 3 hours. In the absence of olefins, the only pathway for the formation of carbonium ions from n-butane is hydride abstraction which requires very strong Lewis acid sites. The initial isobutane formation demonstrates the presence of strong Lewis sites on $AlCl_2(SG)_n$ but their rapid deactivation offers little potential for utilizing such sites in this system. It is well known in the literature[24,31] that olefin protonation requires less energy than hydride abstraction and the above results simply follow that trend.

Reactions of n-hexane with $AlCl_2(SG)_n$

The conversion of n-butane over solid acids can be considered a rather simple reaction, with possible products consisting only of isobutane and cracking products propane and isopentane. N-hexane, in contrast, offers a more complicated reaction chemistry due to its tendency to undergo cracking more easily than butane in addition to skeletal isomerization. The researchers in Gates' laboratory[85,86] have examined the reaction of n-hexane (with 0.1 % 1-hexene promoter) over sulfonic-acid supported Al_2Cl_6 at 85 °C. The initial product distribution consisted of ~15 % branched C6 products and ~65 % cracking products including isobutane (42 %), isopentane (21 %) and n-pentane (2 %). The remaining 20 % of the product stream was unreacted n-hexane for a total conversion of 80 %. After 2 hours the conversion had dropped to 12 %.

Table 2-3 lists the product distribution from the reaction of n-hexane over $AlCl_2(SG)_n$ at 100 °C in a hydrogen atmosphere (no HCl or olefin present). The initially high conversion of 99 % drops to ~40 % in less than one hour, a result which is identical to that observed with n-butane: rapid deactivation of the catalyst in the absence of HCl and olefin promoter. Table 2-4 presents the results for the same reaction with the addition of 1-hexene to the reactant mixture and 10 % HCl to the gas stream. The retention of 90 % conversion after 6 hours of reaction shows that once again the Brönsted activity of $AlCl_2(SG)_n$ is important for hydrocarbon skeletal isomerization.

The selectivity to branched hexane isomers is poor in the flow system experiments due to the predominance of cracking at the temperatures used. As mentioned above, cracking requires more energetic conditions than isomerization given that cracking requires net cleavage of C - C bonds but isomerization can proceed via stabilized 3-center intermediates which do not require the energy necessary for full bond breaking.[87] In order to obtain better selectivity to the branched C6 products, then, a lower temperature must be used. The flow system typically used in our hydrocarbon conversion reactions cannot be used for hexane conversions at lower temperature because the reactant must be in the vapor state. Liquid-phase batch reactions are the only alternative for lower-temperature systems; however, the solvation effects of the solvent result in less efficient catalyst utilization. Nonetheless, the reaction of hexane with $AlCl_2(SG)_n$ in a batch reactor was studied.

Table 2-3. Products from the Reaction of N-Hexane over $AlCl_2(SG)_n$.

PRODUCT	MOLE % t = 10 MINUTES	MOLE % t = 45 MINUTES
Methane	0.08	---
Ethane	0.02	---
Propane	7.4	2.6
Propylene	0.4	---
Isobutane	56.4	21.6
N-Butane	8.6	0.6
Isopentane	17.6	11.0
N-Pentane	4.2	0.6
2,2-Dimethylbutane	2.3	0.8
2-Methylpentane & 3-Methylpentane	2.0	3.3
N-Hexane	1.0	59.6

Conditions:

100 °C, 1.0 g catalyst, hexane feed 0.6 ml/hr,
3 ml/min H_2 flow, CCl_4 bubbler in pre-catalyst stream.

Table 2-4. Product Distribution from the Reaction of N-Hexane Over $AlCl_2(SG)_n$, 1-Hexene Promoter Present.

PRODUCT	MOLE % t = 5 MINUTES	MOLE % t = 4 HOURS	MOLE % t = 6 HOURS
Methane	0.4	0.3	0.8
Propane	13.1	11.7	12.4
Propylene	0.8	---	---
Isobutane	40.1	35.3	37.4
N-Butane	10.6	1.8	1.7
Isopentane	22.4	35.0	33.4
N-Pentane	6.3	1.5	---
2,2-Dimethylbutane	3.0	1.7	1.3
2-Methylpentane & 3-Methylpentane	2.7	5.4	1.5
N-Hexane	0.4	7.5	11.6

Conditions:

1.0 g catalyst, 100 °C, 1 % 1-hexene in liquid feed @ 0.6 ml/hr, 3 ml/min H_2 flow, 0.2 - 0.4 ml/min HCl flow (no CCl_4 bubbler)

A temperature of 25 °C was used for the batch reaction. The catalyst was slurried with 10 ml of 0.1 % 1-hexene in n-hexane and 30 ml CCl_4 under 27 psig H_2. There was a barely detectable amount of isobutane present in the reactor after 18 hours, corresponding to $<<1$ % conversion of the reactant. Interestingly, there was no hexene observed in the product mix. This observation can best be explained by irreversible coordination of the olefin to the acid sites on the catalyst; the 2.3×10^{-3} moles of Al sites on the catalyst are more than enough to form 1:1 complexes with all of the 8.0×10^{-4} moles of 1-hexene used in the experiment.

At higher temperatures, the batch reactor does not offer much improvement. For a reaction performed at 65 °C (no hexene), only 2.5 % conversion of the hexane was observed with minimal branched C6 products obtained. It is apparent from these results that hexane highly favors cracking reactivity with $AlCl_2(SG)_n$, based in part on the level of catalyst acidity and propensity of hexane to undergo cracking over acid catalysts.

Cracking of hydrocarbon polymers

Disposal of plastics and rubber is arguably the biggest problem facing polymer manufacturers today. Recycling efforts are being made in many communities but the recovered plastics are essentially utilized as filler material, such as incorporation of used poly(ethylene terephthalate) in soda bottles and used automobile tires in asphalt. Increasing attention has been given to utilizing spent polymers as a chemical resource,[88] with the ultimate goal of recovering the starting monomer via some depolymerization method.

Hexadecane cracking with $AlCl_2(SG)_n$ occurs very readily at 100 °C.[3,4] Reactions between $AlCl_2(SG)_n$ and polyolefins are expected to be similar based on the obvious structural similarities. The unique aspects of polymers which pose additional complications are the solid physical state and the presence of additives which are not present in petroleum feedstocks.

Despite the possible drawbacks, some recent literature work with acidic aluminum compounds as catalysts for polymer degradation illustrates the potential for utilizing $AlCl_2(SG)_n$ in this type of reaction. A catalytic study using ethylaluminum chloride (Et-$AlCl_2$) to crack poly(isobutylene) in solution[89] has resulted in decreased molecular weight of the polymer and formation of branched structures, both of which indicate a carbonium ion mechanism is occurring in the polymer degradation. Examination of the acids $MAlCl_4 \cdot H_2O$ (M = Li, Na, K) in cracking of poly(ethylene), poly(propylene), poly(isobutylene) and butyl rubber demonstrates a dependence on molecular weight, presence of double bonds and extent of branching for catalyst activity.[90] These results again show a cationic pathway for polymer decomposition, as in the ease of protonation of double bonds to generate carbocations, for example. A recent report with exceptional significance to our work with $AlCl_2(SG)_n$ is the catalytic decomposition of butyl rubber with pure $AlBr_3$.[91] No high molecular weight products were observed, the polymer unsaturation was reported to increase (due to hydride abstraction by $AlBr_3$) and a cationic mechanism was proposed for the reaction.

Table 2-5. Cracking of Polymers Over $AlCl_2(SG)_n$.

POLYMER[a]	MOLES ISOBUTANE/MOLE Al SITES
Poly(ethylene)	0.20
Poly(ethylene)[b]	0.04
Poly(4-methyl-1-pentene)	0.28
Poly(butadiene)	0.08
Poly(styrene)	< 0.0001
Rubber Tire	0.05
Cellulose Acetate	< 0.0001
PE Shopping Bag	0.03
PE Shopping Bag[c]	0.07
N-Hexadecane[d]	0.24

[a] Conditions:
100 °C, 1.0 g catalyst, 2.0 g polymer,
25 ml CCl_4, 25 psig H_2 (unless noted otherwise).

[b] Nitrogen used in place of hydrogen.

[c] Reaction at 175 °C.

[d] Presented for comparison purposes.

The results for polymer cracking with $AlCl_2(SG)_n$ are presented in Table 2-5. The first entry in the table gives the conversion for cracking poly(ethylene) (PE) and the results are very encouraging. The product distribution with PE is identical to that obtained from typical monomeric hydrocarbons: isobutane, isopentane and propane are the major products in a 5:2:1 ratio with minor products n-butane and n-pentane. The amount of isobutane produced per Al site on the catalyst provides a pseudo-turnover number (PTON) and is used as a gauge to compare polymer reactivity. The value of 0.20 for the PTON with PE is within the experimental error of ± 0.02 for the result we obtain with n-hexadecane, 0.24. The identical product distributions and similar conversions suggest that the same carbonium ion mechanism is at work for both monomeric and polymeric cracking with $AlCl_2(SG)_n$. Hydrogen appears to be an integral part of the reaction scheme according to the second entry in the table where N_2 is utilized as the atmosphere and a large difference in activity is observed; only about $1/5^{th}$ of the activity is seen in this case. It is not known whether hydrogen is actually consumed in the reaction or is involved in an as yet undetermined non-consumptive pathway.

To investigate further the involvement of hydrogen in the cracking scheme, a version of the catalyst containing 2 % $PdCl_2$ promoter was used in PE cracking. The ability of palladium to activate hydrogen was found to have an unexpected effect on the product distribution, with the amount of isobutane formed at the exact same level as the unpromoted catalyst (PTON = 0.20) but the amount of

methane and ethane in the product mix increased sharply. The ratio of methane to ethane to isobutane in the product mix was 1.3 : 1.2 : 1. The C1 and C2 products are proposed to arise from a hydrogenation of surface coke or dehydrohalogenation of CCl_4 or a combination of the two. These results imply that the mechanism of polymer cracking involves utilizing hydrogen via a different pathway than that employed by $PdCl_2$.

The branched polymer poly(4-methyl-1-pentene) gives higher activity, as expected, due to its branched structure. The presence of 3° carbons on the polymer (refer to Figure 2-2 for the structure) allows for easier hydride abstraction, which is proposed to be the pathway for generation of the carbonium ion intermediates from saturated hydrocarbons.

It was proposed in the previous section on hexane isomerization with 1-hexene promoter that the olefin can coordinate to the acid sites and thereby inhibit the reaction; this effect is also observed in the reaction of poly(butadiene) where the activity drops by a factor of ~2.5 as compared to PE with the presence of an unsaturated functionality on the hydrocarbon chain. Poly(styrene) is another example of an unreactive polymer. The lack of reactivity observed in this instance can be postulated to be due to the observation that the polymer did not melt under experimental conditions or the presence of aromatic groups which may have a poisoning influence on the acid sites.

Carbon-carbon double bonds are considered to be weak bases due to the electron-donating ability of the pi bond and it has been shown that olefins can

have a detrimental effect on the activity of $AlCl_2(SG)_n$. It is expected that stronger bases like oxygen or nitrogen donors will show an even stronger impact on the reactivity of the catalyst; indeed, water can completely deactivate $AlCl_2(SG)_n$ by coordination of the oxygen lone pairs to the Al sites. Cellulose acetate, by virtue of possessing 5 oxygen donors per repeat unit, exhibits this problem as evidenced by its lack of reactivity in the cracking reaction. Unfortunately, the sensitivity of $AlCl_2(SG)_n$ towards bases presents a severe limitation for application of the catalyst in polymer remediation. Investigations of catalyst reactivity toward commercial plastic and rubber, therefore, will concentrate on materials which are devoid of basic functional groups.

The final entries in Table 2-5 illustrate the use of commercial polymer products in cracking to useful end-products. Utilization of a PE shopping bag results in only a small amount of isobutane under the reaction conditions. Two reasons can be postulated for this: first, the bag is constructed from high-density (highly crosslinked) PE which did not form a melt as did the low-density PE mentioned earlier, and second, the bags are designed for bacterial degradation in landfills by the addition of starch, which contains oxygen functionalities. The extent of starch addition is unknown but may not be excessive; the use of higher temperature to assure polymer melting can determine if the presence of starch is the deactivation factor in this instance. Cracking of the PE bag at 175 °C is presented in Table 2-5 and the resulting low activity indicates that the starch additives may indeed inhibit reaction to a certain extent. The polymer did form a

melt under the reaction conditions but the activity only increased very slightly, which shows that the determining factor in the reactivity is not simply contact of the polymer with the catalyst but also involves additives which can poison the catalyst.

A sample of vulcanized rubber tire provides a PTON of 0.05 despite the fact that no melting of the polymer occurs at experimental conditions. To account for this observation, it can be proposed that either a solid/solid reaction occurred between the catalyst and tire or unidentified organic tire additives were extracted from the rubber matrix by the solvent and were the actual reactants in the cracking reaction. A Soxhlet extraction performed with CCl_4 on a sample of the tire resulted in a brownish-colored liquid phase which evaporated down to a black sludge. Cracking of the tire after extraction gave a PTON of 0.016 ($\pm$ 0.004) as compared to the untreated tire which showed 0.050 ($\pm$ 0.010). Utilization of the sludge extract showed a PTON of 0.006 ($\pm$ 0.002), indicating that the tire extract does indeed provide cracking products. However, based on the reactivity still observed with the extracted tire a solid/solid reaction may be occurring.

The longevity of $AlCl_2(SG)_n$ in the cracking of polyolefins is a parameter which is difficult to assess in a batch reactor but needs to be addressed nonetheless. The cracking of PE in the batch reactor is observed to give consistent PTON results for each replicant experiment. The similarity in the product distribution for each replicate is an indication that an equilibrium exists which determines the maximum amount of products formed for a single batch run.

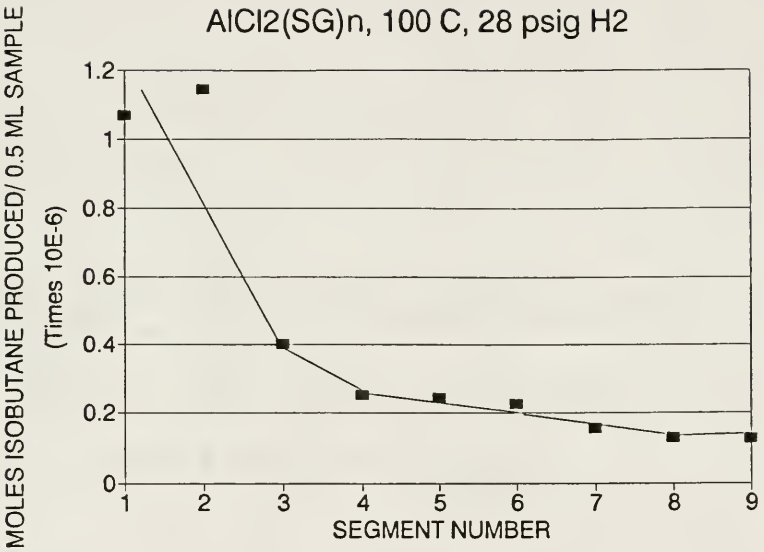

Figure 2-11. Sequential Batch Cracking of Poly(ethylene) with $AlCl_2(SG)_n$.

Figure 2-11 shows a PE cracking experiment where the reactor was purged at elevated temperature after each 18 hour segment; the effect of this is to remove the products and attain greater conversion. The high activity observed in the initial two segments can be attributed to the stronger acid sites on the catalyst. Coking of these sites and their consequential deactivation reduces the efficiency of the catalyst, as seen in comparison of segment two to segment three. The remaining acid sites, being less acidic, do not coke as rapidly so there is a more gradual decline after each segment. This observation correlates well to results obtained for cracking in a flow system[4] where equilibrium is not attained because the carrier gas constantly removes the reaction products. After the 9 segments, the total PTON was 0.80 (± 0.10), which is roughly four times more than obtained in a one-segment experiment. These results demonstrate that the batch polymer cracking is an equilibrium reaction which, if perturbed, presents a method for efficient utilization of the acid catalyst.

Synthesis Variations

Silica hydration studies

The surface of silica has been the subject of many investigations with the goal of gaining an understanding of heterogeneous catalyst preparation. As early as 1940 it was found that silica possesses both silanol groups, Si-OH, and siloxane groups, Si-O-Si, on the surface of a bulk solid that consists of SiO_4 tetrahedra.[92] It is generally accepted that SiOH groups can be condensed reversibly to siloxane groups, as depicted in Figure 2-4. This phenomenon has a distinct influence in the

preparation of $AlCl_2(SG)_n$ because it has been determined that reaction of Al_2Cl_6 with Si-OH groups is the factor which provides stability to the resulting surface aluminum sites.

A review of silica gel surface studies has been presented by Hockey,[93] who describes synthetic procedures and the influence of temperature on silica gel hydroxyl group content. Gel-type silicas are generally prepared by the acid hydrolysis of reactive silicon compounds, such as $SiCl_4$ or $Si(OR)_4$, to obtain polymerized orthosilicic acid, $Si(OH)_4$, which is concentrated to form the gelatinous solid material. These gels typically possess some short-range crystalline order but as a whole are amorphous, due to incomplete condensation of silanol functionalities and imperfect ordering during the polymerization process.

For silica which has not been subjected to calcination (200 °C or higher) the structure can be described as an imperfect semi-crystalline lattice with defects arising from uncondensed proximal SiOH groups. Peri and Hensley[94] have proposed that these lattice defects consist of neighboring geminal hydroxyl groups (two hydroxyls attached to one silicon atom). At ambient temperature, the adjacent silicons are constrained in the gel lattice so that condensation does not occur. Mild heating (to about 100 °C) is enough to allow the silicons to form the siloxane bridge. The strain on the lattice induced by this reaction is the driving force for the reverse reaction at room temperature in the presence of water. If the silica is taken to high temperature, >200 °C, then the surface loses more hydroxyl functionalities and becomes more ordered. This structure reordering at

high temperature can result in alleviation of the ring strain mentioned above and accounts for the hydrophobicity of silicas which are treated at elevated temperatures.

Maciel and Sindorf[54] have derived a surface model of the dehydration/rehydration process, shown in Figure 2-12. The geminal silanols condense with either a geminal neighbor to form two single hydroxyls on vicinal silicon atoms, or a neighboring single silanol to form a new hydroxyl of different orientation. It should be clear from Figure 2-12 that the relationship between the (111) plane and the (100) plane changes dramatically upon even mild heating. This model is certainly an idealized picture of silica gel; Peri and Hensley[94] propose that unheated silica possesses only geminal silanol groups and would have a much more random structure than Figure 2-12 presents.

The interaction of Al_2Cl_6 with the silica surface can take place in a number of ways. Based on the stoichiometry of HCl evolution during the synthesis, the conceptually simplest interaction is reaction of an $AlCl_3$ unit with a lone SiOH moiety to form SiO-$AlCl_2$, giving rise to the active catalyst. Recently revised HCl quantification has shown that the reported one mole of HCl formed for each $AlCl_3$ used is actually closer to 1.5, indicating that SiO-$AlCl_2$ is not a wholly accurate representation of the adsorbed aluminum sites. If reaction of Al_2Cl_6 was favored at single silanol sites, as present on the (111) plane in Figure 2-12, it is expected that dehydration of the silica should not be a determining factor in catalyst preparation because siloxane formation between single silanol groups is

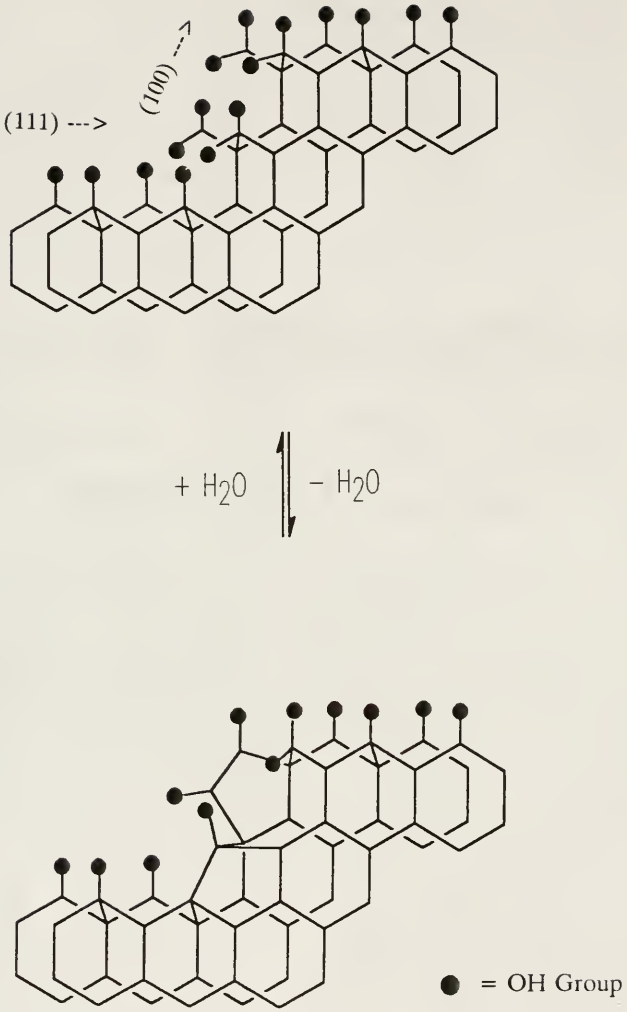

Figure 2-12. Model of Silica Gel Surface Illustrating the Dehydration/Rehydration Equilibrium.

unfavorable at temperatures less than 400 °C due to the major reordering that must occur to accommodate the resulting geometry.

Interaction of aluminum chloride with geminal silanol sites would be notably different than for single silanols. A value of 1.5 moles HCl evolved for each $AlCl_3$ unit indicates that there are at least two SiO-Al bonds for an appreciable quantity of acid sites. The orientation of the geminal hydroxyls pictured in Figure 2-12 appears to be more favorable for formation of two SiO-Al bonds per Al site as compared to the single silanol groups. Furthermore, assuming that there is a predominance of geminal sites on the surface, as proposed by Peri and Hensley, it is likely that Al_2Cl_6 would react with those sites as opposed to single silanol sites. If interaction between Al_2Cl_6 and geminal silanol groups is the preferred reaction, then it is expected that mild dehydration of the silica, which results in condensation of these sites, would have a major influence on the catalyst preparation. In addition, rehydration of the silica by limited exposure to water would restore the geminal sites and return the silica to its active state.

The effect of silica hydration on the preparation of $AlCl_2(SG)_n$ is perhaps best illustrated by comparing the activity of catalysts prepared with "dry" silica (limited quantity of geminal silanol groups), hydrated silica (excess adsorbed H_2O) and conditioned silica (optimum content of geminal sites). Table 2-6 illustrates the activity comparison for the cracking of n-hexadecane in a batch system with the catalysts prepared using the various silica samples. Silica sample A was

Table 2-6. Reactivity of $AlCl_2(SG)_n$ Catalyst Samples Prepared with Silica in Varying Degrees of Hydration.

SAMPLE	COLOR	MOLES HCl PROD./Al	RELATIVE CRACKING ACTIVITY	DETAILS
A	Brown	0.7	0.16	C1 - C3 in large quantity
B	Yellow	1.3-1.7	1.0	standard R^+ distribution
C	White	2.2	$< 10^{-5}$	minimal products observed

Silica Pre-treatment:

Sample A: Activate with 1 M HCl, dry at 80 °C for 72 hours under vacuum.

Sample B: Same as A but exposed to atmospheric water for 24 hours.

Sample C: Activate with 1 M HCl, dry at 40 °C for 24 hours.

activated with 1 M HCl and dried at 80 °C for 72 hours, as reported in references 3,4 and 49. This sample was used directly from the drying oven in the catalyst synthesis procedure. The method gives a brown catalyst intermixed with white particles, indicating less than complete reaction of the Al_2Cl_6 with the silica sample. The reactivity of this catalyst in hexadecane cracking shows isobutane produced in a small amount with additional products of C1 to C3 hydrocarbons. Unsupported Al_2Cl_6 will crack hydrocarbons itself but coordinates very easily to trace olefins which are produced and rapidly deactivates,[49] so the minimal activity seen with this catalyst is not unexpected.

Silica possessing a high adsorbed water content is also unfavorable for $AlCl_2(SG)_n$ preparation. By altering the silica drying procedure to a temperature of 40 °C for 24 hours, the silica retains enough water to hydrate a majority of the Al sites to a less acidic octahedral environment, as evidenced by the white color and excessive HCl formation. With 2.2 moles of HCl formed per Al site, hydrolysis is approaching the limit of 3 for full hydrolysis of Al-Cl bonds. It is therefore not surprising that the catalyst shows no activity in cracking, as the much lower acidity of octahedral Al vs. tetrahedral Al is not sufficient for carbonium ion generation.

It is evident that relatively small variations in silica hydration produce very different materials when reacted with Al_2Cl_6. The active version of the catalyst is prepared with silica which is allowed to absorb water from the atmosphere for a minimum of 24 hours. During this time period, the mass of the silica gel increases

by 0.02 g (± 0.001 g) per gram of dry silica, or 28 mmol water per gram silica. This corresponds to 56 mmol of SiOH groups formed if each molecule of water hydrolyses one Si-O-Si linkage. This is much higher than the estimated 10 to 20 mmol of silanol moieties proposed as the typical concentration of these groups in uncalcined silica. This implies an excess of water is physisorbed on the support but it is not known whether this excess water plays a role in the formation of active catalytic sites. The profound influence of mild dehydration conditions on the catalyst preparation leads to the conclusion that Al_2Cl_6 is interacting primarily with geminal silanol groups on the silica, as they are the only sites which are altered at the mild dehydrating conditions used in the silica pre-treatment.

Infrared examination of adsorbed pyridine. In order to obtain a qualitative assessment of the different acid sites for $AlCl_2(SG)_n$ prepared with silica at various stages of hydration, the infrared spectrum of adsorbed pyridine can be used. The catalyst samples studied in this method are the active catalyst prepared with conditioned silica and the sample prepared with excessively dry silica. The two samples are degassed under vacuum at 200 °C for 3 or more hours, contacted with pyridine vapors for a minimum of 3 hours and finally degassed a second time at various temperatures to remove excess and weakly bound pyridine. Parry[38] has done a thorough assignment of the pyridine bands on acidic surfaces and conclusions can be made based on these assignments. A band at ~1540 cm^{-1} involves C-N^+-H bending in the vibration which justifies its use as a fingerprint for Brönsted acidity. At 1445 cm^{-1} a band occurs which is indicative

of Lewis-bound pyridine and can be used as a gauge for the presence of Lewis acid sites. It should be mentioned that there is also a contribution from hydrogen-bonded pyridine in the 1445 cm^{-1} band which can present problems when assessing Lewis acidity such that other factors should be considered before using this peak for fingerprinting purposes. A third band is present at 1485 cm^{-1} but occurs for both Lewis and Brönsted acidity; conclusions can not be made directly using this particular peak.

Figure 2-13 presents the absorbance IR spectra for the two catalysts made with dry silica and conditioned silica. In both cases, there are significant amounts of both Brönsted and Lewis sites on the catalysts but the patterns for the three fingerprint peaks are sufficiently different that qualitative judgements can be made as to respective amounts of each acid site type. The Brönsted peak at 1540 cm^{-1} for the active catalyst (made with conditioned silica) has an overall intensity close to that seen for the Lewis band at 1445 cm^{-1}; relative to the sloping baseline the Brönsted peak is more intense the Lewis band. This three band pattern is very reproducible for catalytically active $AlCl_2(SG)_n$. In the case where the catalyst is prepared with dry silica, the Brönsted band is much less intense than the Lewis/hydrogen bonding peak. Two explanations for the difference in the two spectra can be proposed. Assuming the validity of the proposed catalyst structure as shown in Figure 1-1, it is apparent that Brönsted acidity for $AlCl_2(SG)_n$ arises from coordination of the oxygen lone pairs of a silanol group to a vicinal Al site which thereby activates the SiO-H bond for proton donation. As the dry silica

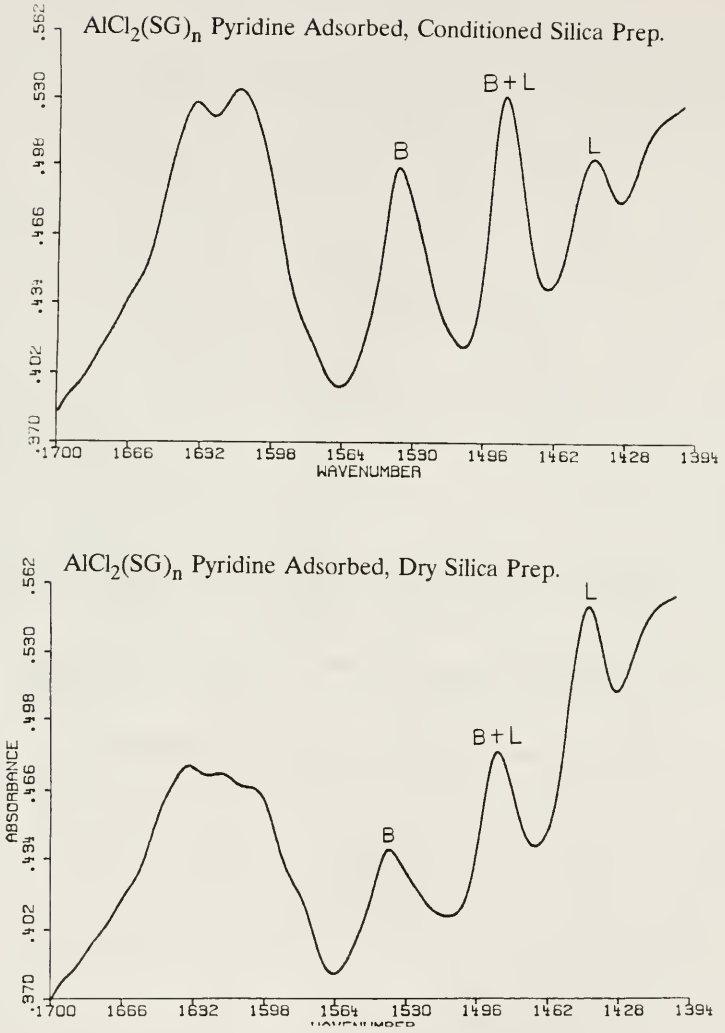

Figure 2-13. Infrared Spectra of Pyridine Adsorbed on $AlCl_2(SG)_n$ Prepared with Conditioned Silica and Dry Silica.

would have a decreased concentration of silanol moieties, the occurrence of a silanol group near an aluminum center is less probable; the result of this is that a greater quantity of silanol groups are available to hydrogen bond with pyridine which would show up as an increased intensity of the 1445 cm^{-1} band. This explanation also accounts for the decreased intensity of the Brönsted peak. The other explanation, which may not be mutually exclusive of the first, is that the large amount of unreacted Al_2Cl_6 present in the dry silica catalyst sample coordinates pyridine via a Lewis interaction and therefore increases the intensity of the 1445 cm^{-1} peak.

Solid State Magic Angle Spinning NMR. One of the most useful methods for elucidation of heterogeneous catalyst structure is solid state magic angle spinning nuclear magnetic resonance (abbreviated SS MAS NMR). The ^{27}Al SS MAS NMR spectrum (300 MHz) for $AlCl_2(SG)_n$ prepared in CCl_4 with conditioned silica is presented in Figure 2-3. The peak at 65 ppm is assigned to a Si-O-$AlCl_2$ moiety, which is consistent with the value of 62.8 ppm obtained for aluminum chlorohydrate (Cl/OH = 2.5).[95]

Figure 2-14(a) gives the spectrum for the corresponding catalyst prepared with dry silica. The spectrum for the conditioned silica catalyst is presented as figure 2-14(b) as a comparison. The conditioned silica spectrum has been sized to match the scale depicted in the figure. A peak at 0 ppm in Figure 2-14(a) indicates the presence of octahedral aluminum. A very prominent feature of this spectrum is the sharp signal at 101 ppm, which coincides with the value of 105

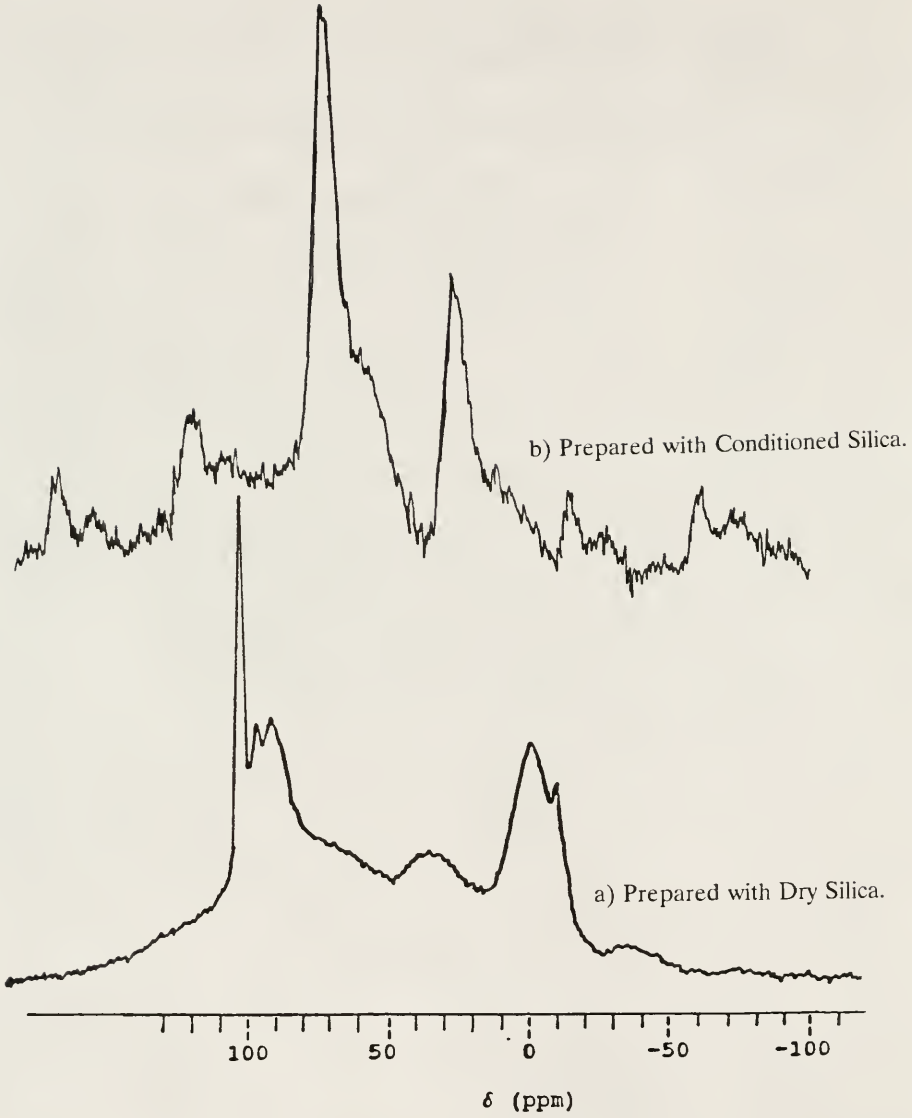

Figure 2-14. SS NMR of $AlCl_2(SG)_n$ Catalysts.
a) Prepared with Dry Silica.
b) Prepared with Conditioned Silica.

ppm reported for anhydrous Al_2Cl_6.[52] This observation along with the increased intensity for the IR band of Lewis-bound pyridine shows that a substantial amount of Al_2Cl_6 has not reacted with the support. The best evidence of unreacted Al_2Cl_6 lies in the observation of desorption of the aluminum chloride at 200 °C under flowing N_2; at least 18 % of the Al_2Cl_6 used to prepare the catalyst desorbs off at this temperature. This result is in stark contrast to that obtained with the catalyst prepared from conditioned silica which shows no desorption of Al_2Cl_6 even at 250 to 275 °C.

The lack of major features in the 40 - 80 ppm range for the dry silica catalyst in Figure 2-14(a) is also quite different than for the spectrum in Figure 2-14(b). This is an indication that the catalytic activity for hydrocarbon conversion reactions is due to the Al species appearing at 65 ppm. The broad peak at 30 ppm in Figure 2-14(a) may be due to a species similar to the one giving rise to the signal at 15 ppm in Figure 2-14(b), proposed to be octahedral aluminum with chloride and oxygen-donor ligands.

The overall result of the silica hydration studies presented here is to demonstrate that minor variations in the silica preparation can have a dramatic effect on the properties of the resulting catalyst. Based on literature studies investigating the dehydration/rehydration of silica gel, the presence of geminal silanol groups appears to be critical for obtaining complete reaction of Al_2Cl_6 with the silica surface and generating active catalytic sites. Reproducibility in catalyst preparation is obtained by optimizing the hydration of the silica support.

Sealed-system catalyst preparation

Preparation of $AlCl_2(SG)_n$ in a sealed system was performed to test the proposal that CCl_4 functions as an unreactive medium. The carcinogenic properties and toxicity of chlorinated solvents[96] provide the motivation for developing alternate methods of catalyst preparation which avoid the use of CCl_4 or other potentially hazardous chlorinated solvents. As mentioned in the background section, vapor deposition methods have been utilized [5-11] for preparation of supported aluminum chloride but presumably due to short contact times Al_2Cl_6 does not form exceptionally stable catalysts with inorganic oxides under standard vapor deposition conditions.

One variation on this vapor deposition technique has arisen which does offer some improvement. The method devised by Schmidt and co-workers[36,37] involves contacting gaseous Al_2Cl_6 with alumina for an extended time period relative to fast-flow vapor deposition techniques. The Schmidt catalyst has reported characteristics quite similar to the Drago/Getty $AlCl_2(SG)_n$ catalyst and serves as a precedent for catalyst preparation using long-term vapor deposition methods.

What appears to be a key aspect of the CCl_4 synthesis procedure is the amount of time the catalyst components are allowed to react. The sealed-system reaction was run for a minimum of 72 hours in order to be consistent with the CCl_4 synthesis. Other syntheses using shorter time periods were also performed to investigate this variable.

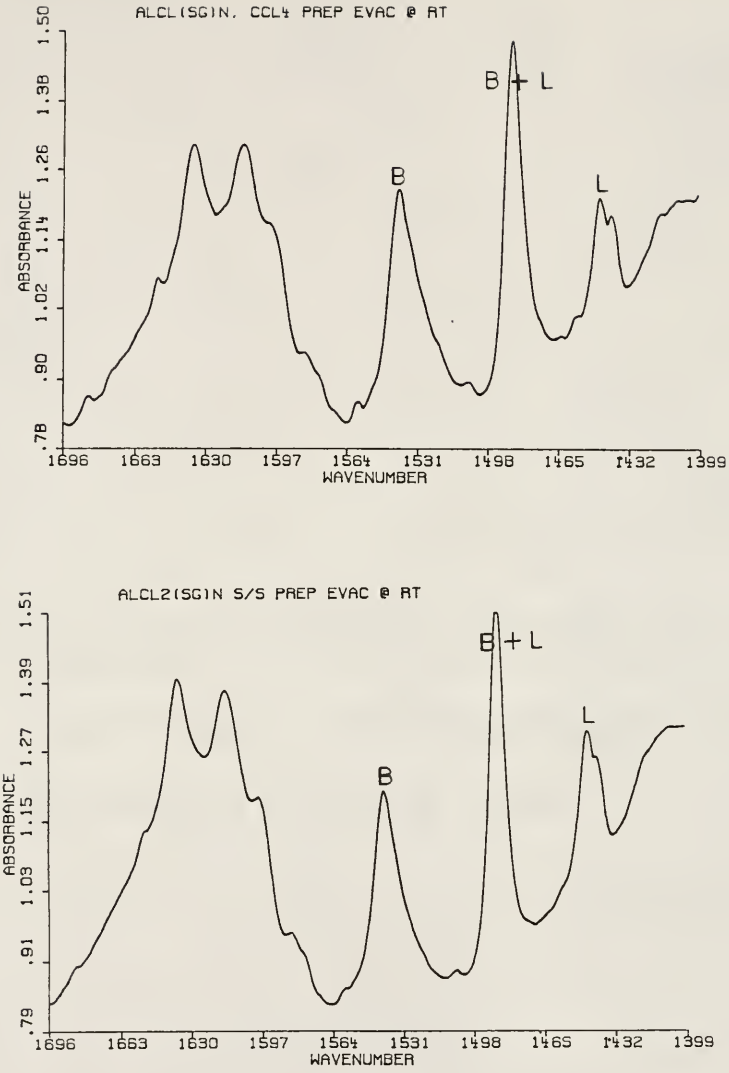

Figure 2-15. Infrared Spectra of Pyridine Adsorbed on $AlCl_2(SG)_n$ Samples Prepared in CCl_4 and in a Sealed System, 72 Hour Reaction.

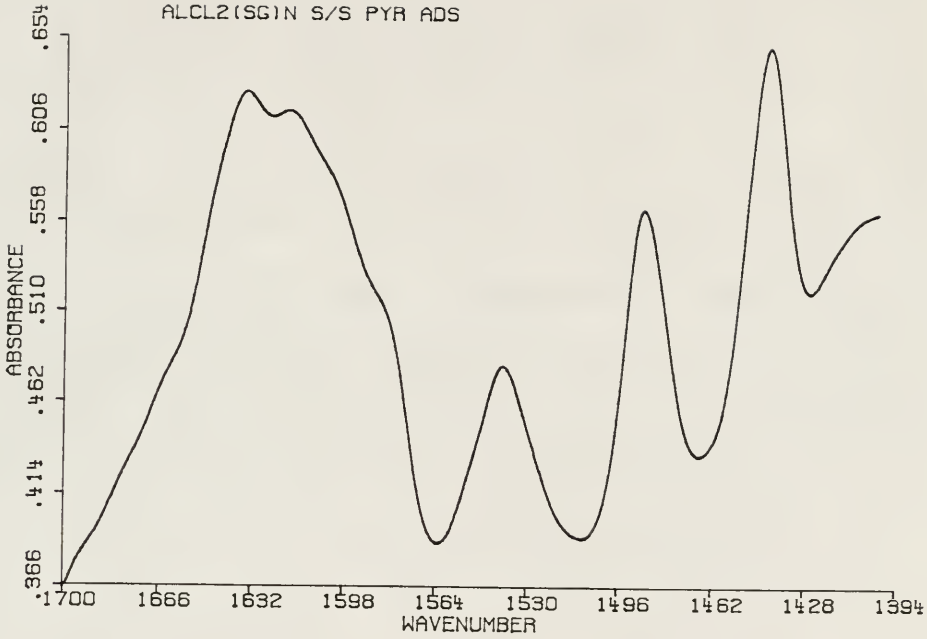

Peak List

1441.1 cm^{-1} (Lewis, H-bonding)

1485.8 cm^{-1} (Lewis & Brönsted)

1538.1 cm^{-1} (Brönsted)

Figure 2-16. Infrared Spectrum of Pyridine Adsorbed on $AlCl_2(SG)_n$ Prepared in Sealed System, 18 Hour Reaction.

Figure 2-15 shows the infrared spectrum of pyridine adsorbed on a catalyst made in CCl_4 and the catalyst made in a sealed system over 72 hours. The peak at ~ 1540 cm^{-1} is assigned to pyridinium ion produced at Brönsted acid sites, labeled (B). The peak at ~ 1445 cm^{-1} is due to Lewis-bound pyridine with some surface hydrogen-bound pyridine peak overlap. This peak is labeled (L). A band at ~ 1490 cm^{-1} exists for both Lewis and Brönsted sites (L + B), therefore it is not conclusive as a fingerprint signal. The overall pattern for the various sites is identical for the catalyst prepared in CCl_4 and in the sealed system which implies a similar distribution of acid sites for both samples. This point becomes more clear after examining Figure 2-16 which shows the IR spectrum for pyridine adsorbed on a catalyst prepared in the sealed system for only 18 hours as opposed to the normal 72 hour period. In this spectrum, there is a significantly different pattern observed, with the Lewis band more intense in relation to the Brönsted peak. This is what would be expected for a case where excess Al_2Cl_6 is present to bind the pyridine preferentially over the weaker silica Brönsted acid sites.

Establishing the strength of the Lewis acid site is also possible by IR spectroscopy. Figure 2-17 presents the spectrum of a catalyst exposed to pyridine and evacuated at 300 °C. This procedure ensures that all the pyridine is removed with the exception of the most tightly bound pyridine. The signal at 1456 cm^{-1} can be assigned to Lewis-bound pyridine. This is a shift of 18 cm^{-1} from the free pyridine stretch at 1438 cm^{-1} and is indicative of a very strong Lewis acid interaction. The shift of the Lewis band as reported for the CCl_4-prepared

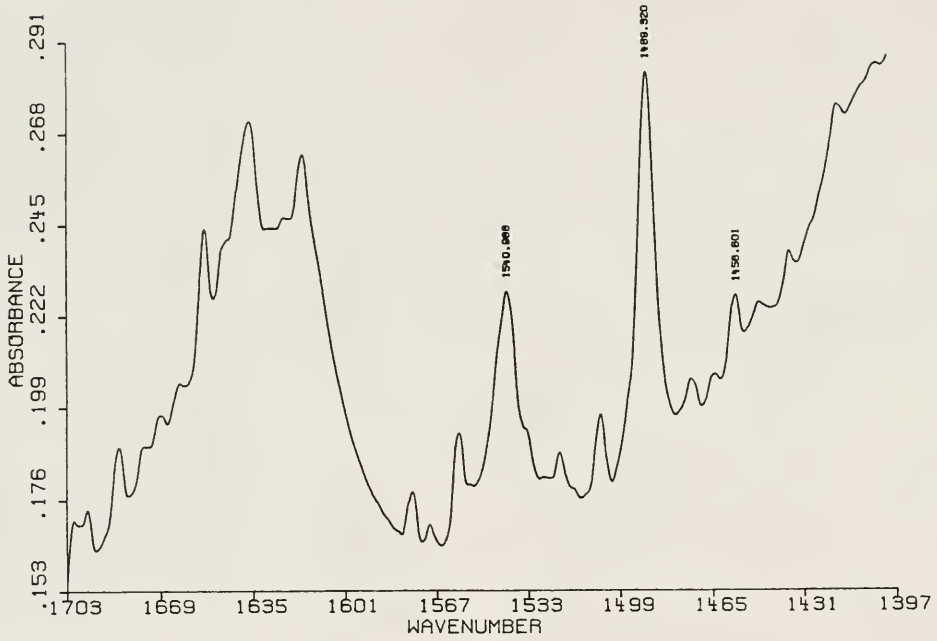

Figure 2-17. Infrared Spectrum of Pyridine Adsorbed on $AlCl_2(SG)_n$ Prepared in a Sealed System, Desorbed at 300 °C.

catalyst[4] is identical to the above result, indicating very similar acid strength for the Lewis sites on the catalysts prepared by two different techniques.

The solid state MAS NMR spectrum for $AlCl_2(SG)_n$ prepared in a sealed system is presented in Figure 2-18. Comparing this spectrum to that of the catalyst prepared in CCl_4 as shown in Figure 2-3, a number of similarities can be pointed out. The signal at 65 ppm is very strong for both samples and both samples exhibit a shoulder at 50 ppm, which could be a spinning side-band. The peaks are attributed to tetrahedral Al sites. The spectrum in Figure 2-18 also exhibits a peak at 0 ppm which can be assigned to octahedral aluminum. The signal at 20 ppm in Figure 2-18 is attributed to an octahedral Al site with both chloride and hydroxo ligands, also similar to the catalyst prepared in CCl_4.

Since the spectroscopic results showed a distinct similarity in acid site distribution, the sealed-system (s/s) catalyst was used in the cracking of n-hexadecane in a batch reaction in order to make a reactivity comparison to the CCl_4-prepared catalyst. At 100 °C under 30 psig hydrogen, 1.0 g of the s/s catalyst gave an isobutane production of 0.22 (± 0.02) moles isobutane/mole Al sites as compared to $AlCl_2(SG)_n$ prepared in CCl_4 which showed 0.24 (± 0.02) moles isobutane/mole Al sites. It is apparent that both catalysts give good activity in cracking reactions and are indistinguishable within the error limits for the experiment. It can be said at this point that the strong acid sites on the catalyst are the same or very similar in structure and reactivity when the catalyst is prepared in carbon tetrachloride or via prolonged vapor deposition. The

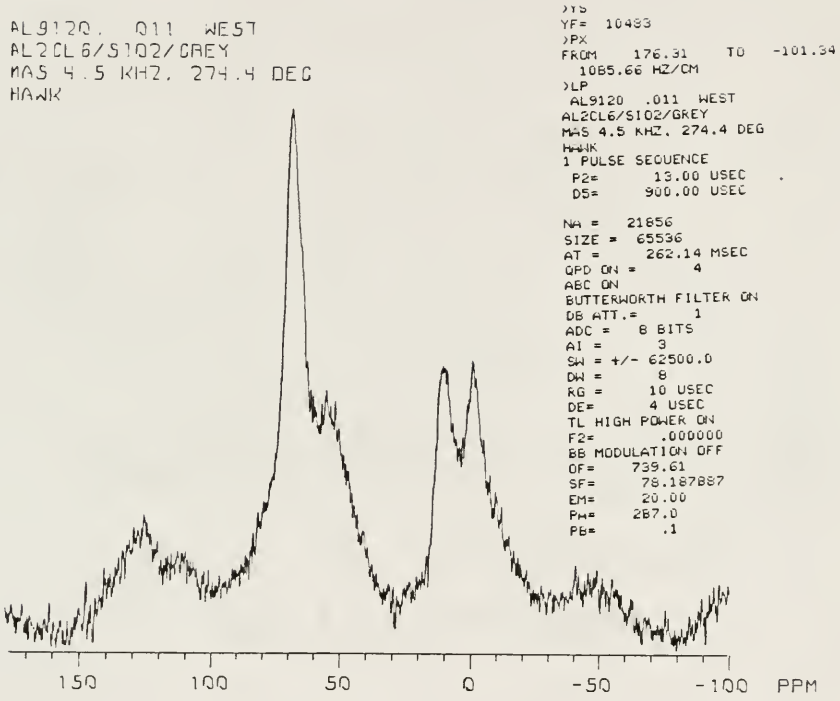

Figure 2-18. SS MAS NMR of $AlCl_2(SG)_n$ Prepared in a Sealed System.

similarity in reactivity for the two catalyst samples further supports the proposal that the NMR resonance at 65 ppm, which is common to the spectra of both samples, is the active site for catalysis.

Conclusions

The goal of the project delineated in this chapter is to examine the reactivity of $AlCl_2(SG)_n$ for various hydrocarbon conversions as well as to develop an alternative preparation for the catalyst and to determine how silica hydration affects catalyst structure and reactivity.

Reactivity Studies

Dehydrohalogenation and hydrodehalogenation of 1,2-dichloroethane was studied with various metal-promoted variations of $AlCl_2(SG)_n$. The activity of $AlCl_2(SG)_n$ was found to increase markedly with the presence of noble metal promoters but these promoted catalysts offered mixtures of hydrodehalogenated and dehydrohalogenated products with poor selectivity to the vinyl chloride target product, presumably due to the propensity of the catalysts to promote hydrodehalogenation. Trichloroethane offered better results, with 90 % conversion of the reactant with 90 + % selectivity to the dehydrohalogenated product. Comparison to a silica blank indicated that the reaction was catalytically and not thermally induced.

Alkylation of aromatic substrates with alkyl halides and olefins did not produce the expected results but offered insight into the mechanism nonetheless. In batch reactions performed in CCl_4, it was determined that alkylated products are obtained readily from 3° halides (t-BuCl, e.g.), less readily from 2° halides and not at all with 1° halides. This reflects the tendency of the catalyst to form the most stable carbonium ions from the corresponding halides. Catalyst poisoning by the aromatic reactant is proposed as a competing pathway which limits cation formation to only the more reactive alkyl halides. Olefins show no reactivity in batch reactions since prolonged contact of the olefin with the catalyst favors π-coordination of the olefin to the Lewis sites over protonation of the olefin to form the reactive carbonium ion intermediate. Acyl chlorides show the expected lack of reactivity due to the coordinative nature of the oxygen donor group which is known to deter hydrocarbon activation activity for $AlCl_2(SG)_n$.

Alkylation in a flow system at more extreme conditions shows that $AlCl_2(SG)_n$ is too vigorous, with t-BuCl reacting to give products arising from oligomerization and cracking of the alkyl halide. Evidence also shows that the alkylaromatic product can dealkylate under the experimental conditions as evidenced by reaction of cumene over $AlCl_2(SG)_n$ to give C3 products and benzene. The cumene cracking activity signifies that formation of alkylaromatic products in the flow system is unfavorable, therefore limiting the use of $AlCl_2(SG)_n$ to low-temperature batch-type reactions.

The supported aluminum chloride catalyst was found to be quite active in the isomerization of n-butane, even at room temperature, if the correct additives are used to initiate and maintain activity. Pure n-butane gave limited reactivity; addition of 4 % 1-butene to the feed resulted in a significant jump to 50 % conversion. A mechanism involving proton addition to the olefin is proposed based on this result. Addition of HCl to the flow is required to maintain activity, presumably by regenerating the Brönsted sites as they are depleted during the reaction.

The chemistry of n-hexane conversion over $AlCl_2(SG)_n$ was found to be somewhat more complex than that seen with butane due to the introduction of cracking as a competing reaction. The presence of branched C6 isomers comprised only 15 % of the products observed under conditions necessary for hexane activation in the flow system. The increased activity and longevity if $AlCl_2(SG)_n$ in the presence of olefins and HCl showed that the mechanism for hydrocarbon activation is similar to that with n-butane; the variation in product distributions results from different reactivity of the respective carbonium ion intermediates.

Polyolefin reactants were used as extended-chain analogs to simple paraffins in cracking reactions for possible application in waste polymer remediation. Poly(ethylene) in a melt state afforded similar results to hexadecane used previously in terms of the moles of isobutane produced per aluminum site on the catalyst. A highly branched polymer, poly(4-methyl-1-pentene), gave the

expected higher activity resulting from the presence of 2° and 3° carbons. Poly(styrene) and cellulose acetate were unreactive with $AlCl_2(SG)_n$ for reasons mentioned previously; namely, coordination of donor groups such as aromatic π-systems or oxygen functionalities serve to poison the acid sites on the catalyst surface. An important result for possible real-world application of polymer recycling arose from the observation that commercial polymeric materials such as rubber tire and plastic poly(ethylene) shopping bags give reasonable cracking reactivity despite the presence of stabilizers and other industrial additives.

Synthetic Studies

A prolonged vapor deposition method, where sublimed Al_2Cl_6 is contacted with silica for an extended period of time (3 to 5 days), was found to result in a catalyst with similar activity in hexadecane cracking to the catalyst synthesized in CCl_4. Infrared spectroscopy on adsorbed pyridine showed identical acid site distribution and identical acid strength for the Lewis sites as determined by the shift of 18 cm^{-1} for pyridine adsorbed on a Lewis site versus free pyridine. Solid-state NMR experiments revealed the presence of a species which has a resonance at 65 ppm in both the CCl_4-prepared catalyst version and the sealed-system catalyst version. The consistency in this signal coupled with the consistency in cracking activity strongly suggests that the species at 65 ppm is the active catalytic site; based on HCl evolution this is probably a $SiO\text{-}AlCl_2$ or $(SiO)_2AlCl$ species.

Finally, the preparation of $AlCl_2(SG)_n$ was investigated from the standpoint of silica hydration. The extent to which silica gel possesses silanol groups was found to have a significant influence on the binding of Al_2Cl_6 to the silica surface. Infrared examination of adsorbed pyridine and solid state MAS NMR indicated the presence of unreacted Al_2Cl_6 as well as drastically different acid sites present on the catalyst prepared with excessively dry silica. Comparing the activity of the catalysts prepared with conditioned and dehydrated silica it was shown that catalytic activity results only when Al_2Cl_6 is condensed with SiOH groups to form the catalytically active moieties.

CHAPTER 3
POROUS, CARBONACEOUS ADSORBENTS AS CATALYSTS AND CATALYST SUPPORTS FOR ACIDIC METAL OXIDES

Background

The application of porous, carbonaceous adsorbents to heterogeneous catalysis is an area which, although known for some time, is receiving increased attention in recent years. In the early 1970s, Trimm and Cooper[97,98] and Schmidt and Walker,[99,100] in independent studies, reported the use of platinum-modified porous carbons for olefin hydrogenation. In their investigations, shape selectivity to the linear isomer of a mixture of linear and branched hydrocarbons was observed; this was an indication of the molecular sieving capability of the carbons as analogous to that seen with zeolites. More recently, Foley[101] has studied the modification of porous carbons with inorganic oxides through a number of different preparative routes for application in catalysis. Pyrolysis (heating to 300 - 1200 °C in an inert atmosphere) of successive layers of polymer material on the surface of a metal oxide particle or pyrolysis of a physical mixture of the two components are two ways of producing a carbon surface over an oxide material. Adsorption of the oxide (or a precursor compound) on a carbon surface is a way to modify a carbon with a catalytic oxide component. The adsorption of oxides on

carbon surfaces is the preferred way to synthesize catalysts from commercially available carbon supports.

A widely used method for preparation of porous carbons, also known as carbon molecular sieves (CMS), is the pyrolysis of macroreticular (macroporous) polymers. The polymers themselves are designed to have high macropore volume to facilitate transport of adsorbates in ion-exchange applications.[102,103] During the pyrolysis procedure the polymer loses hydrogen and becomes essentially a carbon skeleton of the parent polymer, thereby retaining the macropore characteristics of the macroreticular polymer in carbon form. Figure 3-1 presents a proposed scheme for the pyrolysis of poly(styrene/divinylbenzene) which depicts the resulting carbon structure at various temperature levels. The physical strain on the polymer as it undergoes pyrolysis causes the formation of fissures in the carbon matrix. These fissures can be regarded as a separation of two graphite layers, leaving behind slit-like pores of molecular dimensions, or micropores, which impart the molecular sieving properties to the carbon.[101] Volatilization of small molecules out of the matrix is also reported to contribute to micropore formation. The end product of these processes is a highly porous carbon material with high surface area. This high surface area along with the unique pore structure and hydrophobic surface allows for exceptional adsorption of organic molecules which can be utilized as an asset in the application of porous carbons to heterogeneous catalysis.

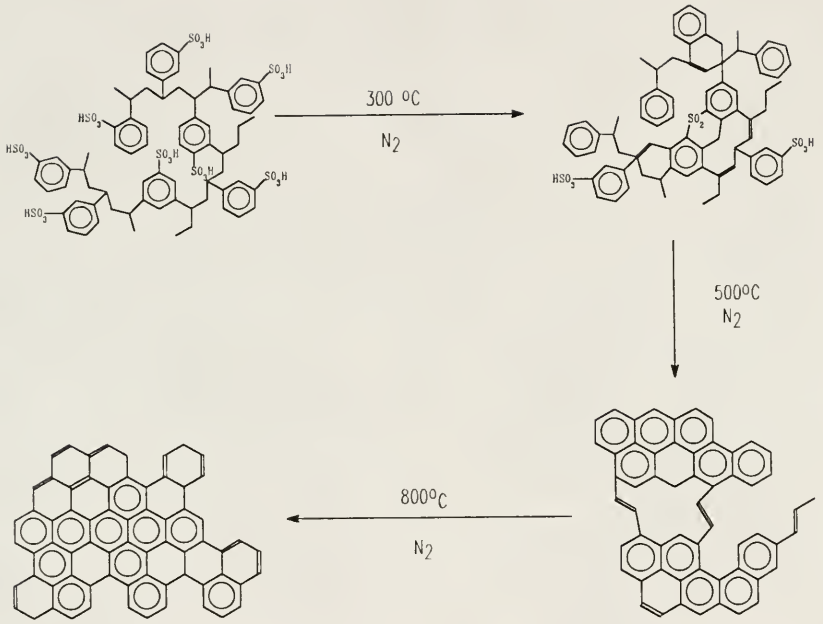

Figure 3-1. Structure of Pyrolyzed Poly(styrene/divinylbenzene) at Various Temperatures.

There have been studies done on the influence of pyrolysis temperature and duration on the pore structure of polymer-derived carbons. Lafaytis et al.[104] have determined that pyrolysis of poly(furfuryl alcohol) at 800 to 900 °C produces the maximum surface area for the final carbon and that higher temperatures can decrease the micropore volume. Furthermore, longer pyrolysis times were found to decrease the overall dimensions of the micropores, as examined by diffusion of CO_2 and n-butane into the carbon pores monitored by gas uptake. This examination demonstrates that microporous carbons can be tailored for predetermined applications so as to optimize the effectiveness of the CMS for adsorption. This tailoring of carbon pore structure has already been shown to be applicable in the development of carbon adsorbents for groundwater purification.[13]

The carbon materials which are used in the catalytic and structural examinations presented in this chapter are derived from poly(vinylaromatic) polymers. Specifically, the pyrolysis of divinylbenzene-crosslinked poly(styrene) ion-exchange resins is the synthetic procedure utilized. The ion-exchange resins possess sulfonate groups which are proposed to stabilize the polymer during pyrolysis and also result in additional micropore structure as the sulfur oxides volatilize off of the surface.[13,105,106]

The presence of slit-like pores is not unique to the divinylbenzene-based carbons used in this work. The phenomenon was first observed with pyrolyzed poly(vinylidene chloride) in 1965 where normal butane was found to adsorb

preferentially into the pores of the carbon from a mixture of normal butane and isobutane.[107] In addition to preferentially adsorbing molecules by size, polymer carbons have been demonstrated to separate molecules by polarity. In a study of adsorption capacity for water and dichloromethane, it was determined that a series of commercial carbons, Carboxen® CMS, had a greatly increased adsorption capacity for dichloromethane as compared to water.[108] The difference was attributed to the hydrophobic surface of the carbon showing preference for hydrophobic molecules. In addition, it was also observed that the extent of chemical activation of the CMS can influence the surface chemistry and hence the relative hydrophobicity of the surface by the introduction of oxygen and/or nitrogen groups. The more activated CMS samples showed a higher affinity for water adsorption. From these studies, it is apparent that polymer carbons can be used as two-function adsorbents; molecules are able to be separated based on size and on hydrophobicity so as to provide remarkable selectivity to target adsorbates. By careful choice of pyrolysis conditions to determine micropore dimensions and by chemical activation to control the surface chemistry, CMS materials are unique in their ability to be tailored for specific applications.

The actual chemical structure of surface species on activated carbons is a subject of much controversy. The transient nature of these moieties, in particular oxygen-containing species, makes identification difficult even for relatively rapid spectroscopic techniques. It should be mentioned, however, that certain chemical reactivity of substituent groups on the carbon surface has been empirically

examined and acidity was found to be a prevalent characteristic. Reaction of basic and acidic dyes was examined on various carbon samples and it was found that the basic dyes showed a much larger extent of reaction as compared to the acidic dyes.[109] The data for surface reactivity of the dyes was correlated with NaOH titration data to establish that acidic groups on the surface are indeed present and are involved in the chemistry observed with activated carbon.

Given the control that can be obtained over the structure of CMS materials, it is somewhat surprising that there is a dearth of research in the literature pertaining to utilization of polymer carbons as catalysts and catalyst supports. The capacity of carbons to function catalytically has been known only for about 15 years, as delineated in a study of ethylbenzene oxidative dehydrogenation using alumina.[110] The activity of the alumina catalyst had been found to be influenced by the coke buildup on the catalyst surface, which in itself is a direct function of the alumina acidity. Further studies of the coke activity[111] show a correlation between the paramagnetism of the coke to the catalytic activity observed. Vrieland and Menon[112] have recently presented a brief review on the role of carbon in the oxidative dehydrogenation of ethylbenzene with the ultimate conclusion that the mechanism of carbon catalysis is as yet undetermined. Literature reports continue to arise on this question, however, and there may be a better understanding of catalysis with carbon materials in the near future. For example, a recent examination of the oxydehydrogenation of ethylbenzene over alumina supports the proposition that carbon oxide species are responsible for the

activity.[113] A number of different techniques were utilized in the study, such as ammonia desorption, X-ray Photoelectron Spectroscopy, Electron Paramagnetic Resonance and Secondary Ion Mass Spectrometry. By process of elimination, the authors were able to narrow the active species down to the oxygen-containing paramagnetic quinone/hydroquinone and aroxyl/phenol groups.

In addition to examination of surface coke as a carbonaceous catalytic agent, there have been studies done on pyrolyzed polymers as active carbon catalysts. The oxidative dehydrogenation of ethylbenzene over a commercial CMS, Anderson AX21, was studied by Grunewald and Drago.[114] The high surface area CMS was determined to be one of the most active catalysts known for the oxidative conversion of ethylbenzene to styrene, with 80 % conversion of the ethylbenzene obtained at 350 °C and selectivity to styrene of 90 %. The same authors also examined the oxidation of alcohols over AX21[115] in terms of the reaction mechanism. The products obtained in the alcohol oxidations demonstrated that CMS can function via hydride abstraction arising from Lewis acidity or in hydrogen atom abstraction, presumably from paramagnetic sites. The reaction mechanism, therefore, is apparently dictated by the reactivity requirements of the particular substrate.

Grunewald and Drago have also examined the Fischer-Tropsch synthesis of hydrocarbons from hydrogen and carbon monoxide over carbon catalysts.[116] The product distribution obtained with carbon-supported ruthenium carbonyl species was found to have a significantly increased selectivity to C2 through C5

hydrocarbons, with no products higher than C5 observed. This result was attributed to the ability of the carbon to disperse metal species, thereby limiting agglomeration and formation of metal crystallites. Scanning electron microscopy supports this proposal[115,117] as no formation of metal crystallites was detected on the carbon in contrast to the analogous alumina or silica catalysts which show metal aggregation. This dispersion and anchoring of metal species can have a major influence on catalyst stability and offers another advantage for the utilization of CMS in heterogeneous catalysis.

One application of carbon-based catalysts which has been devised[117] is the catalytic combustion of halogenated organic compounds. Halogenated hydrocarbons have widespread application as solvents in the chemical industry due to their relative inertness and solvating capacity for organic compounds. Investigations regarding the toxicity and carcinogenic properties of halogenated organics have raised industry awareness on the matter of proper disposal of these hazardous materials.[118] Incineration is presently the preferred method but temperatures exceeding 1000 K are required for the process to obtain complete decomposition[119,120] and dioxin is often a byproduct. In cases of low concentration of contaminant in the gas phase, the process becomes exceedingly inefficient as the entire sample must be heated to the combustion temperature. The cost of the fuel alone can reach about 40 % of the total operating cost for a typical incinerator,[121] so development of low-temperature processes for

halogenated waste disposal can offer significant improvement over present methods.

Spivey[122] presents an exhaustive review (to 1987) of low-temperature oxidative decomposition catalysts for application in environmental remediation. The majority of the catalysts can be put into two categories: transition metal oxides (either unsupported or adsorbed onto an inorganic oxide support) and supported noble metals. The noble metal catalysts (Pd, Pt, Rh, Ru) are poor choices for oxidation of halogenated hydrocarbons because of the high expense involved and the poisoning of the catalysts by Cl_2 and HCl produced in the reaction.[123,124] A number of patents have been issued for the process of destroying halogenated hydrocarbons with metal oxide catalysts[125-137] but optimum temperatures for these systems are usually >300 °C and the halogenated hydrocarbon concentration is typically limited to less than 10,000 ppm.

The purpose of the studies performed in this chapter is to examine CMS materials as catalysts for the catalytic combustion of halogenated hydrocarbons. Examination of the reaction mechanism may provide further insight as to how CMS function as catalysts and catalyst supports.

Characterization of the carbon catalysts is necessary to understand the reactivity of the catalysts and eventually the mechanisms by which the catalysts operate. Due to certain properties inherent to the carbon material, carbon molecular sieves are difficult to characterize. Diffuse reflectance infrared fourier-transform spectroscopy (DRIFTS) and solid state ^{13}C nuclear magnetic resonance

(SS ^{13}C NMR) are two powerful tools for examining the structure of solids; however, these methods are not applicable to CMS. In the case of DRIFTS, the black CMS absorb a large amount of the infrared radiation so that the spectra of surface species is not detected. The porous nature of the carbon also may contribute to the lack of features in the infrared spectrum. In every attempt at using this technique in our laboratory, a featureless spectrum has resulted, even with such normally strong absorbing species such as metal carbonyls. The NMR results are equally useless, with the carbon support showing no discrete signals but rather a very broad signal which is useless for characterization purposes. Carbon molecular sieves are paramagnetic, which often leads to a broadened signal. Furthermore, for defined functional groups such as carbonyl or alcohol moieties varying environments may broaden the resonances.

Despite the above problems, there are a number of techniques available to investigate the carbon structure and the structures of supported metal species. An invaluable procedure for the examination of porous materials is porosimetry. An adsorptive gas, such as nitrogen, is introduced to the carbon at low pressure. The amount of gas adsorbed is then plotted as a function of the increased gas pressure to obtain an adsorption isotherm.[138] The shape of the isotherm along with the slope of the adsorption curve at various points gives information about pore structure, such as the distribution of micropores (defined as < 2 nm in diameter), mesopores (2 - 50 nm) and macropores (> 50 nm), and also the carbon surface area. A number of approximations are made in these calculations which result in

reasonable results in most cases. This technique is referred to as the BET method after Brunauer, Emmett and Teller, the inventors of the procedure. It is a characteristic of porous materials to have extremely high surface areas arising from high micropore volumes; a large pore volume for a small mass of carbon translates into high surface area. Some CMS materials, such as AX21 mentioned previously, have apparent surface areas (3400 m^2/g) greater than the theoretical limit for the unilateral surface area of a carbon monolayer of the same mass. Obviously in those examples the surface area measurement approximations are inaccurate in which case it is reasonable to set an approximate lower limit to the surface area, such as 2000 m^2/g.

A surface method which gives information about metal oxidation states is X-ray photoelectron spectroscopy (XPS), also known as electron spectroscopy for chemical analysis (ESCA). This procedure can provide information about metal species which are supported on the carbon. The technique involves bombarding a surface with x-ray radiation of a known energy and monitoring the energy of the electrons which are ejected from the surface. The difference of the incident and scattered radiation is the energy required to remove the electron from its nucleus, the binding energy, which is often a characteristic of the oxidation state for the parent atom. One of the metals which is of interest in this chapter is chromium due to its high activity in the catalytic combustion reactions. The XPS method has been used successfully for pure chromium compounds where it was found that the $2p^{3/2}$ electrons can be used to determine the chromium oxidation state; in

particular, it can distinguish Cr(VI) from Cr(III) which is of importance in examining chromium redox chemistry.[139]

Photoelectron studies of supported chromium catalysts have also shown that the support can reduce Cr(VI) to Cr(III) at elevated temperature. Chromia/alumina catalysts prepared by impregnation with $Cr(NO_3)_3$ solution and subsequently calcined at 500 °C in air were examined by XPS.[140] It was found that at loading levels of 5 weight % $Cr(NO_3)_3$ or higher there was a mixture of Cr(VI) and Cr(III) on the surface of the alumina. This mixture is also observed for a commercial copper chromite hydrogenation catalyst, consisting of predominantly Cr_2O_3, CuO and SiO_2.[141] In this study it was postulated that calcination temperature has an influence on the relative amounts of the Cr(VI) and Cr(III) species. A study of Cr(VI) oxide supported on silica[142] also presents the temperature dependence of the chromium oxidation state. A 1 % CrO_3/SiO_2 catalyst possessed only Cr(VI) at temperatures up to 500 °C whereas a 9 % catalyst sample showed 50 % Cr(III) and 50 % Cr(VI) at 350 °C, down from > 95 % Cr(VI) at 250 °C. One structure that is postulated to account for the stability of Cr(VI) at low loading levels is presented in Figure 3-2.[143] The existence of this species at low chromium surface concentrations may be an indication of the catalyst possessing isolated metal centers resulting from exceptional dispersion of the dopant. As the surface concentration increases, vicinal Cr(VI) sites can possibly interact through oxygen bridges and form a Cr_2O_3-like structure. The observation that Cr(VI) is stable on silica at 250 °C even at high loadings may be

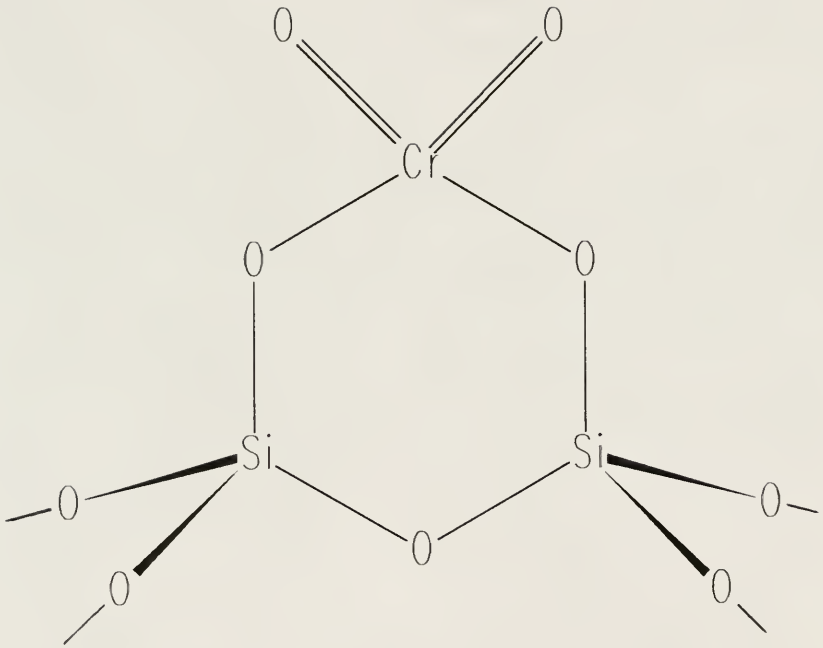

Figure 3-2. Proposed Surface Structure of Silica-supported Chromium(VI) Oxide.

an indication that neighboring chromium sites do not interact at temperatures less than 300 °C.

Magnetic susceptibility is another technique available to examine the oxidation states of supported metal species. An advantage to this procedure is that it is a bulk method; that is, it examines the entire sample as opposed to the external surface. For a porous support, this can allow for examination of metals in the interior pore structure which are inaccessible to typical surface methods like XPS. In the specific example of chromium, magnetic susceptibility has been utilized for pure compounds such as Cr_2O_3 and $CrCl_3$.[144] The chromium oxide samples were observed to exhibit different magnetic properties depending on the method of preparation, in some cases even exhibiting ferromagnetic character. The Curie law of magnetism, which accounts for spin-only forces, is an approximation of the Curie-Weiss law: $\mu_{eff} = 2.828[\chi_m(T - \Theta)]^{1/2}$ where μ_{eff} is the effective magnetic moment, χ_m is the molar magnetic susceptibility and Θ is the Curie temperature. The value for Θ is determined from temperature dependent studies so the Curie law (assume $T-\Theta \approx T$) is used as an approximation for investigations performed at a single temperature. The values of μ_{eff} determined in this way are used to calculate approximate values for n, the number of unpaired electrons per site. For similar systems, the value of n can give a relative assessment of paramagnetic character for metal species. Magnetic susceptibility determined in this way can also be used in conjunction with surface techniques like XPS to complement the conclusions made from the analysis.

One final characterization method which can find use for porous carbon catalysts is scanning electron microscopy (SEM). This procedure is essentially a qualitative technique which is useful for examining large surface structures like metal clusters. This technique has been used successfully for observing the sintering (agglomeration) of metal species on inorganic oxide supports.[145-148] As a visual method it can be utilized to determine if large metal particles are forming on the surface of the carbon catalysts, either before catalysis at elevated temperature or after. As mentioned previously, porous carbon catalysts have been found to possess high metal dispersion and this effect has been observed by SEM.[115]

Experimental

Reagents. A number of porous carbon adsorbents are utilized in this study and their relevant structural properties are listed in Table 3-1. Ambersorb® adsorbents were donated by Rohm and Haas Company. The materials (denoted as A®563 and A®572) are prepared by the pyrolysis of sulfonated ion-exchange resins[13] and have very reproducible surface areas and pore volumes. The sample ER42-30 (also obtained from Rohm and Haas) is a noncommercial, experimental carbon designed to possess the pore characteristics shown in Table 3-1. The Kureha carbon sample is obtained from Kureha Chemical Industry Company, Ltd. through Rohm and Haas. All of the polymer-derived carbons mentioned here are produced in bead form as opposed to powder form for easier handling and

Table 3-1. Structural Parameters of Carbonaceous Adsorbents.

CARBON SAMPLE	SURFACE AREA (m^2/g)	MICRO-PORE VOL. (ml/g)	MESO-PORE VOL. (ml/g)	MACRO-PORE VOL. (ml/g)	CONV'N (%)
A® 563	680	0.32	0.25	0.24	55
A® 572	1200	0.49	0.26	0.41	78
ER42-30	1200	0.45	0.12		73
KUREHA	1000	0.53	0.02	0.02	94
AX21	2000 +	1.7	0.70		23

[a] Proprietary carbon (polymer-based)

[b] Organic-based carbon

increased stability. An ultra-high surface area powdered carbon, termed AX21, was obtained from Anderson Development Company. This support is produced by the reaction of petroleum coke with KOH and subsequent pyrolysis. Washing the salt out of the carbon matrix after pyrolysis gives pores of molecular dimensions; the high surface area of AX21 is attributed to these micropores.[149] AX21 was dried at 100 °C under vacuum before use. The zeolite sample is LZ-Y52 donated by Union Carbide and was dried in vacuo at 100 °C for 12 hours prior to use. The silica support, Davison grade 62, was donated by W. R. Grace Co. and has a surface area of 340 m^2/g. Activation of the silica was achieved by washing with 1 M HCl (aq.), rinsing with water and drying in vacuo at 80 °C for 72 hours.

The chlorinated reactants were purchased from Aldrich Chemical Company. Methylene chloride and carbon tetrachloride were distilled over P_2O_5 prior to use. All other halogenated hydrocarbons were used as received. The metal salts were all purchased from Aldrich and used without further treatment unless otherwise specified. Air, hydrogen, helium, argon and nitrogen were supplied by Liquid Air Company. 1-Butene (C.P. grade) was purchased from Matheson. All gases were used without further purification.

Instrumentation. Reaction products were analyzed on a Varian 3700 gas chromatograph equipped with a 3 m x 1/8" stainless steel Porapak Q (100/120 mesh) column and a thermal conductivity detector. Light gases (CO_2, CO, N_2, O_2, H_2O) were analyzed on a 15' x 1/8" Carboxen® 1000 (60/80 mesh) column on

the same detector. GCMS was accomplished on a Varian 3400 GC linked to a Finnegan 700 ion-trap mass spectrometer. Magnetic susceptibility was performed on a Johnson-Matthey JME balance. The porosimetry method used was single-point BET and was performed at Rohm and Haas on a Micromeritics ASAP 2400 porosimeter. X-ray photoelectron spectroscopy was preformed on a Kratos XSAM-800 spectrometer using a Mg Kα radiation (nonmonochromatic) operating at 15 kV and 12 mA, with the sample at 5 x 10^{-9} torr. Acknowledgement goes to Dr. Vaneica Young of the University of Florida for running the XPS experiments. Scanning electron microscopy was performed on a Jeol JSM 35C electron microscope using an electron acceleration voltage of 15 kV. The micrographs were taken at 6000 X and 30,000 X. The author acknowledges Mr. Richard Crockett of Major Analytical Instrumentation Center at the University of Florida for performing the microscopy.

Reactor. A packed-bed flow reactor was used for all catalytic experiments. Figure 2-6 shows a schematic representation of this apparatus. The reaction tube is heated by either a commercially available Thermolyne Briskheat flexible electric heat tape or a resistance oven consisting of nichrome wire wrapped around a 4" pyrex tube with quartz wool packing material for even heating. The heating element is controlled by a digital temperature controller model CN-2041 (Omega Engineering) equipped with a J-type thermocouple. In all cases temperature varied only ± 2 °C once equilibrated. A 2.0 g sample of catalyst (48 mm bed height) is the typical amount utilized in the catalytic experiments and this sample

is covered with a 6-inch length of glass beads for mixing and heating the reactants prior to catalyst contact. A model FL-320 rotameter (Omega Engineering) is used to obtain flow control of gas feeds from 0.2 ml/min up to 50 ml/min. A soap bubble meter in the post-catalyst zone is used to determine overall flow rates of the gases. The halogenated reactants are delivered either by vaporization from a reservoir to the air stream which flows over the catalyst bed or by pumping a liquid feed to the top of the heated zone by a custom-built motorized syringe pump. The vapor pressure of the hydrocarbon and the temperature of the reservoir sets the concentration in the air stream for the reservoir delivery method; the constant delivery volume per time sets the concentration for the syringe method. The typical hydrocarbon concentration is 60,000 ppm for optimum decomposition efficiency at 1.0 ml/min air flow. The liquid volume feed rate for the halogenated reactants are 0.01 - 0.05 ml/hr for the reservoir method and 0.05 - 0.10 ml/hr for the syringe pump method. Gas samples taken before and after the catalyst bed are compared to determine conversions. A halogen mass balance is performed by reacting the HX gas in an aqueous NaOH bubbler placed at the reactor outlet and back-titrating to quantify the HX produced. The mass of the catalyst is checked after most reactions to determine if loss of carbon occurs; for all experiments at 250 °C there is no degradation of the catalyst, even after 150 hours of reaction.

Catalyst preparation. All catalysts are prepared by a pore-filling method (incipient wetness) whereby only enough solvent is used to fill the void space of

the carbon; this procedure ensures intimate contact of the dopant solution with the interior support surface. CrO_3, $TiCl_4$, $KMnO_4$, $Ce(NO_3)_3$, $SbCl_5$, NH_4VO_3, H_2SO_4, $Co(NO_3)_2$ and $FeCl_3$ are the soluble precursor species utilized in the catalyst preparations. In all cases water is the solvent with the exception of $TiCl_4$ which utilizes a 1M solution in CH_2Cl_2. Once impregnated, the catalysts are converted to the hydrated oxide forms in a number of different ways. $TiCl_4$ is hydrolyzed in moist air whereas iron and antimony chlorides are treated with base to obtain the oxides. In all other cases, heating of the impregnated support to the reaction temperature of 250 °C is the only step required for oxide formation. The catalysts are all 14 % metal oxide by mass unless otherwise noted.

Results and Discussion

Catalytic Combustion Reactivity Studies

Initial investigations into the catalytic combustion of halogenated hydrocarbons used methylene chloride, due to its high vapor pressure and the simple stoichiometry:

$$CH_2Cl_2 + O_2 \text{ ----> } CO_2 + 2\ HCl \qquad (3\text{-}1)$$

Carbon monoxide is also present in the product stream, indicating that the reaction is not as simple as presented above; however, the chloride balance is the same for reactions producing CO or CO_2. The activities of the metal

oxide/carbon adsorbent catalysts for the above reaction at 250 °C are presented in Table 3-2. An interesting observation can be made concerning the blank reactions with the untreated A®572 and A®563 supports. Unexpectedly, substantial oxidation of CH_2Cl_2 was observed for the undoped carbons. This ability of carbon to function as a catalyst without a metal dopant, albeit unanticipated, is a documented phenomenon. Detailed studies of oxidative dehydrogenation reactions over acid catalysts have shown[110,111,150,151] that coke formed from the hydrocarbon reactant at the acid sites is actually the active species in the reaction, with oxygen-containing carbon species playing an important role for the redox chemistry observed.[113]

Four of the supported metal oxide catalysts in Table 3-2 stand out as being superior to the others. CrO_3/563, CrO_3/572, $KMnO_4/Ce(NO_3)_3$/572 and TiO_2/572 all show conversions higher than 90 % and in the case of the chromium catalysts the conversion is essentially 100 %. Alumina-supported Cr_2O_3 is known to be effective in the catalytic decomposition of methylene chloride[121] and chloroform[152] at temperatures of 350 °C to 550 °C. A rapid drop in activity of this catalyst was accounted for by loss of the metal as volatile CrO_2Cl_2. It should be mentioned that no volatilization of the metal species is seen with the Ambersorb catalysts even after 150 hours of reaction. This observation demonstrates the unique ability of the carbon adsorbents to form exceptionally stable metal/support interactions, a topic which will be discussed in more detail in the characterization section. A blank experiment was performed with CrO_3 on

Table 3-2. Activity of Various Metal Oxide/Porous Carbon Catalysts in the Catalytic Combustion of Methylene Chloride.

CATALYST	CONVERSION (%)
CrO_3/563	99.9 (± 0.1)
CrO_3/572	99.9 (± 0.1)
TiO_2/572	93 (± 1)
$KMnO_4$/$Ce(NO_3)_3$/572	95 (± 1)
Sb_2O_5/572[a]	52 (± 3)
V_2O_5/572	82 (± 3)
H_2SO_4/572	83 (± 3)
Cobalt Oxide/572	75 (± 4)
Iron Oxide/572[a]	65 (± 4)
572	78 (± 3)
563	69 (± 3)
563, CrO_3[b]	48 (± 3)

[a] Metal chloride-doped carbon support treated with base to obtain hydrated metal oxide species.

[b] A layer of 563 over a layer of CrO_3, separated by a plug of glass wool.

Conditions:

250 °C, 1 ml/min air flow, 2.0 g catalyst, $[CH_2Cl_2]$ = 60,000 ppm, 72 hour reaction time.

Conversions based on GC analysis and HCl product quantification.

silica (prepared in the same fashion as the Ambersorb catalysts) in the methylene chloride decomposition at 250 °C and showed initially 90 % conversion of the substrate with a gradual drop over time to 25 % after 24 hours. Concurrent with this activity loss was the appearance of a residue on the walls of the reactor in the post-catalyst zone which appeared to be a mixture of red CrO_2Cl_2 and an unidentified green Cr(III) material.

The iron and antimony oxides supported on carbon gave conversions which were lower than for the support itself. The common aspect of the two catalysts is treatment of the chloride precursor with base to obtain the hydrated oxide form of the metal. These results indicate a dependence of the catalytic combustion reaction on acidity as has been noted for the decomposition of 1,2-dichloroethane over TiO_2/SiO_2.[153] To further investigate the importance of acid centers, samples of a blank support, A®563, were treated with base to determine the effect on the activity. The results of the experiments are presented in Table 3-3. The addition of ammonia to the carbon catalyst resulted in a slight drop in activity of about 10 - 15 %, which is measurable but not totally conclusive. Addition of sodium hydroxide to the carbon, however, produced an even larger drop in activity of ~30 to 40 % which is strong evidence that base directly influences the catalytic activity of the unmetallated carbon catalysts in the deep oxidation reaction.

The catalytic cycle of the oxidative combustion reaction requires that oxygen be able to regenerate reduced surface species back to the active oxidized state. The effectiveness of the oxygen regeneration step is an indicator of the

Table 3-3. Activity of Base-Treated Carbon Adsorbents for the Catalytic Combustion of Methylene Chloride.

BASE	AMOUNT ADDED	CONVERSION
none	---	69 % (± 3)
NH_3	8.29×10^{-2} moles	52 % (± 4)
KOH	8.82×10^{-3} moles	32 % (± 4)

projected lifetime of the catalyst as it is subjected to repeated oxidation/reduction cycles. Figure 3-3 presents the results of a deep oxidation experiment using $563/CrO_3$ where air and nitrogen were alternated through the reactor. The initial air stage showed a high activity but upon changing to N_2 a gradual loss of activity ensued. Upon reintroducing air to the system the activity resumed at a level virtually identical to the first stage. These results are consistent with a mechanism whereby the catalyst is reduced by the organic reactant and oxygen completes the catalytic cycle by re-oxidizing the catalyst to the active state. The observation that the catalyst continues to operate even 8 hours after air is removed from the system shows that there is a significant concentration of catalytically active sites on the surface which are used effectively in the reaction. At the end of the N_2 stage the catalyst is in a reduced state but it resumes full activity almost immediately upon contact with air; this result demonstrates the effectiveness of the catalyst regeneration step. The capacity of the Ambersorb catalysts to rapidly obtain their original activity after complete reduction illustrates their potential for long lifetimes in industrial applications.

Pore structure of the carbons is the determining factor in adsorption efficiency[13] and therefore has a significant impact on the catalytic efficiency of the low-temperature combustion process. Table 3-1 lists the pore volumes and surface areas for various carbon samples and also their respective activities in the decomposition of methylene chloride. Similar conversions are obtained with Ambersorb 572 and ER42-30, a non-commercial polymer-based carbon adsorbent

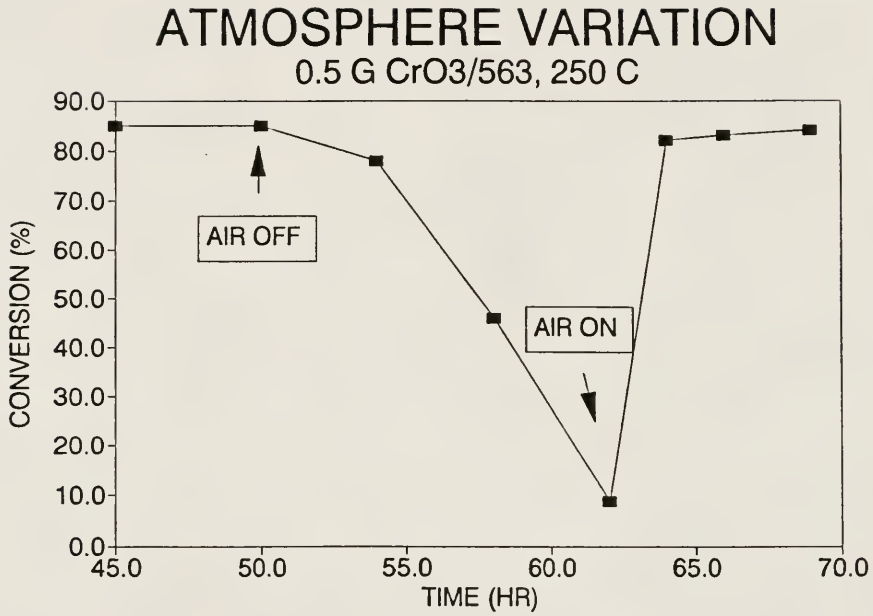

Figure 3-3. Influence of Air on the Catalytic Activity of CrO_3/563 in CH_2Cl_2 Deep Oxidation.

provided by Rohm and Haas. The structural character of the two samples is similar with the exception of different macro- and mesopore dimensions. The observed similarity in reactivity implies that the larger pores do not contribute to the kinetics of reaction. The trend is observed in the other carbons as well, with 563 showing less reactivity due to less micropore volume and finally the all-micropore Kureha sample giving very high conversion. A recent study on carbon-supported molybdenum catalysts[154] noted that surface area, which is often quoted to be a decisive factor in the activity of inorganic oxide catalysts, does not necessarily play an important role for carbon catalysts. AX21 is listed in Table 3-1 as a carbon which gives very low activity in this reaction despite the extremely high surface area. The difference in activity between AX21 and the other carbons can be accounted for by the fact that AX21 is derived from petroleum coke and would be expected to have vastly different pore characteristics and surface chemistry than the polymer-derived carbons. In particular, the slit-shaped pores which are inherent in the polymer-derived carbons would not be expected to be present in AX21 because the majority of the micropore volume for AX21 is generated by removal of KOH, which generates cage-like pores. In addition, the KOH used in AX21 activation can impart basic character to the carbon which destroys deep oxidation activity. It can also be postulated that a minimum percent of the total pore volume is required to be meso- or macroporous for efficient adsorption kinetics to occur and AX21 does not possess an appropriate amount of these larger pores. The observation that Kureha carbon is extremely active in the

catalytic combustion reaction despite its very low meso- and macropore volume, however, argues against this supposition.

Kinetic Experiments

Data for the methylene chloride reaction at 250 °C were fit to a plug-flow model[155] for a first order or pseudo-first order reaction in CH_2Cl_2. An assumption is made in this model that the oxygen concentration is large enough to remain essentially unchanged through the course of the reaction, thereby allowing for determination of the rate constants with respect to methylene chloride concentration. The results are presented in Table 3-4. The rate constants obtained are quite consistent throughout the range, with an exception of the value of 3.46 E-3 for a flow rate of 1 ml/min. A slow air flow allows a significant amount of methylene chloride to build up over the reservoir which effectively decreases the O_2 to CH_2Cl_2 ratio. At 1 ml/minute the molar ratio of oxygen to methylene chloride is calculated to be 2.3. The ratio appears to be low enough that oxygen is not in large excess throughout the reactor and thus oxygen enters into the rate equation, altering the rate constant value. This observation is in contrast to the study done by Weldon and Senkan[152] where it was determined that the catalytic oxidation of chloroform using Cr_2O_3/Al_2O_3 was zero order in oxygen. The comparison implies that adsorption of oxygen onto the carbon is an integral part of the mechanism whereas non-porous inorganic oxides are less able to achieve oxygen adsorption.

Table 3-4. Values of the Rate Constant for the Catalytic Combustion of Methylene Chloride at Various Flow Rates.

FLOW RATE (ml/min)	RESIDENCE TIME (s)	k (s^{-1})
1.0	234	3.46×10^{-3}
2.0	117	5.71×10^{-3}
3.0	78.0	4.84×10^{-3}
4.0	58.5	5.33×10^{-3}
5.0	46.8	5.40×10^{-3}
6.0	39.0	4.84×10^{-3}
10.0	23.4	5.46×10^{-3}

[a] Conditions: 250 °C, 2.0 g A®563

An Arrhenius plot for the temperature range of 250 °C to 375 °C is shown in Figure 3-4 for a flow rate of 3 ml/min. Variation of the rate constant with temperature reveals information about the activation energy of the reaction. The best-fit line for the points is given as: $\ln k = (-E_a/RT)(1/T) + \ln A$. The activation energy (E_a) derived from a least squares treatment on this plot is 11.0 kcal/mol, which is comparable to that observed for the same reaction over cerium and chromium oxides supported on zeolites.[156] In that study, the oxygen pickup and acidity were correlated to the activity and a dual-site mechanism for oxygen adsorption and hydrocarbon adsorption was proposed. Brönsted acid sites were indicated as the sites where methylene chloride is adsorbed and the cationic metal sites as the place where oxygen is adsorbed. However, empirical evidence to support this mechanism was not provided. Furthermore, inconsistent observations, such as oxygen uptake with a non-metallated zeolite, discredit the proposed mechanism. It is interesting to note that oxygen adsorption on zeolites was proposed to occur at the cationic metal sites whereas the carbon catalysts utilized here do not appear to require a metal for efficient oxygen adsorption.

Isotope effects were examined in the methylene chloride reaction by the utilization of CD_2Cl_2 as the reactant. Conditions for comparing the deuterated to the undeuterated reactant were kept as similar as possible by using the same catalyst sample (Ambersorb® 563) and the same flow rates. A smaller bed height was employed than for the reactions presented in Table 3-2. The deuterated reactant gave 35 % (± 2) as compared to 49 % (± 2) for CH_2Cl_2. This effect,

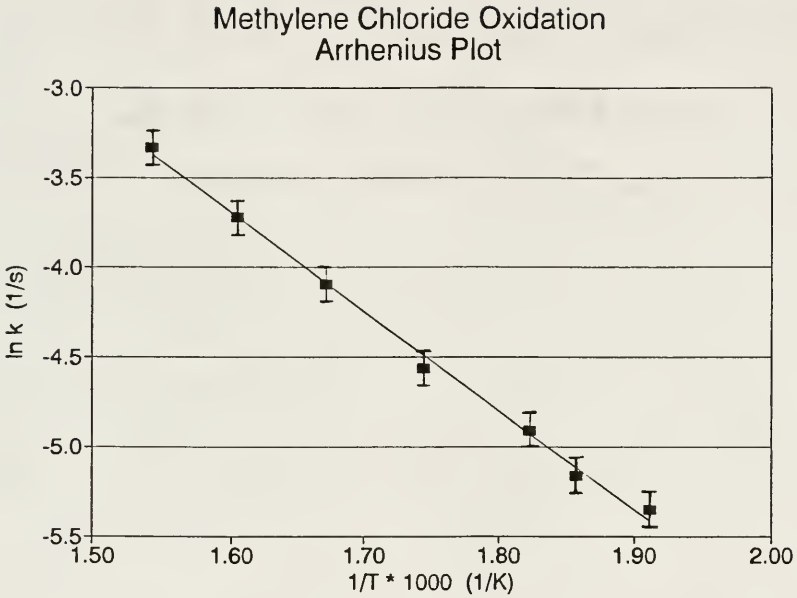

Figure 3-4. Arrhenius Plot for CH_2Cl_2 Deep Oxidation with Ambersorb® 563.

k_H/k_D = 1.4, implies that C-H bond cleavage is involved in the rate determining step but secondary isotope effects cannot be excluded based solely on this result. The reported ability of carbon materials to function as both hydride and hydrogen atom abstractors[157,158] and investigations of alcohol reactivity in terms of C-H bond cleavage[115] over carbon catalysts offers precedence for this type of reactivity.

In addition to methylene chloride, a number of other halogenated reactants were employed in the catalytic combustion reaction and the results are presented in Table 3-5. The carbon catalyst utilized for these reactions is CrO_3/563. The flow rates and reactant feed rates are presented in order to make comparisons with regard to catalyst reactivity for different substrates. 1,2,4-trichlorobenzene was utilized as a model for polychlorinated biphenyls (PCBs) and it is observed that the reactivity is comparable to that seen for methylene chloride at a similar feed rate, given in entry two of the table. Since there was no attempt to optimize the feed rate for trichlorobenzene, it is expected that complete decomposition can be achieved at slower feeds. The example with 1,1,2,2-tetrachloroethane shows that a substrate with excess chlorine relative to hydrogen can be decomposed if an external hydrogen source is provided. In this instance the amount of water in the reaction was not varied, so again better conversions are anticipated once the reaction is optimized. Methylene bromide serves to show that chlorinated organics are not exclusive to this reaction; it should be mentioned that the halogen balance was off by ca. 50 % which indicates that only half of the Br present in the

Table 3-5. Reactivity of CrO_3/563 in the Catalytic Combustion of Halogenated Organics.

SUBSTRATE	FLOW RATE (ml/min)	FEED RATE (ml/hr)	CONV'N (%)
Methylene Chloride	1.0	0.010	99.9 +
Methylene Chloride	5.0	0.050	32
1,2,4-Trichlorobenzene	6.0	0.060	19
Tetrachloro-ethylene[a]	1.0	0.050	16
1,1,2,2-Tetra-chloroethane[a]	1.0	0.010	63
Methylene Bromide	1.0	0.005	93

[a] H_2O added as proton source

CONDITIONS: 2.0 g CrO_3/563, 250 ^oC, 1 atm.

reactant was converted to HBr. The other product(s) of the reaction have not been identified but could include volatile organic bromides.

Experiments done with 1,2-dichloroethane (DCE) are interesting from the standpoint of the influence of water on catalyst reactivity; results are given in Table 3-6. For the DCE reaction, water is expected to be a product according to the following stoichiometry:

$$Cl\text{-}CH_2\text{-}CH_2\text{-}Cl + 5/2\ O_2 \text{ ---> } 2\ HCl + 2\ CO_2 + H_2O \qquad (3\text{-}2)$$

Reactivity of DCE under standard reaction conditions with TiO_2/572 is impressive with 99.7 % conversion. Upon addition of water to the reaction at a feed rate about 10 times that of DCE, the activity is still high at 94 % conversion. With the unmodified support, the conversion with water and without water is identical at 97 % (± 2) within the error limits. These results are in stark contrast to literature reports for the reaction catalyzed by zeolites[156] where a drop of between 10 and 60 % was observed with water addition. Indeed, use of LZ-Y52 zeolite in our system showed a significant water sensitivity as seen in Table 3-6. These observations with the carbon catalysts show that the reaction is not equilibrium controlled because addition of a product (H_2O) does not decrease the reactivity. It can also be said that competitive adsorption of water, which is known to occur with aluminosilicates, is not a major factor on these carbon surfaces and the

Table 3-6. Influence of Water on 1,2-Dichloroethane Reactivity Over Carbon and Zeolite Catalysts.

CATALYST	WATER FEED RATE (ml/hr)	CONVERSION (%)
TiO_2/572	0.0	99.7
TiO_2/572	0.12	94
572	0.0	97
572	0.12	97
LZ-Y52	0.0	23
LZ-Y52	0.12	4

hydrophobic nature may even deter water adsorption at metal sites as seen in the comparatively small activity drop with the titanium oxide catalyst.

Carbon tetrachloride is a model compound for the general category of fully chlorinated, non-olefinic hydrocarbons. The reactivity of CCl_4 in the catalytic combustion system was investigated in order to determine the importance of C - Cl bond cleavage in the reaction as compared to cleavage of C - H bonds. Table 3-7 presents the bond enthalpies for a number of C - H and C - Cl bonds in chlorinated methane derivatives.[159] The energies for C - Cl bonds are on the order of 20 kcal/mol lower than the C - H energies, which indicates the thermodynamic favorability of C - Cl bond cleavage over C - H bond cleavage. Table 3-8 shows the results of the catalytic combustion of carbon tetrachloride using Ambersorb® 563 (undoped). An interesting thing to notice is the conversion after five hours of 73 %. Comparing this result to the methylene chloride conversion of 55 % under identical conditions indicates that cleavage of C - Cl bonds is facile over CMS and follows the trend of bond enthalpies. The decline of activity after 120 hours shows that a reactant is being depleted; in this case it is most likely the hydrogen necessary to form the HCl product. Addition of water at 0.06 ml/hr increases conversion from 5 % to 15 %. At 0.60 ml/hr the conversion rises to 47 %, indicating that water can provide the hydrogen needed for product formation. It should be apparent from the excessive amount of water used relative to carbon tetrachloride that water is not used efficiently in this reaction, probably because the carbon is hydrophobic.

Table 3-7. Bond Energies for Chlorinated Methane Compounds.

C-X Bond	$\Delta H°_{C-X}$ (kcal/mol)
Cl_2HC-H	99 (± 1)
ClH_2C-H	100 (± 1)
Cl_3C-H	96 (± 1)
H_3C-Cl	84 (± 1)
H_2ClC-Cl	79 (± 1)
HCl_2C-Cl	77 (± 1)
Cl_3C-Cl	71 (± 1)

Table 3-8. Deep Oxidation of CCl_4 Over Ambersorb® 563.

Time (hr)	Conversion (%)	Water Feed (ml/hr)
5	73	0
48	47	0
120	5	0
140	15	0.06[a]
170	47	0.60[b]

[a] 3.33×10^{-3} moles/hr

[b] 3.33×10^{-2} moles/hr

Conditions:

250 °C

1.44×10^{-4} moles/hr CCl_4 feed

2.0 g Ambersorb 563

In order to support the proposal that hydrogen is being depleted from the carbon surface, elemental analysis of Ambersorb® 563 was performed on a fresh sample and the sample removed from the carbon tetrachloride reaction; the results are given in Table 3-9. The excess carbon tetrachloride present after reaction was purged from the catalyst by passing 0.60 ml/hr of water in air over the catalyst at 250 °C followed by flushing the reactor with pure air for 18 hours. Error limits shown are based on duplicate analyses. The observation that the carbon to hydrogen ratio increases after reaction supports the contention that surface hydrogen is being depleted by the hydrogen-deficient reagent. Another interesting result is the large drop in percent carbon after reaction. Obviously an additional element must be present in this sample to account for the missing 26 percent, and chlorine is the most likely candidate. Oxygen could account for the missing mass but it is unlikely that a large amount of oxygen functionality would be imparted to the carbon surface without a concurrent CO or CO_2 generation, which is not observed. This observation suggests that the carbon is being chlorinated by CCl_4 or by Cl_2 formed as an intermediate in the deep oxidation reaction. Chlorination of carbon adsorbents by elemental chlorine is known to occur readily under mild conditions[13] and would readily explain the missing 26 % percent for the after-reaction sample.

With the exception of the activation energy studies, all of the reactions mentioned thus far in this chapter are performed at 250 °C. This temperature is apparently the optimum temperature for the system; increasing the temperature to

Table 3-9. Elemental Analysis of Ambersorb® 563 Before and After CCl_4 Deep Oxidation.

	Before Reaction	After Reaction
% C	86.5 (± 1.0)	63.2 (± 1.0)
% H	1.9 (± 0.1)	1.0 (± 0.2)
% N	0.0	0.0
C/H	45.5	63.2

300 or 350 °C results in oxidation of carbon from the support and decreasing the temperature results in irreversible adsorption, or condensation, of the organic into the carbon pores causing the reaction to stop because of oxygen deficiency at the active sites. The critical temperature for methylene chloride is 237 °C, consequently at temperatures lower than that the gas can condense into the pores of the carbon. It is desirable, however, to attain lower temperatures in this reaction in order to apply the technology to existing adsorbent regeneration methods which operate at 140 to 170 °C.[13] The carbon adsorbents, once they are utilized commercially in wastewater extraction, are regenerated with superheated steam to remove the organic contaminant. Catalytic combustion operating at these lower temperatures would provide a way by which the organic would be removed and destroyed simultaneously. Because water acts as a regeneration agent by desorbing the organic from the carbon, the catalytic combustion experiment was performed at lower temperature in the presence of water vapor to inhibit the irreversible adsorption of the reactant and thereby extend catalyst activity to lower temperature. The results of this experiment are presented in Figure 3-5. The catalyst used in this experiment is Ambersorb® 563 and the water is introduced by saturating the air stream in a water bubbler before contacting the reactor. In a typical experiment without water there is a threshold point at 215 °C where irreversible adsorption of the organic material results in a sudden drop in activity to 0 %. Upon heating to 225 °C or higher a large plug of methylene

chloride is expelled from the catalyst which shows the concentrating effect of the carbon pores at low temperature.

Figure 3-5, with a water-saturated air flow, shows a fairly smooth decline in activity down to 150 °C where 15 % conversion is still maintained. The apparent increase in conversion at 140 °C is misleading; the post-catalyst concentration of methylene chloride was observed to drop at this point which gives the false impression of increased activity when the actual cause is the irreversible adsorption as mentioned above. Water is apparently ineffective at preventing irreversible adsorption of methylene chloride at temperatures lower than 150 °C which possibly accounts for the fact that commercial regeneration of the adsorbents is done at temperatures higher than 140 °C.

Oxidative Dehydrogenation of 1-Butene

As mentioned in the background section of this chapter, the first major application for carbon materials as catalysts in their own right was the oxidative dehydrogenation of ethylbenzene to styrene. This reaction has major importance based on the need for styrene as a polymer precursor. Another significant polymer precursor is 1,4-butadiene. Butadiene, in an analogous manner to styrene, can be prepared by the oxidative dehydrogenation of 1-butene. The reaction involves the reaction of two moles of butene with one mole of O_2 to form two moles of butadiene and two moles of water. Literature reports concerning this reaction involve the use of metal salts or inorganic oxides as catalysts.

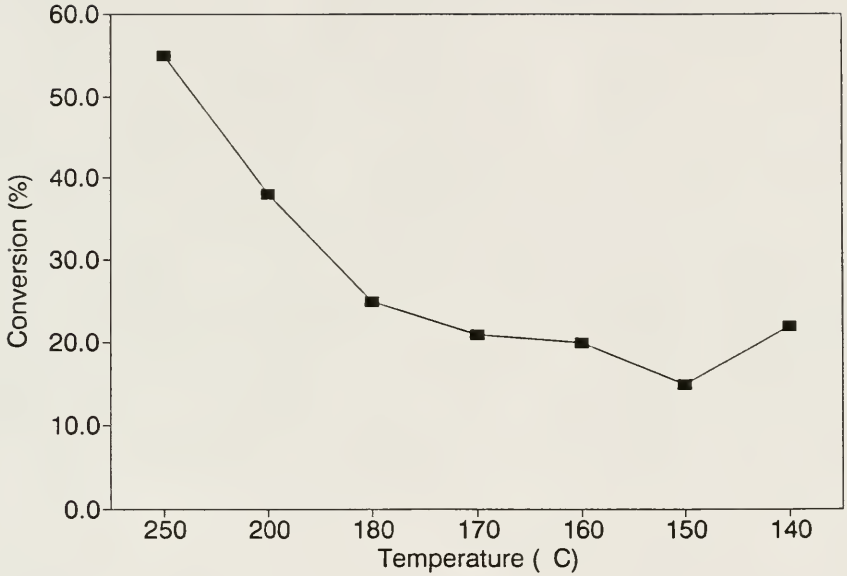

Figure 3-5. Low-Temperature Catalytic Combustion Using a Water Co-Feed.

Lambert and Germain[160] report the use of tin cadmium phosphates, obtained by calcination of $Cd(PO_4)$ and $Sn(OH)_2$ at 550 °C, for the oxidative dehydrogenation of 1-butene at 470 °C. They reported that the catalysts offer good activity and selectivity: 88 % conversion of 1-butene with 71 % selectivity to butadiene. Matsuura and co-workers[161] have investigated oxydehydrogenation of butene with bismuth molybdates and reported excellent selectivity to butadiene of 95 % but only 40 % conversion at 500 °C. Clearly, with conventional metal catalysts there is the need for relatively high temperature (> 400 °C) to activate the catalysts. This high temperature results in poor selectivity for the more active systems while the less active systems show poor conversion.

The above results are presented as comparison studies in Figure 3-6 along with the results for Ambersorb® catalysts. The conditions are such that the butene to oxygen ratio is 2, which fits the stoichiometry mentioned above. The CrO_3/563 catalyst shows the best selectivity of all the catalysts studied, at 98 %. The temperature for optimizing activity and selectivity is 300 °C with this catalyst. Conversion at this selectivity level is 75 %, which is only surpassed by tin cadmium phosphate. The carbon with no metal operates at 350 °C for optimal reactivity of 50 % conversion with 87 % selectivity. Clearly the metal is a vital component for efficient utilization of the catalyst. The temperature for the AX21 reaction is 250 °C. At higher temperatures AX21 lost bed height and mass, indicating oxidation of the carbon was occurring.

A very important aspect of the carbon catalysts is their ability to perform this reaction around 300 to 350 °C, which is 50 to 200 ° less than the other catalysts reported in the literature. Once again, the extraordinary adsorption capability of CMS is most likely the influential characteristic which allows for better activity at lower temperature as compared to inorganic oxides. Comparison of the Ambersorb catalysts to AX21 indicates once again that acidity and/or slit-shaped micropores are important for catalytic activity.

Catalyst Characterization

X-ray photoelectron spectroscopy

The materials examined in the X-ray photoelectron experiments were CrO_3 supported on 563, both before and after the catalytic combustion of methylene chloride, and CrO_3 supported on silica gel before and after reaction. Because the carbon catalysts are in bead form and have a fairly smooth surface, the effect of takeoff angle, θ, on XPS response was studied as a way of determining if the chromium oxidation state changes as a function of depth. This angle is defined as 0 ° when the detector is perpendicular to the surface and 90 ° when parallel with the surface plane. At 0 ° for a smooth surface, 95 % of the intensity of the XPS signal originates from the upper 3 nm of surface coverage.[162] Higher takeoff angles, up to 90 °, allow for enhanced intensity from the lower layers. Figure 3-7 presents the chromium spectrum for CrO_3/563 before reaction at θ = 0 °. Comparing this to Figure 3-8 for the same sample where θ = 90 ° it can be

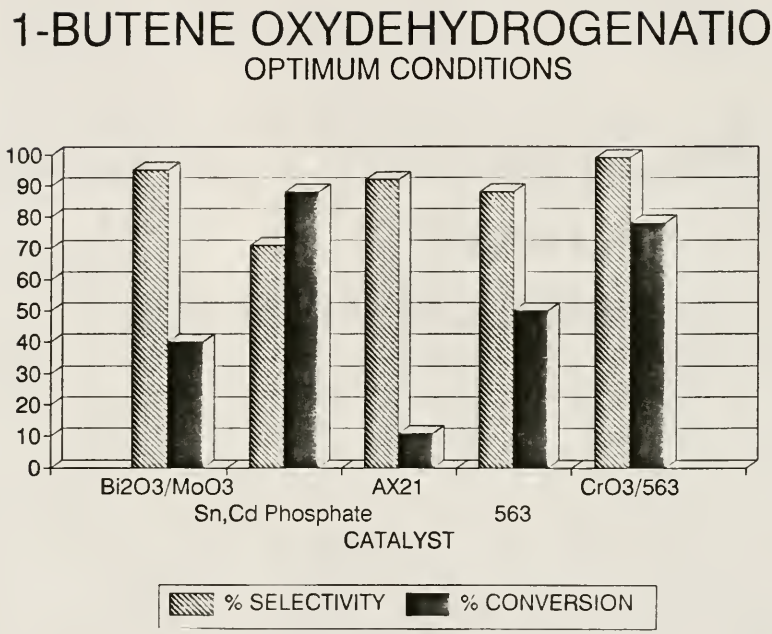

Conditions:

0.5 g catalyst

1.2 ml/min air

0.5 ml/min 1-butene

Variable temperature

Figure 3-6. Oxydehydrogenation of 1-Butene with Various Catalysts.

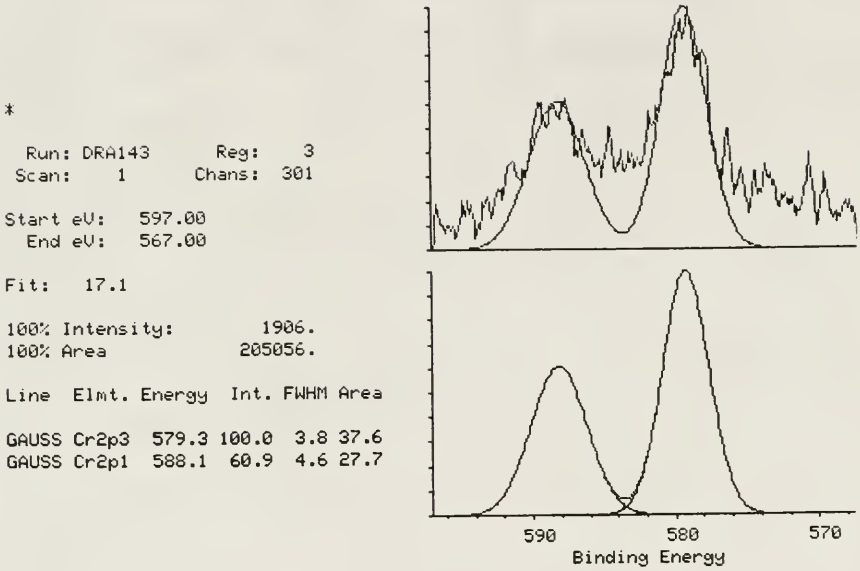

Figure 3-7. XPS Spectrum of CrO_3/563 Before Reaction, θ = 0 °.

observed that the $2p^1$ and $2p^3$ peaks appear broadened at 90 ° relative to the 0 ° spectrum. Deconvolution of these peaks reveals two signals corresponding to Cr(VI) and Cr(III). The peak deconvolution is certainly not conclusive in peak identification but nonetheless is a sign that different Cr oxidation states are present.

Table 3-10 shows a summary of the XPS data for a number of the chromium catalysts utilized in the methylene chloride catalytic combustion reaction. As mentioned above, there appear to be two different peaks for chromium on the carbon at 90 ° takeoff angle, in contrast to one peak for 0 ° which is attributed to Cr(VI). From this observation alone, it can be proposed that Cr(III) is present on the catalyst and exists at the interface between carbon and Cr(VI). In defense of the deconvolution method, the binding energies presented in the table for both Cr(VI) and Cr(III) correlate almost perfectly with those reported in the literature for Cr(VI) and Cr(III) oxo-compounds.[139-142] This is compelling evidence that there are actually two different chromium oxidation states present on the carbon catalyst. In addition, if the intensity values are compared for the used catalyst versus the fresh catalyst (the intensity values on this table are not percentages but arbitrary units), the Cr(VI) to Cr(III) ratio seems to decrease from 5 to 3.5 after reaction. The indication is that chromium is in a slightly more reduced state after the reaction, possibly due to redox chemistry occurring in the catalysis.

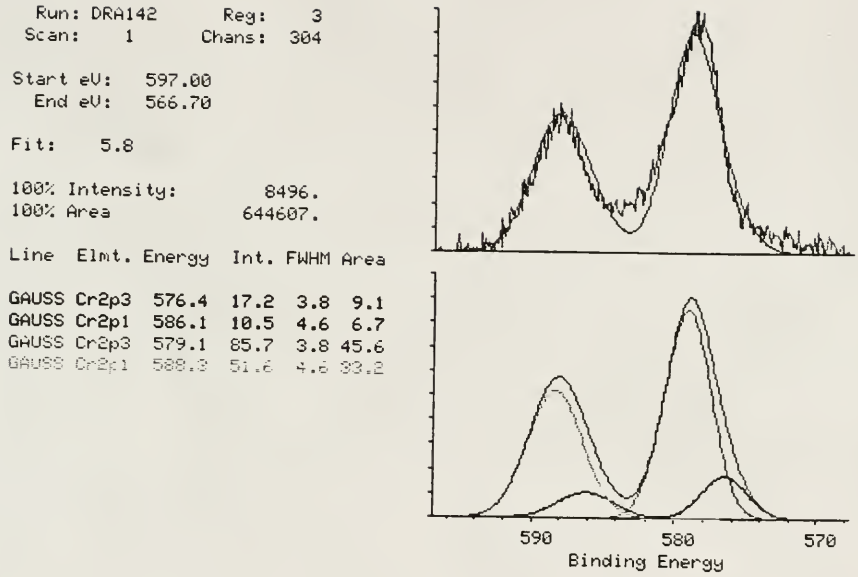

Figure 3-8. XPS Spectrum of CrO_3/563 Before Reaction, θ = 90 °.

Table 3-10. Summary of XPS Data for Chromium Catalysts.

CrO_3/563

SAMPLE	PEAK MAX (eV)	INTEN.	ASSIGN.
BEFORE RXN, θ = 0°	579.3	100	Cr(VI)
BEFORE RXN, θ = 90°	576.4	17.2	Cr(III)
	579.1	85.7	Cr(VI)
AFTER RXN, θ = 0°	579.7	95.1	Cr(VI)
AFTER RXN, θ = 90°	576.7	20.0	Cr(III)
	579.2	71.9	Cr(VI)

CrO_3/SiO_2

SAMPLE	PEAK MAX (eV)	INTEN.	ASSIGN.
BEFORE RXN	582.0	89.8	Cr(VI)
AFTER RXN	581.7	67.0	Cr(VI)
	578.4	28.0	Cr(III)

In the case of a silica-supported CrO_3 catalyst, before reaction there is only one signal observed. Because the silica is amorphous changing the takeoff angle offers no change in the spectrum. The binding energies are slightly higher most likely due to the presence of Si^{4+} Lewis acid centers on the silica support. After reaction there is a considerable amount of Cr(III) formed with the Cr(VI) to Cr(III) ratio of 2.1. The reduction of chromium in this example indicates that the silica catalyst is somewhat less stable than the carbon analogs. The catalytic results themselves indicate a less stable catalyst, with only 60 % average conversion obtained (initial 97 % conversion with gradual drop to 20 % after 24 hours), loss of chromium from the support as observed by collection of red and green compounds (probably volatile oxychlorides) in the post-catalyst zone and coking of the silica during the reaction.

Magnetic susceptibility

An additional method for assessing the oxidation state of supported metal species is magnetic susceptibility. It is fortunate for the susceptibility experiments that Cr(VI) is diamagnetic and Cr(III) is paramagnetic; determination of the paramagnetism of a catalyst sample can indicate the particular oxidation state of the chromium. One complication arises in the observation that the carbon adsorbents are paramagnetic themselves, so the sample susceptibility must be divided into a metal and a support contribution. Determining the magnetic susceptibility of the sample and subtracting out the paramagnetic contribution

from the carbon will give the metal species contribution. The magnetic susceptibility, χ_g (magnetic susceptibility per gram, c.g.s. units) for Ambersorb® 563 is 3.15 x 10^{-6}. The catalyst sample CrO_3/563 gives a χ_g value of 5.51 x 10^{-6}. Correcting the result obtained with CrO_3/563 to remove the carbon contribution results in χ_g = 2.80 x 10^{-6} for 0.14 g Cr species; this translates into 2.00 x 10^{-5} per gram of Cr species present on the catalyst. The value of χ_m is determined; assuming a formula weight of 100 g/mol (based on CrO_3), one gets a χ_m of 2.00 x 10^{-3} and a μ_{eff} ($\mu_{eff} = 2.828(\chi_m T)^{1/2}$) of approximately 2.18 Bohr Magnetons. The spin-only formula, $\mu_{eff} = [(n + 2)n]^{1/2}$, gives an estimate of n = 1.4 for the number of unpaired electrons per Cr atom. This number is indicative of the presence of mixed oxidation states for the catalyst. Specific assignments for oxidation states are difficult because of complications arising from anti-ferromagnetic coupling and a multitude of possible oxidation states. The values obtained in this experiment for χ_g (2.0 x 10^{-5}) can be compared to literature values of 2.5 - 3.0 x 10^{-5} for pure Cr_2O_3[144] and presents further support for the presence of Cr(III). A sample of the same catalyst utilized in the catalytic combustion experiment resulted in a value of n = 1.5. The slight increase in paramagnetism after reaction is also observed in the XPS analysis. The remarkably good association of the magnetic susceptibility results with the XPS experiments is compelling evidence for the validity of the oxidation state assignments.

The chromium oxidation state distribution was examined further in catalytic experiments. An attempt was made to isolate the reduced species in the catalytic combustion reaction by replacing the oxygen reactant by nitrogen and examining the catalyst once the reaction had stopped. For CrO_3/563, however, a stable conversion level of 30 % was maintained for ~100 hours even in the absence of oxygen. The carbon balance in this reaction was very poor because minimal amounts of carbon oxides and organic products were observed in the post-catalyst stream. Magnetic susceptibility of this catalyst sample showed no change from the fresh catalyst (n = 1.4). The reaction was repeated using helium with identical results, showing that the reactivity was not due to an oxygen impurity in the nitrogen. The carbon without CrO_3 demonstrated no activity under nitrogen.

The results presented above lead to a number of speculations about the reaction mechanism. The chromium appears to be functioning non-oxidatively, which is unexpected. The possibility exists for a stoichiometric reaction of methylene chloride with Cr(VI) and subsequent reduction to Cr(III) by sequential electron transfer processes, proceeding through intermediate oxidation states Cr(V) and Cr(IV). However, the amount of methylene chloride reacted in the experiment (10.1 mmol) is more than the oxidation equivalents available from the chromium (8.4 mmol of electrons, if each chromium atom loses three electrons). These numbers presuppose that all chromium is Cr(VI) initially, which is not the case. In addition, the magnetic susceptibility shows absolutely no change in the paramagnetism. Precedence for chromium functioning in a non-oxidative process

is seen in the reaction of CrO_3 with HCl to form CrO_2Cl_2[163] and the ability of water to hydrolyze chromyl chloride back to HCl and chromate. It is possible that a species similar to chromyl chloride exists on CrO_3/CMS and trace amounts of water in the reactor serve to perform the apparent catalysis.

The results for the SiO_2/CrO_3 catalyst are different. Magnetic susceptibility on the catalyst after reaction shows a significant amount of Cr(III) formed in the reaction: n = 1.46 for the after reaction catalyst in contrast to n = 0 for the fresh material. The XPS studies presented earlier also show this result. The reactivity of the catalyst also decreases over time, reaching a level of just 20 % after 24 hours, regardless of the atmosphere. Loss of the metal from the silica and the observation of metal reduction demonstrate that the silica catalyst is very different than the carbon analogs. A large amount of coking was observed in these reactions as observed by the intense black color of the catalyst after reaction. Despite the differences between the silica and carbon catalysts, this type of process may be involved in the poor carbon balance observed with the Ambersorb catalysts. At this point there is no strong evidence to support this proposal, primarily because the observation of carbonaceous coke on a carbon-based catalyst is not a trivial matter.

A blank sample consisting of a heterogeneous mixture of 563 and pure CrO_3 was utilized in the magnetic susceptibility experiment. χ_g obtained for the sample was 5.21×10^{-7}, which is lower than for 563 untreated. This indicates pure CrO_3 makes only a diamagnetic contribution to the sample susceptibility. If this

experiment is compared to the results for the prepared catalyst, it can be inferred that the carbon acts as a reducing agent upon preparation of the catalyst to form lower valent chromium species which do not appear in the physical mixture.

Assuming the validity of the above results with regard to a mixture of oxidation states, the active oxidation state for catalytic combustion should be determined in order to better understand the reaction. To do this, 0.5 g of CrO_3/563, which gives 93 % conversion in the CH_2Cl_2 experiment under these conditions, was pretreated with H_2 for 1 hour in order to reduce any Cr species present to Cr(III). Activity of this reduced catalyst in the methylene chloride reaction gave 59 % (± 2) conversion. This value is within the error limit for the reactivity of the blank support, at 55 % (± 3). Magnetic susceptibility measurements on the reduced catalyst gave n = 3.1 unpaired electrons per Cr atom, which is consistent with the full reduction to Cr(III). We can state, therefore, that a high oxidation state chromium species, most likely Cr(VI), is the active metal oxidation state for low-temperature oxidative combustion. It can also be stated that the Cr(III) formed from hydrogen reduction is not regenerated to Cr(VI) under the conditions of the experiment.

Scanning electron microscopy

Scanning electron micrographs of A® 563 are presented in Figure 3-9 (6000 magnification) and Figure 3-10 (30,000 magnification). At 6000 magnification, there is a large fault in the sample which provides a view of the interior pore

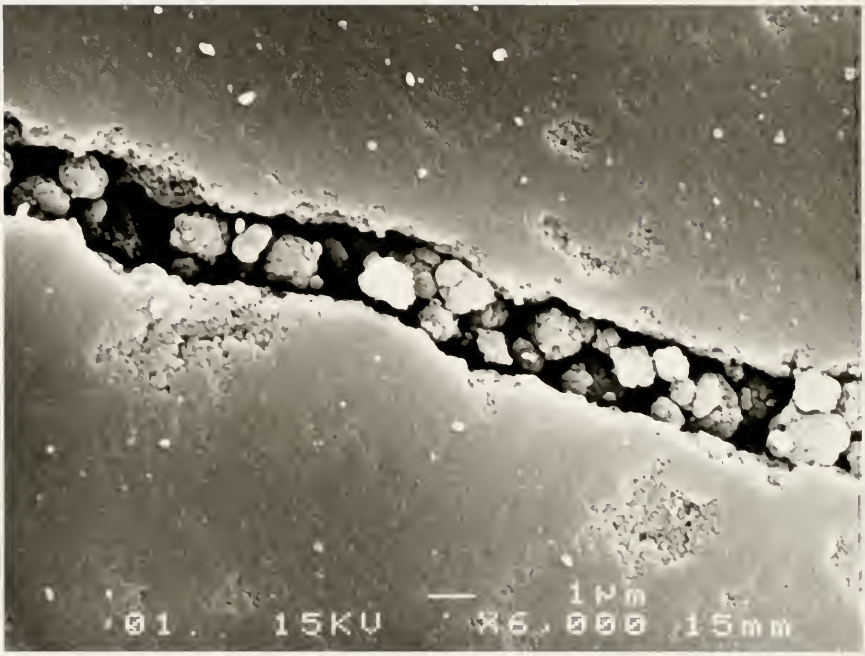

Figure 3-9. SEM of Ambersorb® 563, 6000 Magnification.

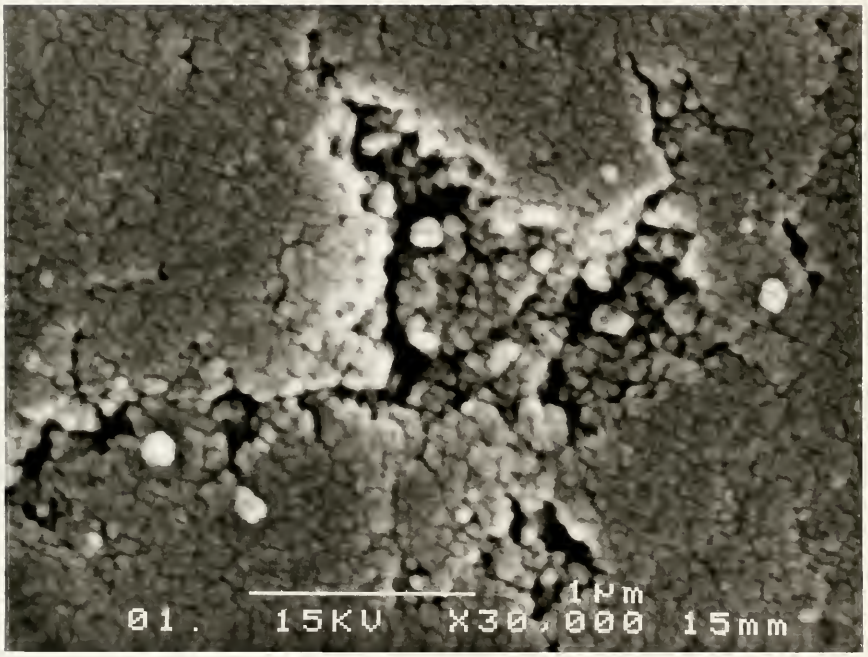

Figure 3-10. SEM of Ambersorb® 563, 30,000 Magnification.

structure arising from the copolymer precursor. The micrograph at 30,000 x illustrates the detail for a pore of macroporous dimensions with mesopores observed as small cracks in the surrounding surface. Micropores on the surface of the carbon bead, which in these figures are too small to see, are often cited to be the defining character which accounts for the molecular sieving action observed for certain carbon materials.[107,164,165]

The micrographs in Figure 3-11 and Figure 3-12 are of CrO_3/563 at 6000 and 30,000 magnification, respectively, and reveal some qualitative information about catalyst structure. This sample is one that has been used in a catalytic reaction; that is, taken to 250 °C for an extended period of time. One would expect that CrO_3, which has a melting point of 195 °C, would melt and recrystallize upon cooling into aggregates, or large crystallites, unless it was highly dispersed and anchored to the surface. The lack of large crystallites in Figures 3-11 and 3-12 is strong evidence that dispersion and coordination to the surface has occurred. Grunewald and Drago[115] have demonstrated this effect with MoO_3 supported on high surface area carbon materials. The synergistic activity of CrO_3/563 presented in Table 3-2 is also indicative of this high level of dispersion and coordination of CrO_3 to the carbon surface.

Porosimetry

Nitrogen porosimetry is a useful method for examining changes in surface area and pore volumes for different samples. Adsorption of nitrogen onto porous

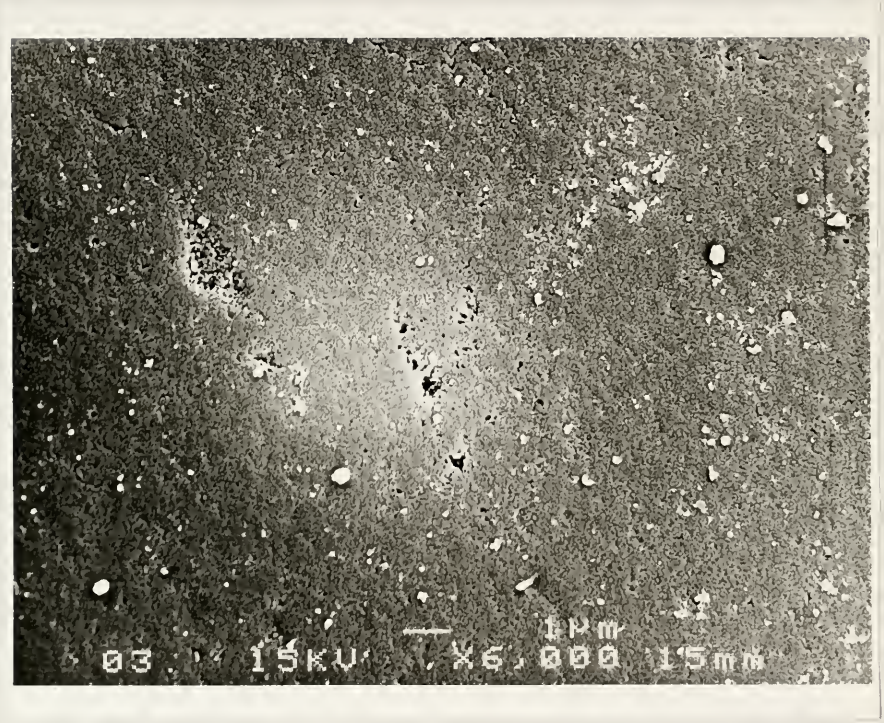

Figure 3-11. SEM of 563/CrO_3, 6000 Magnification.

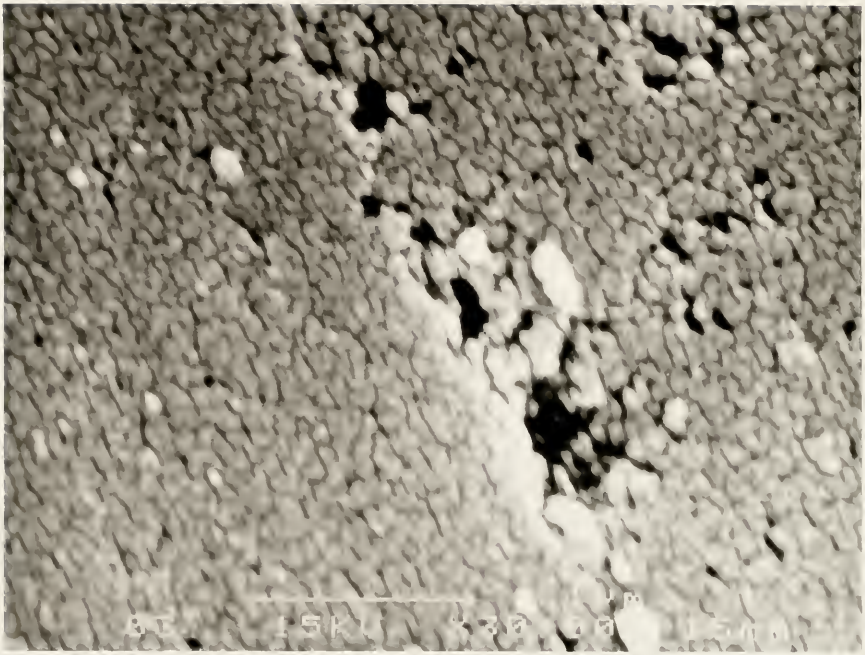

Figure 3-12. SEM of 563/CrO_3, 30,000 Magnification.

solids occurs principally through dispersion forces which are assumed to be constant for different supports with widely varying properties. This phenomenon forms the basis behind the BET method of surface area analysis. Equation 3-3 presents the relationship between the surface area of the support (A_s) with the amount of nitrogen adsorbed in one complete monolayer (n_m) and the area occupied by one nitrogen molecule in the monolayer on the surface (a_m):

$$A_s = (n_m)(L)(a_m) \qquad (3\text{-}3)$$

The constant L is Avogadro's number (6.02×10^{23}). The BET experiment is performed to determine the value of n_m; L is known and a_m is derived from a close-packed structure to be 0.162 nm^2 at 77 K.[138] To determine n_m, a sample of support is degassed and a measured amount of gaseous nitrogen is introduced to the sample. The relative pressure in the system (p/p^o) is then plotted against the actual amount of nitrogen adsorbed (n). The relationship between p/p^o and n is described by the BET equation:[166]

$$\frac{p/p^o}{n[1-(p/p^o)]} = \frac{1}{n_m c} + \frac{(c-1)(p/p^o)}{n_m c} \qquad (3\text{-}4)$$

The parameter denoted c is a constant related to the heat of adsorption. For nitrogen on porous solids, c is usually calculated to be large (> 100) which implies

that the plot of n vs. p/p^o passes through the origin of the coordinate system. Mathematically, it means that 1/c is a negligible quantity and (c-1)/c is approximately equal to 1. Putting these approximations into equation 3-4 gives a simple relationship for n_m and n, depicted in equation 3-5:

$$n_m = n\ (1 - p/p^o) \qquad (3\text{-}5)$$

Equation 3-5 allows for determination of n_m from one point on the adsorption isotherm and is aptly referred to as the single-point BET method.

The determination of pore volumes is accomplished by utilizing a t-plot.[166] The amount of gas adsorbed, n, is plotted against a related parameter, t. The t parameter is referred to as the statistical thickness of the surface film and is obtained from the isotherm of a reference solid with negligible pore volume but surface area comparable to the support being examined. Because the t value does not account for pore structure, any deviation from linearity in the n vs. t plot signifies the presence of mesopores or micropores and the pore volumes can be determined by manipulation of the plot data.

The single-point BET method was used to determine the changes upon supporting CrO_3 on 563 and the results comparing the modified with the unmodified support are presented in Table 3-11. The lack of significant change in the total surface area and the micropore volume upon adding CrO_3 indicates that the oxide does not penetrate or cover the openings to the micropores. The

Table 3-11. Porosimetry of Ambersorb® 563 and CrO_3/563.

CATALYST	SURFACE AREA (m^2/g)	MICROPORE VOLUME (ml/g)	TOTAL PORE VOLUME (ml/g)
A® 563	680	0.26	0.79
CrO_3/563	682	0.25	0.60

decrease observed for the total pore volume shows that the CrO_3 did indeed enter the pores of the carbon bead but is contained in the meso- and macropores rather than the micropores. It is expected that the micropores would not be penetrated by the impregnation solution due to the fact that 563 is very hydrophobic and water was the solvent used to prepare the catalyst. Furthermore, H_2CrO_4 and its polymer aggregates ($H_2Cr_2O_7$, for example) are too large to enter the micropores.

Conclusions

The goal of the research presented in this chapter was to develop a low-temperature catalytic combustion process using catalysts derived from porous, carbonaceous adsorbents. It was found that at 250 °C, a series of metal oxides supported on carbon adsorbents were able to convert 60,000 ppm of methylene chloride completely to CO, CO_2 and HCl. Investigation of the catalytic activity for the unmodified carbons showed that the adsorbents were active even in the absence of metal additives. This activity was found to correlate with the micropore volume of the carbon material. In comparison of polymer-derived carbons (e.g., Ambersorb® series) with organically-derived carbons (e.g., AX21) it was proposed that the catalytic activity is dependent on the surface chemistry (the presence of basic groups, for example) or the physical shape of the micropores present. The same comparison also reveals that the surface area of the carbon is not a feasible criterion by which to judge support applicability if surface chemistry

is not taken into account, as demonstrated by the low activity of the ultra-high surface area AX21.

Acidity of the carbon was shown to be an important factor in carbon activity as indicated by the base sensitivity for Ambersorb® 563 in the deep oxidation reaction. Possibly related to this are the deuterium isotope effect studies where a k_h/k_d of 1.4 indicated that C-H bond scission may be involved in the rate determining step. Literature precedence for C-H bond cleavage by carbon catalysts[115] corroborates this observation.

The kinetics of the catalytic combustion reaction over an unmodified carbon catalyst were found to exhibit first-order dependence on $[CH_2Cl_2]$ at excess oxygen levels; when $(O_2/CH_2Cl_2) < 3$ a deviation from first order behavior in $[CH_2Cl_2]$ was observed. Determination of the rate constant at different temperatures provided the data for an Arrhenius plot (ln k versus 1/T); a least-squares fit of the linear trend resulted in an activation energy of 11.0 kcal/mol for the deep oxidation process. The E_a value obtained in this manner is relatively low compared to typical catalyzed oxidation reactions but is comparable to literature values for similar catalytic combustion reactions.[156]

Catalysts comprised of metal oxides supported on the carbon adsorbents generally afforded the best conversions in the methylene chloride deep oxidation reaction. The metal species with optimal performance were chromium, titanium and mixed-metal manganese/cerium oxides. Expanding the catalytic combustion reaction to other substrates, it was determined that the carbon catalysts are

effective for the destruction of a variety of halogenated hydrocarbons such as chlorinated aromatics (as PCB models), chlorinated olefins, fully chlorinated hydrocarbons and bromine compounds.

The influence of water was studied to determine the effectiveness of the carbon catalysts in the real-world application of wastewater treatment. The overall effect of adding water to the reaction was negligible in the case of the unmodified carbon catalysts. For metal oxide/carbon catalysts water was found to slightly hinder the activity. In contrast, a zeolite catalyst showed a drastic drop in activity in the presence of water vapor. The hydrophobicity of the carbon supports is proposed to account for the observed results. Water was also used to examine the deep oxidation reaction at temperatures lower than 200 °C. In this instance the effect of water was to deter the irreversible adsorption of methylene chloride onto the carbon which is seen at temperatures of 225 °C or less in the absence of water. Superheated steam at 140 °C or higher is used in the process of regenerating carbon adsorbents after standard wastewater treatment[13] and this effect was utilized in the deep oxidation reaction. Conversion of methylene chloride was observed at temperatures as low as 150 °C using water vapor in the air stream as compared to a dramatic drop from ~40 % conversion at 225 °C to 0 % conversion at 215 °C when no water is present. Condensation of CH_2Cl_2 in the pores of the carbon is postulated to account for the abrupt dropoff in activity at 225 °C, as this is close to the critical temperature for methylene chloride at 237 °C.

The effectiveness of the catalytic combustion process was demonstrated in an experiment where the atmosphere was altered and the activity monitored. Switching from air to nitrogen resulted in a gradual drop in activity over a span of 12 hours, indicating efficient use of oxidized surface sites even as the oxygen concentration approached zero. Reestablishing the air environment caused an almost immediate recovery of activity to the original level, illustrating that reoxidation of the catalyst is facile and non-destructive. This experiment also demonstrated the requirement of oxygen to the catalytic process and supports a redox mechanism for the reaction.

The use of the carbon catalysts in the oxidative dehydrogenation of 1-butene to butadiene provided remarkable results in a reaction notably different than catalytic combustion. The combination of activity and selectivity observed with the Ambersorb® catalysts was shown to be among the most effective methods known for conversion of 1-butene to butadiene, as compared with literature reports for the same reaction. The relatively low temperature and pressure needed to effect the high activity are an indication of how efficient the carbon catalysts are at promoting hydrocarbon conversion reactions.

The catalysts chosen for characterization studies were the most effective ones in the catalytic combustion reactions; namely, chromium (VI) oxide supported on carbon adsorbents. These analyses can help in determining the important factors for optimizing catalytic activity. The chromium species on the carbon was determined to exist in a mixture of oxidation states, as indicated by

magnetic susceptibility and supported by XPS analysis. The most likely combination is Cr(VI) and Cr(III). Takeoff angle variation in the XPS study showed the presence of Cr(III) at a position underneath the Cr(VI) layer which is suggestive of Cr(III) being present at the interface of the carbon and the Cr(VI) species and points to the capacity of the carbon support to reduce the metal at the lower molecular layers.

Magnetic susceptibility was also useful in determining the active oxidation state of the metal. After complete reduction of surface Cr(VI) to Cr(III) by hydrogen and confirmation of the reduction by the observation of increased paramagnetism by magnetic susceptibility, the activity of the catalyst was no higher than that for the unmodified carbon; that is, the catalytic effect of the metal was destroyed by reduction. This is convincing evidence that a higher oxidation state such as Cr(V) or Cr(VI) is the active species. The experiment also shows that Cr(III) as formed by hydrogen reduction is not reoxidized under the conditions of the experiment.

The comparison of undoped carbons to CrO_3/CMS catalysts in reactions without air presented the observation that chromium can function in the catalytic combustion process with no air flow for at least 100 hours whereas the carbon itself requires oxygen to perform the reaction. Magnetic susceptibility on the catalyst after reaction indicated no major change in oxidation state for the chromium as compared to the fresh catalyst, which is a strong indication that the chromium dopant functions non-oxidatively.

The physical placement of the metal dopant was indicated by porosimetry and scanning electron microscopy. The lack of large crystallites of CrO_3 on the carbon, even after reaction above the melting point of the metal oxide, signifies that good dispersion and anchoring of the chromium is achieved by the carbon supports. Literature reports are consistent with this observation.[115] The porosimetry results demonstrate that the metal was effective in pore penetration, as seen by reduction in total pore volume with regard to the unmodified carbon, but the micropores were left essentially unaffected. The high level of metal dispersion was also observed in porosimetry by the retention of high surface area even at high metal loading levels. The characterization results taken as a whole give a reasonable picture of catalyst structure and offer insights into how the carbon adsorbents can function as supports for metal oxides.

CHAPTER 4
SUMMARY

Supported Aluminum Chloride

A recently developed catalyst comprised of aluminum chloride supported on silica was utilized in a number of acid-catalyzed hydrocarbon reactions. The catalyst demonstrated remarkable activity in standard carbonium-ion catalyzed reactions such as butane isomerization, hexane cracking, Friedel-Crafts reactions and dehydrohalogenation. A more novel application of solid acids, cracking of polyolefins, was also found to give impressive results with $AlCl_2(SG)_n$.

In order to circumvent the use of hazardous chlorinated solvents, a preparation for the acid catalyst was developed which involved prolonged vapor deposition, or an extended reaction of sublimed Al_2Cl_6 with the silica support. This version of the catalyst showed essentially identical reactivity to the CCl_4 prepared catalyst and possessed a similar surface structure, as demonstrated by MAS NMR and FTIR spectroscopy. In further structural investigations, it was determined that the properties and activity of the catalysts samples are directly influenced by the level of hydration for the silica used to prepare the catalyst. This parameter is one that has not been discussed previously as being important

to catalyst preparation. In particular, it was proposed that the presence of geminal silanol groups are crucial for obtaining an active version of the catalyst.

Porous Carbon Adsorbents

Carbon molecular sieves are novel materials which have application for supporting metal species as acid catalysts. The employment of transition metal oxides supported on these polymer carbons has been investigated for a number of unique hydrocarbon conversion reactions. The catalytic combustion of halogenated hydrocarbons is a relatively new approach to toxic waste disposal; the metal doped carbon catalysts have been studied in this process and were found to be the most effective catalysts reported to date for the conversion of chlorinated hydrocarbons to HCl and carbon oxides.

Mechanistic aspects of the catalytic combustion reaction have been elucidated by a number of comparison studies performed. It was found that the carbon catalysts are active even without metal additives and that this activity is apparently linked to surface acidity as demonstrated by base sensitivity. In addition, the micropore volume of the carbon was shown to be a determining factor in catalytic activity as opposed to surface area which is often used for assessment of inorganic oxide catalysts. The kinetics of methylene chloride catalytic combustion were determined to be first order in $[CH_2Cl_2]$ with an activation energy of 11.0 kcal/mol, which indicates a very facile reaction with the carbon catalysts.

Addition of water to the deep oxidation system was shown to have little effect on catalytic activity with the carbon-based catalysts in direct contrast to results obtained with zeolite catalysts which demonstrated competitive adsorption of water, effectively reducing the activity of the catalyst. The catalytic combustion of methylene chloride at temperatures less than 200 °C required the presence of water in order to prevent apparent condensation of methylene chloride in the micropores of the carbon and allowed for deep oxidation activity to occur at 150 °C.

Characterization of the most active catalysts which utilized chromium oxide revealed some significant aspects of catalyst structure. Remarkable dispersion and stability for the catalysts was observed as well as the pore environment of the metal additive. Chromium was determined to exist as mixed oxidation states, of which Cr(VI) was proposed to be the active one. Atmosphere variations illustrated that chromium can function in the absence of air when supported on carbon and possibly acts in a non-oxidative fashion.

The work contained in this thesis demonstrates the overall utility of acid catalysis, from new applications with known catalysts to the development of novel materials and processes. Through this work a better understanding of structural influences on catalytic activity has been achieved as well as insight into the mechanisms of hydrocarbon conversions using acid catalysts.

REFERENCE LIST

1. Campbell, I. M. Catalysis at Surfaces; Chapman and Hall: London, 1988, p. 5.

2. a.) Drago, R. S.; Getty, E. E. U.S. Patent No. 4,719,190; Jan. 12, 1988.

   b.) Drago, R. S.; Getty, E. E. U. S. Patent No. 4,929,800; May 29, 1990.

3. Drago, R. S.; Getty, E. E. J. Am. Chem. Soc., **1988**, 110, 3311.

4. Drago, R. S.; Getty, E. E. Inorg. Chem., **1990**, 29, 1186.

5. Kelly, T. T.; Sechrist, C. N. U.S. Patent No. 3,248,343; April 26, 1966.

6. Olah, G. A.; Messina, G. U.S. Patent No. 3,993,587; Nov. 23, 1976.

7. Hamner, G. P.; Mattox, W. J. U.S. Patent No. 3,961,036; June 1, 1976.

8. Smith, R. M. U.S. Patent No. 2,927,087; March 1, 1960.

9. Herbstman, S.; Webb, A. N.; Estes, J. H. U.S. Patent No. 4,066,716; Jan. 3, 1978.

10. Herbstman, S.; Webb, A. N.; Estes, J. H. U. S. Patent No. 4,113,657; Sept. 12, 1978.

11. Myers, J. W. U.S. Patent No. 3,449,264; Nov. 27, 1961.

12. Getty, E. E.; Petrosius, S. C.; Drago, R. S. J. Mol. Catal., **1991**, 67, 127.

13. Neely, J. W.; Isacoff, E. G. Carbonaceous Adsorbents for the Treatment of Ground and Surface Waters; Marcel Dekker, Inc.: New York, 1982.

14. Evering, B. L. Advan. Catal., **1954**, 6, 197.

15. Oelderick, J. M.; Platteeuw, J. C. Proc. 3rd Int. Cong. Catal., **1964**, 735.

16. Rodewald, P. U.S. Patent No. 3,925,495; 1975.

17. Krzywicki, A.; Marczewski, M.; Malinkowski, S. React. Kinet. Catal. Lett., **1978**, 8, 25.

18. Ono, Y.; Tanabe, T.; Kitajima, N. J. Catal., **1979**, 56, 47.

19. Fuentes, G. A.; Gates, B. C. J. Catal., **1982**, 76, 440.

20. Rodewald, P. U.S. Patent No. 3,962,133; 1976.

21. Rodewald, P. U.S. Patent No. 3,984,352; 1976.

22. Rodewald, P. U.S. Patent No. 3,992,473; 1976.

23. Fuentes, G. A.; Boegel, J. V.; Gates, B. C. J. Catal., **1982**, 78, 436.

24. Olah, G. A.; Surya Prakash, G. K.; Sommer, J. Superacids; Wiley: New York, 1985.

25. Olah, G. A., Ed. Friedel-Crafts and Related Reactions; Interscience: New York, 1963.

26. Friedel, C.; Crafts, J. M. C. R. Acad. Sci. Paris, **1877**, 84, 1292.

27. Friedel, C.; Crafts, J. M. C. R. Acad. Sci. Paris, **1877**, 84, 1450.

28. Olah, G. A.; Farooq, O.; Farnia, M. F.; Olah, J. A. J. Am. Chem. Soc., **1988**, 110, 2560.

29. Laszlo, P.; Mathy, A. Helv. Chim. Acta, **1987**, 70, 577.

30. Olah, G. A.; Kaspi, J.; Bukala, J. J. Org. Chem., **1977**, 42, 4187.

31. Pines, H. The Chemistry of Catalytic Hydrocarbon Conversions; Academic Press, Inc.: New York, 1981.

32. Uemichi, Y.; Ayame, A.; Kashiwaya, Y.; Kanoh, H. J. Chromatogr., **1983**, 259, 69.

33. Nanbu, H.; Ishihara, Y.; Honma, H.; Takesue, T.; Ikemura, T. J. Chem. Soc. Jpn., **1987**, 765.

34. Uemichi, Y.; Makino, Y.; Kanazuka, T. J. Anal. Appl. Pyrol., **1989**, 14, 331.

35. Uemichi, Y.; Kashiwaya, Y.; Ayame, A.; Kanoh, H. Chem. Lett., **1984**, 41.

36. Schmidt, R. J.; Stine, L. O. U.S. Patent No. 4,783,575; Nov. 8, 1988.

37. Schmidt, R. J. U.S. Patent No. 4,834,866; May 30, 1989.

38. Parry, E. P. J. Catal., **1963**, 2, 371.

39. Vedrine, J. C.; Auroux, A.; Bolis, V.; Dejaifre, P.; Naccache, C.; Weirzchowski, D.; Derovane, E. G.; Nagy, J. B.; Gilson, J.; Van Hooff, J. H. C.; Van Denberg, J. P.; Wolthoizen, J. J. Catal., **1979**, 59, 248.

40. Jacobs, P. A. in Chemical Industries; Vol. 15 (Delannay, F., Ed.), Marcel Dekker, Inc.: New York, 1984, p. 367.

41. Hair, M. L. Infrared Spectroscopy in Surface Chemistry; Marcel Dekker, Inc.: New York, 1967.

42. Schwarz, J. A.; Russell, B. G.; Harnsberger, H. F. J. Catal., **1978**, 54, 303.

43. Monterra, C.; Coluccia, S.; Chiorino, A.; Boccuzzi, F. J. Catal., **1978**, 54, 348.

44. Primet, M.; Ben Taarit, Y. J. Phys. Chem., **1977**, 81 (13), 1317.

45. Monterra, C.; Chiorino, A.; Ghiotti, G.; Garrone, E. J. Chem. Soc. Faraday Trans. I, **1979**, 75, 271.

46. Monterra, C.; Chiorino, A.; Ghiotti, G.; Garrone, E. J. Chem. Soc. Faraday Trans. I, **1979**, 76, 2102.

47. Take, J.; Tsuruya, T.; Sato, J.; Yoreda, Y. Bull. Chem. Soc. Jpn., **1972**, 45, 3404.

48. Corrsin, L.; Fax, B. J.; Lord, R. C. J. Chem. Phys., **1953**, 21 (7), 1170.

49. Getty, E. E. Ph.D. Dissertation, University of Florida, Gainesville, FL., 1988.

50. Thomas, J. M.; Klinowski, J. in Advances in Catalysis; Vol. 33 (Eley, D. D.; Pines, H.; Weisz P. B., Ed.), Academic Press, Inc.: Orlando, FL., 1985, p. 199.

51. Chaing, C. D.; Chu, C. T. W.; Miale, J. N.; Bridger, R. F.; Calvert, R. B. J. Am. Chem. Soc., **1984**, 106, 8143.

52. Akitt, J. W. Annual Reports on NMR Spectroscopy, **1975**, 5A, 466.

53. Maciel, G. E. in Heterogeneous Catalysis; Vol. 2 (Shapiro, B. L., Ed.), Texas A & M University Press: College Station, Texas, 1984, p. 349.

54. Maciel, G. E.; Sindorf, D. W. J. Am. Chem. Soc., **1983**, 105, 1487.

55. Weiss, K. D. Ph.D. Dissertation, University of Florida, Gainesville, FL., 1986.

56. Levanova, S. V. Zh. Vses. Khim. Obva., **1987**, 30, 68.

57. Weiss, A. H.; Gambhir, B. S.; Leon, R. B. J. Catal., **1971**, 22, 245.

58. Weiss, A. H.; Krieger, K. A. J. Catal., **1966**, 6, 167.

59. Weiss, A. H.; Valinski, S.; Antoshin, G. V. J. Catal., **1982**, 74, 136.

60. Gambhir, B. S.; Weiss, A. H. J. Catal., **1972**, 26, 82.

61. Van Barneveld, W. A. A.; Porec, V. J. Catal., **1984**, 88, 382.

62. Sonin, E. V.; Shkalyabin, O. K.; Treger, Y. A. Zh. Vses. Khim. Obva., **1987**, 30, 15.

63. Stille, J. K. Industrial Organic Chemistry; Prentice-Hall, Inc.: Englewood, N.J., 1968.

64. Mochida, I.; Uchino, A.; Fojitsu, H,; Takeshita, K. Chem. Lett., **1975**, 745.

65. Mochida, I.; Kamon, N.; Fojitsu, H.; Takeshita, K. J. Jpn. Petrol. Inst., **1978**, 21, 285.

66. Mochida, I.; Watanabe, H.; Fujitsu, H.; Takeshita, K. J. Chem. Soc. Chem. Comm., **1980**, 793.

67. Mochida, I.; Watanabe, H.; Fujitsu, H.; Takeshita, K. Ind. Eng. Chem. Prod. Res. Div., **1983**, 22, 38.

68. Mochida, I.; Miyazaki, T.; Takagi, T.; Fujitsu, H. Chem. Lett., **1985**, 833.

69. Olah, G. A.; Meidar, D. Nouv. J. Chim., **1979**, 3, 269.

70. Olah, G. A.; Meidar, D.; Malhota, R.; Olah, J. A.; Narang, S. C. J. Catal., **1980**, 61, 96.

71. Prakash, G. K. S.; Olah, G. A. in Acid-Base Catalysis; (Tanabe, K., Ed.), Kodansha, Ltd.: Tokyo, 1989, p. 59.

72. Olah, G. A.; Kaspi, J.; Bukala, J. J. Org. Chem., **1977**, 42, 4187.

73. Clark, J. H.; Kybett, A. P.; Macquarrie, D. J.; Barlow, S. J.; Landon, P. J. Chem. Soc. Chem. Comm., **1989**, 1353.

74. Laszlo, P.; Cornelis, A. Synthesis, **1985**, 909.

75. Lalancette, J. M. U.S. Patent No. 3,880,944; 1975.

76. Schrall, H.; Schunack, W. Sci. Pharm., **1974**, 42, 248.

77. Morrison, R. T.; Boyd, R. N. Organic Chemistry; 4th Ed., Allyn and Bacon. Inc.: Boston, 1983.

78. Asselin, G. F.; Block, H. S.; Donaldson, G. R.; Haensel, V.; Pollitzer, E. L. Prepr. Am. Chem. Soc. Div. Petr. Chem., **1972**, 17 (3), B4.

79. Ware, K. J.; Richardson, A. H. Hydrocarbon Process., **1972**, 51 (11), 161.

80. Grote, H. W. Oil Gas J., **1958**, 56 (13), 73.

81. Ono, Y.; Tanabe, T.; Kitajima, N. Chem. Lett., **1978**, 625.

82. Ono, Y.; Sakuma, S.; Tanabe, T.; Kitajima, N. Chem. Lett., **1978**, 1061.

83. Ono, Y.; Yamaguchi, K.; Kitajima, N. J. Catal., **1980**, 64, 13.

84. Pines, H.; Wackher, R. C. J. Am. Chem. Soc., **1946**, 68, 599.

85. Magnotta, V. L.; Gates, B. C.; Schuit, G. C. A. J. Chem. Soc. Chem. Comm., **1976**, 342.

86. Magnotta, V. L.; Gates, B. C. J. Catal., **1977**, 46, 266.

87. Olah, G. A.; White, A. M. J. Am. Chem. Soc., **1969**, 91, 5801.

88. Poller, R. C. J. Chem. Tech. Biotech., **1980**, 30, 152.

89. Khalafov, F. R.; Novruzova, F. A.; Krentsel, B. A.; Dzhafarov, O. I.; Mekhtiev, S. A.; Kuliev, A. M.; Nurullaev, G. G. Vysokomol. Soedin. Ser. B., **1990**, 32 (3), 194.

90. Ivanova, S. R.; Gumerova, E. F.; Berlin, A. A.; Minsker, K. S. Vysokomol. Soedin. Ser. A., **1991**, 33 (2), 342.

91. Sal'nikov, S. B.; Tsailingol'd, V. L.; Bychkova, T. I.; Travina, V. N. Kauch. Rezina, **1990**, 7, 13.

92. Carman, P. C. Trans. Faraday Soc., **1940**, 35, 964.

93. Hockey, J. A. Chem. Ind., **1965**, 57.

94. Peri, J. B.; Hensley, A. L., Jr. J. Phys. Chem., **1968**, 72, 2926.

95. Pinnavaia, T. J. in Heterogeneous Catalysis; Vol. 2 (Shapiro, B. L., Ed.), Texas A & M University Press: College Station, Texas, 1984, p. 142.

96. Hanson, D. Chem. Eng. News, March 12, 1990, 4.

97. Trimm, D. L.; Cooper, B. J. J. Chem. Soc. Chem. Comm., **1970**, 477.

98. Trimm, D. L.; Cooper, B. J. J. Catal., **1973**, 31, 287.

99. Schmitt, J. L., Jr.; Walker, P. L., Jr. Carbon, **1971**, 9, 791.

100. Schmitt, J. L., Jr.; Walker, P. L., Jr. Carbon, **1972**, 10, 87.

101. Foley, H. C. Am. Chem. Soc. Symp. Ser., **1988**, 368, 335.

102. Kunin, R.; Meitzner, E. F.; Bortnick, N. M. J. Am. Chem. Soc., **1962**, 84, 305.

103. Millar, J. R.; Smith, D. G.; Marr, W. E.; Kressman, T. R. E. J. Chem. Soc., **1963**, 218.

104. Lafaytis, D. S.; Tung, J.; Foley, H. C. Ind. Eng. Chem. Res., **1991**, 30, 865.

105. Neely, J. W. U.S. Patent No. 4,040,990; Aug. 9, 1977.

106. Maroldo, S. G.; Betz, W. R.; Borenstein, N. U.S. Patent No. 4,839,331; June 13, 1989.

107. Lamond, T. G.; Metcalfe, J. E.; Walker, P. L., Jr. Carbon, **1965**, 3, 59.

108. Betz, W. R.; Maroldo, S. G.; Wachob, G. D.; Firth, M. C. Am. Ind. Hyg. Assoc. J., **1989**, 50, 181.

109. Graham, D. J. Phys. Chem., **1955**, 59, 896.

110. Alkhazov, T. G.; Lisovskii, A. E. Kinet. Katal., **1976**, 17, 434.

111. Fiedorow, R.; Przystajko, W.; Sopa, M.; Dalla Lana, I. G. J. Catal., **1981**, 68, 33.

112. Vrieland, G. E.; Menon, P. G. Appl. Catal., **1991**, 77, 1.

113. Cadus, L. E.; Gorriz, O. F.; Rivarda, J. B. Ind. Eng. Chem. Res., **1990**, 29, 1143.

114. Grunewald, G. C.; Drago, R. S. J. Mol. Catal., **1990**, 58, 227.

115. Grunewald, G. C.; Drago, R. S. J. Am. Chem. Soc., **1991**, 113, 1636.

116. Grunewald, G. C.; Drago, R. S. J. Chem. Soc. Chem. Comm., **1988**, 1206.

117. Grunewald, G. C. Ph.D. Thesis, University of Florida, 1989.

118. Norstrom, R. J.; Simon, M.; Muir, D. C. G.; Schweinsburg, R. E. Environ. Sci. Tech., **1988**, 22, 1063.

119. Josephson, J. Environ. Sci. Tech., **1984**, 18, 222A.

120. Huang, S. L.; Pfefferle, L. D. Environ. Sci. Tech., **1989**, 23, 1085.

121. Manning, M. P. Hazard. Waste, **1984**, 1, 41.

122. Spivey, J. J. Ind. Eng. Chem. Res., **1987**, 26, 2165.

123. Mendyka, B.; Rutkowski, J. D. Environ. Prot. Eng., **1984**, 10, 5.

124. Tichenor, B. A.; Pallazolo, M. A. in "AIChE Annual Meeting, November 10-15, 1985," No. 486.

125. Hyatt, D. E. U.S. Patent No. 3,989,806; Nov. 2, 1976.

126. Sare, E. J.; Lavanish, J. M. U.S. Patent No. 4,059,677; Nov. 22, 1977.

127. Sare, E. J.; Lavanish, J. M. U.S. Patent No. 4,065,543; Dec. 27, 1977.

128. Johnston, E. L. U.S. Patent No. 3,989,807; Nov. 2, 1976.

129. Sims, V. A. U.S. Patent No. 3,453,073; July 1, 1969.

130. Harley, A. D. U.S. Patent No. 4,816,609; March 28, 1989.

131. Kageyama, Y. U.S. Patent No. 4,053,557; Oct. 11, 1977.

132. Livingston, D. A.; Surls, J. P. U.S. Patent No. 4,587,116; May 6, 1986.

133. Reitmeier, R. E.; Mayfield, F. D.; Mayes, J. H. U.S. Patent No. 3,437,703; April 8, 1969.

134. Frevel, L. K.; Kressley, L. J. U.S. Patent No. 3,376,113; April 2, 1968.

135. Wolford, T. L. U.S. Patent No. 4,423,024; Dec. 27, 1983.

136. Dockner, T.; Sauerwald, M.; Krug, H.; Irgang, M. U.S. Patent No. 4,943,671; July 24, 1990.

137. Manning, H. E. U.S. Patent No. 3,859,375; Jan. 7, 1975.

138. Sing, K. S. W.; Everett, D. H.; Haul, R. A. W.; Moscov, L.; Pierotti, R. A.; Rouquerol, J.; Siemieniewska, J. Pure Appl. Chem., **1985**, 57, 603.

139. Allen, G. C.; Curtis, M. T.; Hooper, A. J.; Tucker, P. M. J. Chem. Soc. Dalton Trans., **1973**, 1675.

140. Okamoto, Y.; Fujii, M.; Imanaka, T.; Teranishi, S. Bull. Chem. Soc. Jpn., **1976**, 49, 859.

141. Schreifels, J. A.; Rodero, A.; Swartz, W. E., Jr. Appl. Spectr., **1979**, 33, 380.

142. Cimino, A.; DeAngelis, B. A.; Luchetti, A.; Minelli, G. J. Catal., **1976**, 45, 316.

143. Hogan, J. P. J. Polym. Sci., **1970**, 8A-1, 2637.

144. Bhatnagar, S. S.; Cameron, A.; Harbard, E. H.; Kapur, P. L.; King, A.; Prakash, B. J. Chem. Soc., **1939**, 1433.

145. Commereuc, D.; Chauvin, Y.; Hugues, F.; Basset, J. M.; Olivier, D. J. Chem. Soc. Chem. Comm., **1980**, 154.

146. Chojnacki, T. P.; Schmidt, L. D. J. Catal., **1989**, 115, 473.

147. Kiwi, J.; Italiano, P. J. Mol. Catal., **1989**, 50, 131.

148. Audier, M.; Klinowski, J.; Benfield, R. J. Chem. Soc. Chem. Comm., **1984**, 626.

149. O'Grady, T. M.; Wennerberg, A. N. in "Petroleum-Derived Carbons," ACS Symposium Series 1986, 303, 302.

150. Menon, P. G. J. Mol. Catal., **1990**, 59, 207.

151. Alkhazov, T. G.; Lisovskii, A. E.; Gulakhmedova, T. K. React. Kinet. Catal. Lett., **1979**, 12, 189.

152. Weldon, J.; Senkan, S. M. Combust. Sci. Technol., **1986**, 47, 229.

153. Imamura, S.; Tarumoto, H.; Ishida, S. Ind. Eng. Chem. Res., **1989**, 28, 1449.

154. Solar, J. M.; Derbyshire, F. J.; DeBeer, V. H. J.; Radovic, L. R. J. Catal., **1991**, 129, 330.

155. Laidler, J. Chemical Kinetics; 3rd ed.; Harper & Row Publ. Inc.: New York, 1987.

156. Chatterjee, S.; Greene, H. L. J. Catal., **1991**, 130, 76.

157. Manassen, J.; Wallach, J. J. Am. Chem. Soc., **1965**, 87, 2671.

158. Manassen, J.; Khalif, S. J. Am. Chem. Soc., **1966**, 88, 1943.

159. Furuyama, S.; Golden, D. M.; Benson, S. W. J. Am. Chem. Soc., **1969**, 91, 7564.

160. Lambert, J. C.; Germain, J. E. Bull. Soc. Chim. Fr., **1982**, 33.

161. Matsuura, I.; Schut, R,; Hirakawa, K. J. Catal., **1980**, 63, 152.

162. Defosse, C. in Characterization of Heterogeneous Catalysts (Delannay, F., Ed.); Marcel Dekker: New York, 1984; p. 241.

163. Cotton, F. A.; Wilkinson, G. Advanced Inorganic Chemistry; 5th ed.; John Wiley and Sons, Inc.: New York, 1988.

164. Eguchi, Y. Sekign Gokkai Shi, **1970**, 13(2), 105.

165. Koresh, J. E.; Soffer, A. J. Chem. Soc. Farad. Trans. I, **1981**, 77, 3005.

166. Gregg, S. J.; Sing, K. S. W. Adsorption, Surface Area and Porosity; 2nd ed.; Academic Press: London, 1982.

BIOGRAPHICAL SKETCH

Steven C. Petrosius was born in Quincy, Massachusetts, on November 9, 1965. He attended Boston College High School and graduated in May 1983. The following fall he enrolled in the University of Massachusetts at Boston. He graduated cum laude in 1987 and was awarded senior honors in chemistry. From there he went on to attend graduate school at the University of Florida where he studied inorganic chemistry under the tutelage of Professor Russell Drago. The author has published two articles and has filed two patents as well as presented papers at numerous ACS meetings, Florida Catalysis Conferences and UF Industrial Affiliate Meetings. Several other publications are currently in preparation.

I certify that I have read this study and that in my opinion it conforms to acceptable standards of scholarly presentation and is fully adequate, in scope and quality, as a dissertation for the degree of Doctor of Philosophy.

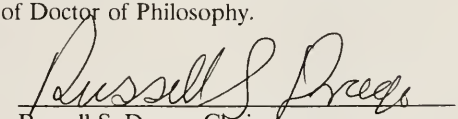

Russell S. Drago, Chairman
Graduate Research Professor of
Chemistry

I certify that I have read this study and that in my opinion it conforms to acceptable standards of scholarly presentation and is fully adequate, in scope and quality, as a dissertation for the degree of Doctor of Philosophy.

William M. Jones
Distinguished Service Professor of
Chemistry

I certify that I have read this study and that in my opinion it conforms to acceptable standards of scholarly presentation and is fully adequate, in scope and quality, as a dissertation for the degree of Doctor of Philosophy.

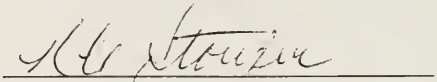

Robert C. Stoufer
Associate Professor of Chemistry

I certify that I have read this study and that in my opinion it conforms to acceptable standards of scholarly presentation and is fully adequate, in scope and quality, as a dissertation for the degree of Doctor of Philosophy.

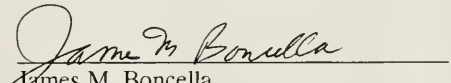

James M. Boncella
Assistant Professor of Chemistry

I certify that I have read this study and that in my opinion it conforms to acceptable standards of scholarly presentation and is fully adequate, in scope and quality, as a dissertation for the degree of Doctor of Philosophy.

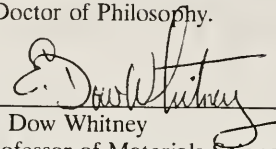

E. Dow Whitney
Professor of Materials Science and Engineering

This dissertation was submitted to the Graduate Faculty of the Department of Chemistry in the College of Liberal Arts and Sciences and to the Graduate School and was accepted as partial fulfillment of the requirements for the degree of Doctor of Philosophy.

August, 1992

Dean, Graduate School